

FEDERAL UNIVERSITY OF SAO CARLOS (UFSCAR)  
CENTER FOR EXACT SCIENCES AND TECHNOLOGY (CCET)  
DEPARTMENT OF MECHANICAL ENGINEERING (DEMEC)  
POSTGRADUATE PROGRAM IN MECHANICAL ENGINEERING (PPGEMEC)

DIMITRI HOOGEWIJS

RESEARCH AND DESIGN OF AN AUTONOMOUS  
AND COLLABORATIVE GUIDED VEHICLE  
PROTOTYPE, TO BE APPLIED IN INDOOR AND  
OUTDOOR ENVIRONMENTS AND DIFFERENT  
TYPES OF FLOOR

SAO CARLOS -SP  
2020



DIMITRI HOOGEWIJS

RESEARCH AND DESIGN OF AN AUTONOMOUS AND COLLABORATIVE GUIDED  
VEHICLE PROTOTYPE, TO BE APPLIED IN INDOOR AND OUTDOOR ENVIRONMENTS  
AND DIFFERENT TYPES OF FLOOR

Master thesis presented to the  
PostGraduate Program in Mechanical  
Engineering from Federal University of  
Sao Carlos as part of the procedure do  
obtain the title of Master in Mechanical  
Engineering.

Advisor: Prof. Dr. Luis Antonio Oliveira  
Araujo

São Carlos-SP  
2020



## ERRATUM

HOOGEWIJS, Dimitri. **Research and design of an autonomous and collaborative guided prototype, to be applied in indoor and outdoor environments and different types of.** 2020. 82. Master thesis - DEMec, UFSCar, São Carlos, 2020.

Page	Line	Where you read	Should be read as
Page n°	Line n°	Point here the error	Point the correction

FEDERAL UNIVERSITY OF SAO CARLOS (UFSCAR)  
CENTER FOR EXACT SCIENCES AND TECHNOLOGY (CCET)  
DEPARTMENT OF MECHANICAL ENGINEERING (DEMEC)  
POSTGRADUATE PROGRAM IN MECHANICAL ENGINEERING (PPGEMEC)

## **Approval Page**

Jury composition and signature. Defense presentation on 31/08/2020:

---

Prof. Dr. Luis Antonio Oliveira Araujo  
UFSCar

---

Prof. Dr. Carlos Ventura  
UFSCar

---

Ing. Bram Creve  
KU Leuven

---

Ing. Theo Vercruyssen  
KU Leuven

## ACKNOWLEDGEMENTS

This thesis is the concluding piece of my educational program, master of science in mechanical engineering with option mechatronics and robotics. The road to this final project was a tough but joyful learning experience. It gave me knowledge, experience and made me mature which I all can use in my further life. But luckily I wasn't alone in this journey, and therefore I would like to take the time to express my gratitude to a few people.

First of all I would like to thank Prof. Luis Antonio Oliveira Araujo, he guided me not only with great care in this project but he made me also feel very welcome in the prodigious, but in the beginning still unknown for me, Brazil. With the COVID-19 pandemic the situation of this project was not ideal, but Prof. Luis was there for me when I had questions or doubts, I will be forever grateful for the opportunity he gave me to make the best of my international exchange.

Next I wish to show my appreciation for Prof. Marc Juwet, he presented me this opportunity and guided me to the right people to make this exchange possible.

This exchange project wouldn't be possible without the people from the department of International relations of KU Leuven and UFSCar. They helped me with my pre departure questions and made the interscholastic agreement possible. Therefore I would like to thank everybody who helped to made it possible and in particular Hilde Lauwereys and Marcelo Fila Pecenin.

During my whole school career I made some great friends which helped me evolve in the person that I am today. They supported me in and outside school and therefore wish to extend my special thanks to them.

Last but not least I would like to thank my parents, they gave me the possibility to pursue my educational dreams and supported my financially and mentally.

Dimitri Hoogewijs

**“Unless you try to do something beyond what you have already mastered,  
you will never grow.” - Ronald E. Osborn [1]**



## **ABSTRACT**

This thesis is an initial attempt to investigate and design a prototype of an Autonomous Guided Vehicle (AGV) which could operate in indoor and outdoor applications. Currently an AGV is designed to work in application where the driving surface is clean, flat and solid. This takes some planning and timing before implementation. Therefore a suitable solution needs to be found which will make the vehicle usable in multiple environments without the need for clean surfaces. Firstly information is gathered about industrial AGV's to know what an AGV is made of and what are the strengths or flaws of the current ones. After that several concepts are proposed for designing problems like: wheel geometry, backlash while steering, which kind of suspension, etc. The main problem is solved by adding a suspension, which contains a shock absorber and coil spring, to the vehicle. This will make the wheels keep contact to the surface, even when it is loose and/or uneven like sand. To be able to manoeuvre in all directions, there is opted for a four wheel drive and steering solution. A dynamic model of the vehicle is made to see how the suspension and the chassis of the vehicle will react of a different load and a step in the road. Technical drawings, motor and suspension calculations, electrical structure, risk analysis and a cost estimation are also included in this study.

**Key words:** AGV. Suspension. Outdoor. Prototype.



## LIST OF FIGURES

Figure 1: Diagram design process	3
Figure 2: Unit load AGV with roller conveyor [6]	5
Figure 3: (a) Low capacity towing AGV [7], (b) high capacity towing AGV [8].	6
Figure 4: Forklift AGV [9]	7
Figure 5: Monobloc frame from Kiva AGV [10]	8
Figure 6: Sheetmetal frame [11]	8
Figure 7: (a) Frame structure with square tubes [12], (b) ITEM-profiles [13]	8
Figure 8: Different basic wheel types [14]	9
Figure 9: (a) Leaf spring [17], (b) Shock absorber with coil spring	14
Figure 10: Saga Robotics' Thorvald II AGV suspension [19]	15
Figure 11: Suspension of the Agbott II [20]	15
Figure 12: (a) Flooded Lead-acid battery, (b) Sealed Lead-Acid battery	17
Figure 13: Preparation for magnetic navigation [5]	18
Figure 14: Scheme working LiDAR sensor [21]	19
Figure 15: Safety areas [5]	21
Figure 16: Swedish omniwheel steering [23]	23
Figure 17: Four steering and driving wheels geometry	24
Figure 18: Six wheel configuration	24
Figure 19: Drive concept, motor on axle	25
Figure 20: Drive concept, drive belt	26
Figure 21: Drive concept, mechanical chain	26
Figure 22: Backlash between gears [26]	27
Figure 23: Backlash, adjustment of centre distance [26]	28
Figure 24: Backlash, anti-backlash gear [26]	28
Figure 25: Suspension placement sketch	29
Figure 26: Suspension: concept 1	30
Figure 27: Spring rate of an air suspension [27]	31
Figure 28: Frame	33
Figure 29: Suspension unit	34
Figure 30: Wheel support	35
Figure 31: (a) Suspension unit, (b) bottom view mesh between slewing gear and anti-backlash gear, (c) anti-backlash gear	35
Figure 32: Frame with suspension unit	36
Figure 33: (a) Top view drawer, (b) 3D-view drawer	37
Figure 34: Rolling resistance with arm of rolling friction [28]	40
Figure 35: Forces on a slope with decomposed gravity force	40
Figure 36: Specifications driving motor	44
Figure 37: Gear ratios ATO worm gearbox	45
Figure 38: Efficiency worm gearbox [33]	45
Figure 39: Trajectory AGV	46

Figure 40: v-t diagram motor cycle	46
Figure 41: Speed-Torque diagram, driving motor	49
Figure 42: Steering angle wheel, top view	50
Figure 43: Specifications steering motor	51
Figure 44: Gear ratios steering motor	52
Figure 45: Schematic diagram of a vehicle's suspension [27]	56
Figure 46: Influence of different damping ratio's [27]	58
Figure 47: Adding generalized profile in Abaqus	59
Figure 48: Cross-section of ITEM-profile with stress calculation points	60
Figure 49: Model with constraints, spring and dashpot	61
Figure 50: Load and boundary conditions	61
Figure 51: Sketch bump	62
Figure 52: Maximum stress in frame with $D=0,1$	64
Figure 53: Displacement frame in static step	65
Figure 54: Stress in frame and displacement from compression spring with $D=0,1$	65
Figure 55: Detail overshoot front suspension with $D=0.1$	66
Figure 56: Peak stress for different damping ratios	67
Figure 57: Detail oscillation with a few damping ratios	67
Figure 58: Detail overshoot front wheels with different damping ratios	68
Figure 59: Detail front wheels come down (left), detail unload (Right)	68
Figure 60: Positioning safety laser scanners, top view	69
Figure 61: A non-contact safety switch from Pilz [37]	70
Figure 62: Hazard zone marked on the floor [38]	71
Figure 63: Electrical diagram	73

## LIST OF TABLES

Table 1: overview chassis types	9
Table 2: Wheel configurations [14]	11
Table 3: Overview batteries	17
Table 4: Overview wheel geometry concepts	25
Table 5: Overview drive concepts	26
Table 6: Overview backlash steering	29
Table 7: Overview suspension concepts	31
Table 8: Design table	33
Table 9: Rolling resistance	41
Table 10: Static power	42
Table 11: Maximum acceleration	43
Table 12: Dynamic power	43
Table 13: Total power	43
Table 14: Cycle situations v-t	47
Table 15: Nominal torque driving motor	47
Table 16: total torque per situation	48
Table 17: Battery capacity calculations	54
Table 18: Total capacity and energy required for batteries	55
Table 19: Damping coefficient for different damping ratios	58
Table 20: Amplitudes wheels on bump	63
Table 21: Damping coefficients for dynamic simulation	63
Table 22: Price estimation	75

## LIST OF ABBREVIATIONS

ABS	Acrylonitrile butadiene styrene
AC	Alternating Current
AGM	Absorbent Glass Mat
AGV	Autonomous Guided Vehicle
BLDC	Brushless Direct Current motor
CAE	Computer-Aided Engineering
DC	Direct Current
DoD	Depth of Discharge
EN	European Norm
FLA	Flooded Lead-Acid
GPS	Global Positioning System
IMU	Inertial Measurement Unit
KU	Koninklijke Universiteit
PhD	Doctor of Philosophy
PLC	Programmable Logic Controller
QUT	Queensland University of Technology
RFID	Radio-Frequency Identification
RMS	Root Mean Square
RP	Reference Point
SLA	Sealed Lead-Acid battery
SVM	Stress Von Mises
VRLA	Valve Regulated Lead-Acid battery

## LIST OF ACRONYSM

ANSI	American National Standards Institute
CAD	Computer-Aided Design
DOF	Degrees of Freedom
ISO	International Organization for Standardization
Laser	light amplification by stimulated emission of radiation
LiDAR	Light Detection And Ranging
SLAM	Simultaneous Localization And Mapping
UFSCar	Universidade Federal de São Carlos

## LIST OF SYMBOLS

$a$	Acceleration	[m/s <sup>2</sup> ]
$b$	Width of the tire	[m]
$b_f$	Arm of the rolling friction	[m]
$b_w$	Distance between wheel centres	[m]
$c$	Damping coefficient	[Ns/m]
$c_c$	Critical damping	[Ns/m]
$C_{rr}$	Coefficient of rolling resistance	[/]
$D$	Damping ratio	[/]
$D_{sg}$	Outer diameter slewing gear	[m]
$D_w$	Diameter of the wheel	[m]
$E$	Energy	[J]
$E$	Young's modulus	[N/m <sup>2</sup> ]
$E_{rot}$	Rotational kinetic energy	[J]
$E_{trans}$	Translational kinetic energy	[J]
$f_0$	Natural frequency	[Hz]
$F$	Applied (axial) force	[m]
$F_R$	Static friction force	[N]
$F_{Rf}$	Rolling resistance, on a flat surface	[N]
$F_U$	Peripheral force	[N]
$g$	Gravitational acceleration	[m/s <sup>2</sup> ]
$G$	Shear modulus	[N/m <sup>2</sup> ]
$h$	Height of centre of mass	[m]
$i$	Gear ratio	[/]
$i_g$	Gearbox ratio	[/]
$i_{sg}$	Gear ratio with slewing gear	[/]
$I$	Current	[A]
$I_{11}$	Area moment of inertia around x-axis	[m <sup>4</sup> ]
$I_{12}$	Product moment of area	[m <sup>4</sup> ]
$I_{22}$	Area moment of inertia around z-axis	[m <sup>4</sup> ]
$j$	Backlash	[m]
$J$	Moment of inertia	[kgm <sup>2</sup> ]



$J^*$	Moment of inertia after gearbox	[kgm <sup>2</sup> ]
$k$	Spring stiffness	[N/m]
$m$	Mass of the vehicle	[kg]
$m'$	Mass on each driving tire	[kg]
$n$	Rotations per minute	[RPM]
$n_m$	Rotations per minute motor	[RPM]
$P_D$	Dynamic power of the load	[W]
$P_S$	static power	[W]
$P_{max}$	Maximum power	[W]
$P_n$	Nominal Power	[W]
$P_{tot}$	Total power	[W]
$Q$	Capacity	[Ah]
$r$	Radius of the wheel	[m]
$R$	Reaction Force	[N]
$t$	Time	[s]
$T_{acc}$	Acceleration torque	[N/m]
$T_{nom}$	Nominal torque	[N]
$T_{RMS}$	Root mean square torque	[N/m]
$v$	Speed of the vehicle	[m/s]
$v_t$	tangential velocity	[m/s]
$\Delta W$	Change of load on front wheels	[N/m]
$x$	Deflection of the spring from its original state	[m]
$\alpha_m$	Angular acceleration of the motor	[rad/s <sup>2</sup> ]
$\eta$	Efficiency gearbox	[/]
$\theta$	Steering angle	[°]
$\mu_0$	Static friction coefficient	[/]
$\nu$	Poisson ratio	[/]
$\rho$	Density	[kg/m <sup>2</sup> ]
$\gamma$	Slope angle	[°]
$\omega$	Angular velocity	[rad/s]
$\omega_0$	Natural oscillation	[rad/s]

The logo for 'ufiscan' features the text in a bold, black, sans-serif font. A grey swoosh curves around the letters, and a small orange sphere is positioned at the top right of the swoosh.

**ufiscan**

The logo for KU Leuven consists of the text 'KU LEUVEN' in white, bold, sans-serif capital letters, centered within a dark blue rectangular box with a light blue border.

**KU LEUVEN**

**TECHNOLOGIECAMPUS GENT**

The logo for 'Engenharia mecânica' features the text in a bold, black, sans-serif font. The word 'Engenharia' is in a smaller font size above 'mecânica'. The text is overlaid on a detailed line drawing of a gear and a bolt.

**Engenharia  
mecânica**

## SUMMARY

<b>ACKNOWLEDGEMENTS</b>	<b>I</b>
<b>ABSTRACT</b>	<b>III</b>
<b>LIST OF FIGURES</b>	<b>V</b>
<b>LIST OF TABLES</b>	<b>VII</b>
<b>LIST OF ABBREVIATIONS</b>	<b>VIII</b>
<b>LIST OF ACRONYMS</b>	<b>IX</b>
<b>SUMMARY</b>	<b>XIII</b>
<b>1 INTRODUCTION</b>	<b>1</b>
1.1 INSTITUTIONS	1
1.2 ISSUE STATEMENT	1
<b>2 LITERATURE REVIEW</b>	<b>5</b>
2.1 WHAT IS AN AGV?	5
2.2 COMMERCIAL AGV'S	5
<b>2.2.1 Types of AGV [5]</b>	<b>5</b>
2.2.1.1 Unit load	5
2.2.1.2 Towing	6
2.2.1.3 Forklift	6
2.3 PARTS OF AN AGV	7
<b>2.3.1 Chassis</b>	<b>7</b>
2.3.1.1 Frame	7
2.3.1.2 Wheel configuration [14]	9
2.3.1.3 Suspension	13
<b>2.3.2 Power supply [5]</b>	<b>16</b>
2.3.2.1 AGM and gel cell	16
2.3.2.2 Lithium-ion	16
2.3.2.3 Flooded Lead-Acid	17
<b>2.3.3 Navigation system [5]</b>	<b>18</b>
2.3.3.1 Magnetic	18
2.3.3.2 LiDAR	18
2.3.3.3 GPS	19
2.3.3.4 Combination of navigation systems	20
<b>2.3.4 Safety system [5]</b>	<b>20</b>
	xiii

2.3.4.1	<i>Active safety devices or sensors</i>	20
2.3.4.2	<i>Passive safety devices</i>	22
2.3.4.3	<i>Exception</i>	22
<b>3</b>	<b>DESIGN CONCEPTS</b>	<b>23</b>
3.1	WHEEL GEOMETRY	23
3.1.1	<b>Concept 1</b>	<b>23</b>
3.1.2	<b>Concept 2</b>	<b>24</b>
3.1.3	<b>Concept 3</b>	<b>24</b>
3.1.4	<b>Overview</b>	<b>25</b>
3.2	DRIVE	25
3.2.1	<b>Concept 1: on axle</b>	<b>25</b>
3.2.2	<b>Concept 2: drive belt</b>	<b>25</b>
3.2.3	<b>Concept 3: mechanical chain</b>	<b>26</b>
3.2.4	<b>Overview</b>	<b>26</b>
3.3	BACKLASH STEERING	27
3.3.1	<b>Concept 1</b>	<b>27</b>
3.3.2	<b>Concept 2</b>	<b>28</b>
3.3.3	<b>Concept 3</b>	<b>28</b>
3.3.4	<b>Overview</b>	<b>29</b>
3.4	SUSPENSION	29
3.4.1	<b>Concept 1</b>	<b>30</b>
3.4.2	<b>Concept 2</b>	<b>30</b>
3.4.3	<b>Concept 3</b>	<b>31</b>
3.4.4	<b>Overview</b>	<b>31</b>
<b>4</b>	<b>DESIGN</b>	<b>33</b>
<b>5</b>	<b>CALCULATIONS</b>	<b>39</b>
5.1	DRIVING MOTOR	39
5.1.1	<b>Rolling resistance</b>	<b>39</b>
5.1.2	<b>Static power</b>	<b>41</b>
5.1.3	<b>Dynamic power</b>	<b>42</b>
5.1.4	<b>Motor choice</b>	<b>43</b>
5.1.5	<b>Gear ratio</b>	<b>44</b>
5.1.6	<b>Torque</b>	<b>45</b>

5.2	STEERING MOTOR	49
5.2.1	Static friction resistance	49
5.2.2	Static Power	50
5.2.3	Dynamic power	50
5.2.4	Motor choice	51
5.2.5	Gear ratio	52
5.2.6	Torque	52
5.3	BATTERY CAPACITY	53
5.4	SUSPENSION	55
<b>6</b>	<b>DYNAMIC SIMULATION</b>	<b>59</b>
6.1	STRUCTURE STATIC MODEL	59
6.2	RESULTS	63
<b>7</b>	<b>SAFETY MEASURES</b>	<b>69</b>
7.1	ACTIVE SAFETY DEVICES	69
7.2	PASSIVE SAFETY DEVICES	70
7.3	EXCEPTION	71
<b>8</b>	<b>ELECTRICAL DIAGRAM</b>	<b>73</b>
<b>9</b>	<b>PRICE ESTIMATION</b>	<b>75</b>
<b>10</b>	<b>CONCLUSIONS</b>	<b>77</b>
	<b>REFERENCE LIST</b>	<b>79</b>
	<b>APPENDIX A – LIST OF DRAWINGS</b>	<b>A.1</b>
	<b>ATTACHMENT A – DATASHEETS</b>	<b>A.2</b>
	ATTACHMENT A.1 – IMOBRAS BRUSHED DC-MOTOR	A.2
	ATTACHMENT A.3 – DRIVING MOTOR WITH GEARBOX	A.4
	ATTACHMENT A.4 – ITEM PROFILES	A.5
	ATTACHMENT A.5 – SLEWING GEAR	A.6
	ATTACHMENT A.6 – DRAWER SLIDER	A.7
	ATTACHMENT A.7 – 48 V BATTERY	A.8
	ATTACHMENT A.8 – 24 V BATTERY	A.9
	ATTACHMENT A.9 – CABLE CARRIER	A.10
	ATTACHMENT A.10 – ENCODER	A.11
	ATTACHMENT A.11 – DAMPER	A.12
	ATTACHMENT A.12 – WHEEL	A.13

<b>ATTACHMENT B – PRICES</b>	<b>A.14</b>
ATTACHMENT B.1 – STEERING MOTOR	A.14
ATTACHMENT B.2 – DRIVING MOTOR	A.14
ATTACHMENT B.3 – ITEM PRODUCTS	A.15
ATTACHMENT B.4 – SLEWING GEAR	A.16
ATTACHMENT B.5 – DRAWER SLIDER	A.16
ATTACHMENT B.6 – 48 V BATTERY	A.17
ATTACHMENT B.7 – 24 V BATTERY	A.17
ATTACHMENT B.8 – CABLE CARRIER	A.18
ATTACHMENT B.9 – ENCODER	A.18
ATTACHMENT B.9 – COMPRESSION SPRING	A.18
ATTACHMENT B.10 – WHEEL	A.19

# 1 INTRODUCTION

## 1.1 INSTITUTIONS

This study is an international collaboration between two universities, UFSCar from Brazil and KU Leuven from Belgium.

### **UFSCar**

Universidade Federal de São Carlos, is the federal funded university in São Carlos, São Paulo, Brazil which was founded in 1970. It has four campuses with the main campus in São Carlos itself. The city is known as the National Capital of Technology due to its high concentrations of PhD inhabitants, 1 out of 5.423 inhabitants has a PhD degree. The university has around 25.000 students and is considered the 10<sup>th</sup> best Brazilian Institution following the ranking prepared by Quacquarelli Symonds (QS). This thesis is made with the mechanical engineering department (DEMec). [2]

### **KU Leuven**

The Katholieke Universiteit van Leuven, is the catholic university in Leuven, Belgium. It was founded 1425, which makes it one of the oldest universities in Europe and has up to today 13 different campuses all around Belgium. KU Leuven has 52.822 students enrolled for the academic year 2019-2020. This project is in collaboration with the Robotics, Automation and Mechatronics department (RAM) from the technology campus in Ghent. [3]

## 1.2 ISSUE STATEMENT

Over the last years, robotics and artificial intelligence have reached a high technological level. Currently, we can see developments and applications as mobile robots, autonomous vehicles, massive application of industrial robots and automation, etc. Autonomous Mobile Robots are presented in most of technological roadmaps, as one of the research fields with substantial investments in the next decades. Robot mobility has plenty of benefits: cost reduction, repeatability improvement, sped up logistics, etc. Several of those benefits have great contributions for the industry. Mobile Robots already has a variety of conceptions: as Autonomous Guided Vehicles (AGV's) is the most common.

Traditionally, an AGV is conceived by a rigid chassis with electric motor wheels, following trajectories defined in advanced. They demand considerable planning for implementation, as the level of cleaning the floor - to guarantee adherence - and extra maintenance of the line track, magnets or even guide ports.

This thesis has as goal to do research and design an autonomous and collaborative guided vehicle prototype, to be applied in indoor and outdoor environments and different types of floor. The autonomous refers the ability to transport loads without

any direct human interference, except safety situations. The collaborative characteristics is a group of qualities as: easy to use interface, safety operations, low weight, working together with human with a level of safety. The indoor and outdoor environment make the reference to the capacity of navigation inside house and also outside house. This possibility increases options for logistic routes even if the environment is aggressive, as rain, snow, sun, humidity, etc. Together with this characteristic, the field must be considered. In general, in a plant factory, the outside floor is different from inside floor. The vehicle needs to be able to transport a load of 500 kg and has size limitations of 1,5 m long and 1 m wide.

Figure 1 shows the design process of this thesis. First there needs to be a demand from the market. This is what just was stated before, there is a need for an AGV for indoor and outdoor applications. So the first step of the thesis, chapter 2, is to do a literature review to find what is already on the market and what the possibilities are. Thereafter the product is defined and the initial parameters are set. The next step in the process is finding solutions for several problems: finding the right wheel geometry, calculating the needed motor and battery and looking for a suspension. This happens in chapter 3 and 4.

Next in line, chapter 5, is the actual design of the vehicle. In the chapter the reasoning and material selection of most partial problems are explained. After that the CAD-model is controlled by a CAE-model (chapter 6). If the structure is not strong enough there has to be returned to the previous step to adapt the design. If the model is ok, the design part is finished.

In addition there is made an electrical structure diagram (chapter 7), safety analysis (chapter 8) and a cost estimation (chapter 9).

And to finish the project, chapter 10, there is a conclusion about the project which also includes reflection and things to improve



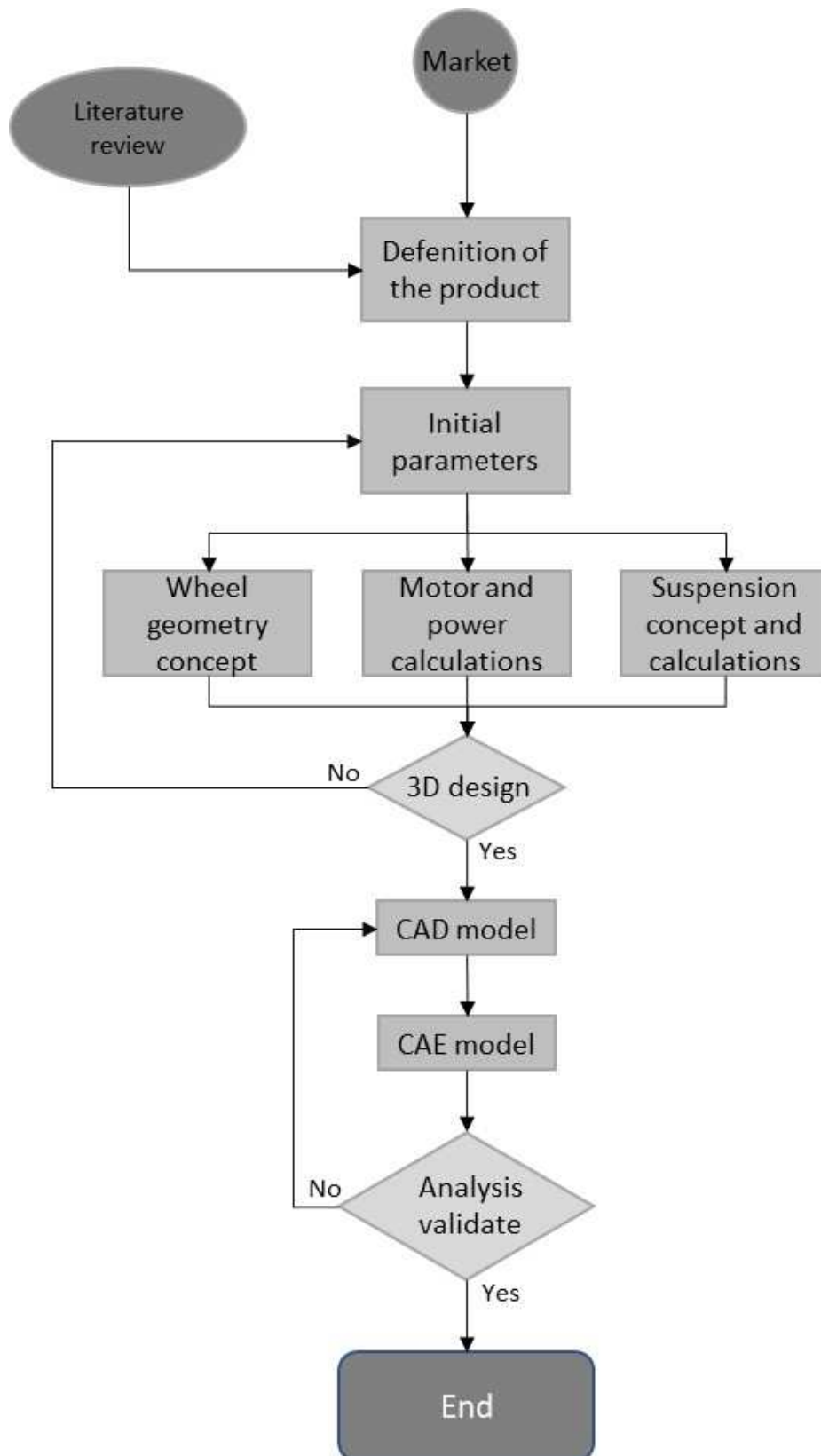


Figure 1: Diagram design process



## 2 LITERATURE REVIEW

### 2.1 WHAT IS AN AGV?

AGV is an abbreviation of Autonomous Guided Vehicle. It's an vehicle that navigates from point A to point B without any human intervention. These AGV's are most common in industrial settings such as big warehouses like Amazon [4], production lines, storage places, etc. But also in the agricultural sector the AGV's are on the rise, to be more precise, in the precision agriculture.

### 2.2 COMMERCIAL AGV'S

When developing a new kind of AGV, it's important to know what's already on the market. In this chapter, the general structure of the commercial AGV's will be discussed. This will help to point out the good points and the flaws of the AGV's of today.

#### 2.2.1 Types of AGV [5]

This prototype will be a unit load AGV, but there are several types of AGV with different purposes and applications. In this chapter the applications, advantages and the disadvantages of these types will be looked into to show what kind of variety is possible.

##### 2.2.1.1 Unit load

Unit load AGV's are vehicles which transport one or a few loads to a different location by carrying them. It's one of the most basic types and is actually not more than a driving platform.

The different kinds of unit load AGV's are specified by how the load is transferred on and off the platform. This transfer can be done by a roller (Figure 2) or belt conveyer, a lifting platform or just a regular flat platform. This makes unit load AGV's perfect for manufacturing and warehouse distribution.



Figure 2: Unit load AGV with roller conveyor [6]

The great advantage of this kind of vehicles is that you have a huge range of load

capacity, this capacity can extend up to 20 tons or more. A disadvantage is that there isn't a high reach height.

### 2.2.1.2 Towing

A towing or tugger AGV can be compared with a train locomotive. The vehicle tows one or multiple wheeled carts without a driver.

The towing capacity varies much but is limited to around 5000 kg. The ones with a lower towing capacity (<2000 kg) are compact and only have an autonomous operation mode (Figure 3a). Vehicles with a higher capacity have mostly an autonomous and a manual operation mode (Figure 3b). There are also AGV's which can tow up to 20 Tons, these are more referred to as tow tractors and will be used more in outdoor applications.



Figure 3: (a) Low capacity towing AGV [7], (b) high capacity towing AGV [8].

One of the greatest disadvantages of this kind of vehicle is the difficult autonomous hooking of the carts. In most applications it will be done manually. On the other hand, towing AGV's are quite fast with a maximum speed of around 1 m/s. But the combination of human interaction and the speed limit, the safety measures are more difficult.

These kinds of AGV's are mostly used to supply components to an assembly or production line or/and transport finished product at the end of the line.

### 2.2.1.3 Forklift

As the name suggests, a forklift AGV is an autonomous kind of forklift. The applications are also mostly the same but with the advantage that you don't need a driver. In this kind of AGV, you still have different types. The automated pallet mover, the counterbalance forklift, the straddle forked AGV and VNA AGV (Very Narrow Aisle). These can all be used at different kinds of applications but the main objective stays the same: to load and unload goods at different heights.



Figure 4: Forklift AGV [9]

The maximum load capacity is around 3000 kg for regular forklift AGV's. The main advantage of a forklift is the reach of height, up to 8 meters. Lifting can be done at 0,1 m/s and driving up to 2 m/s.

## 2.3 PARTS OF AN AGV

There are many things to consider when designing a new AGV or prototype. To keep everything clear and structured the vehicle will be divided in different parts.

### 2.3.1 Chassis

The chassis is a key part of an AGV, it's literally and figuratively the backbone of the vehicle. It will be the main subject of this thesis, trying to design and evaluate a light, rigid chassis which can perform in different environments. The chassis consist of 4 main parts: the frame, the wheel configuration, the steering and the suspension.

#### 2.3.1.1 Frame

The frame will hold all the parts of the vehicle together. When deciding what kind of frame to choose, there are a few points to consider. First and foremost, the strength and rigidity of the frame. It must be able to hold the weight of the load plus the weight of the other parts of the AGV. But it also needs to be rigid enough so when accelerating, the frame isn't shaking. Because this vehicle is a prototype, it would be a surplus if the frame is easy to handle so assembling and disassembling parts from the frame can be done quickly and without much deconstruction.

For the frame there are 3 main options: a monobloc, a sheet metal frame and a frame structure with profiles.

#### **Monobloc**

The frame is made by machining a solid block of metal where the other pieces of the vehicle will be mounted on. The machining process takes quite some time due to programming hours and machine hours but on the other hand, it gives a very accurate result. The size of a monobloc frame is limited by the size

of the machine tool. Because of this are these monobloc solution mostly used on small AGV's. An example of this is the Kiva AGV (Figure 5).

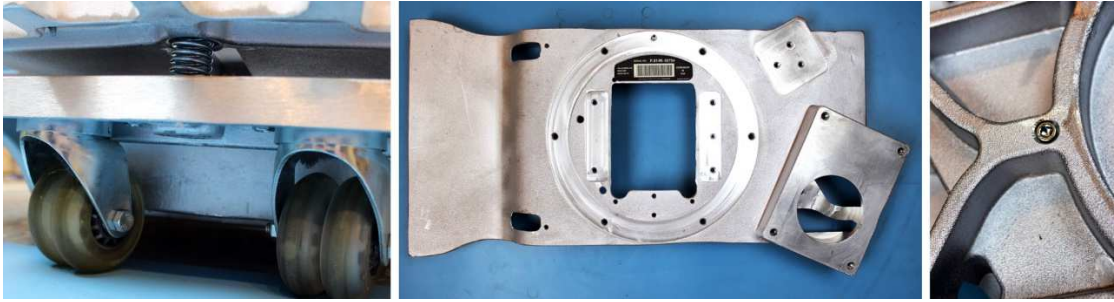


Figure 5: Monobloc frame from Kiva AGV [10]

### Sheetmetal frame

This frame type consist of different metal plates which are assembled. To give strength to the structure, the sheet metal gets bended. This kind of frame results in a very light structure with less material then a monobloc. The difficulty lies in to know where to bend to get a strong construction. In Figure 6 a sheet metal frame is shown, it's not in an application of AGV's but it shows the possibilities of a big seized sheet metal structure.

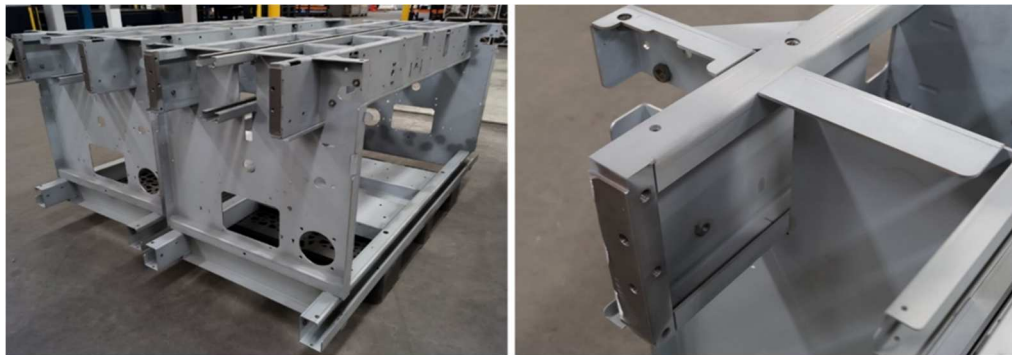


Figure 6: Sheetmetal frame [11]

### Frame structure

The most used type of frame is a structured frame with metal profiles. These pipes could be the regular square or rectangular profiles ( Figure 7a), but also a tube like an ITEM-profile ( Figure 7b). These last ones have the advantage of easy assembly and disassembly but are a bit more expensive in purchase.

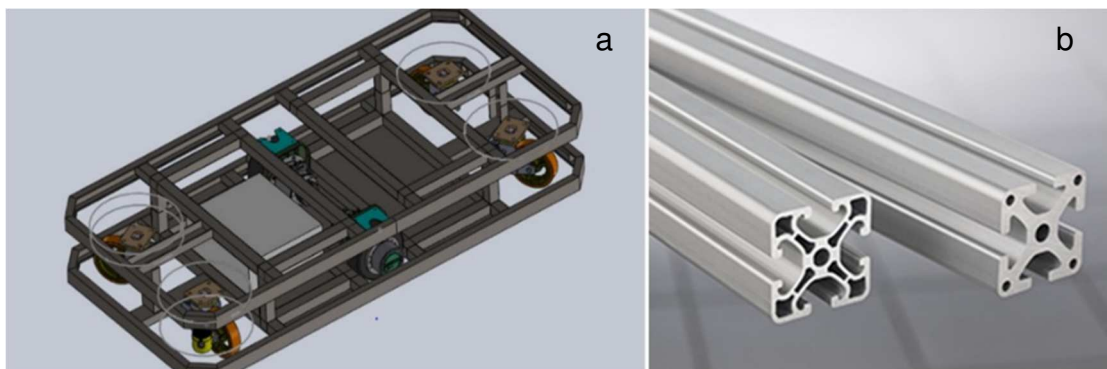


Figure 7: (a) Frame structure with square tubes [12], (b) ITEM-profiles [13]

Table 4 shows an overview of advantages and disadvantages of the different chassis types.

Table 1: overview chassis types

	Monobloc	Sheet metal	Profiles
Easy rigidity	++	-	+
Time manufacturing	-	-	+
Size possibilities	-	+	+
Adaptability	-	-	+

### 2.3.1.2 Wheel configuration [14]

The big variety of applications of AGV's results in many possibilities for wheel configurations. The wheel design and geometry are the basis of the configuration.

**Wheel design:** Figure 8 shows the four basic wheel types:

- A standard wheel which has two degrees of freedom (DOF): rotation around the contact point and around the whether or not motorized wheel axle.
- A castor wheel with two DOF: rotation around an offset steering joint and the wheel axle
- A Swedish wheel has three DOF: a rotation around the rollers, the contact point and the motorized wheel axle.
- A spherical wheel has multiple DOF, realization is technically difficult.

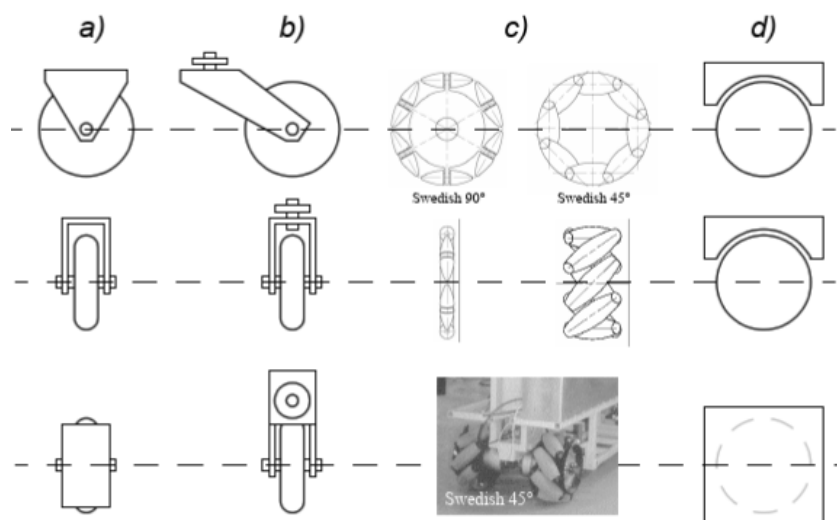


Figure 8: Different basic wheel types [14]

The choice of the wheel type has a big consequence on the kinematics of the whole AGV because of the all the wheels itself have a different kinematics. Both the standard and the castor wheel move in the same way, but with the big

difference that the castor wheel turns around the centre of the wheel with an offset. This causes an extra force on the chassis of the vehicle.

The Swedish wheel has one more DOF than the previous two wheel and is called an omnidirectional wheel. Although it also powered on only one axle, the wheel can move in different directions with little friction.

The spherical wheel can rotate around all axle therefore it's truly an omnidirectional wheel.

### **Wheel geometry**

Choosing the right wheel type is heavily connected to the arrangements of the wheels, or wheel geometry. When designing a robot these two go hand in hand. This choice will affect three essential characteristics: manoeuvrability, controllability, and stability. The big variety of environments that an AGV can be faced makes it impossible to have a wheel configuration where all three characteristics are always optimal.

Stability: A minimum of three wheels are required to have a static stable vehicle, provided that the centre of mass is within the triangle which the contact points of the wheel make. Actually it is two wheel, but for this thesis this is out of the question. Adding extra wheels to the configuration will increase stability, but will make the structure hyperstatic. Therefore a suspension will need to be added for driving on uneven undergrounds.

Manoeuvrability: The manoeuvrability has a lot to do with the rotation axis where the whole vehicle turn around. Omnidirectional means that it can move in any direction at any time on the ground, regardless of the orientation around its vertical axis. Examples of this are the Swedish wheel of a four wheel configuration with active steering and translation. Automotive vehicles use the Ackerman steering configuration. This configuration makes the vehicle turn with a diameter which is larger than the car. This makes short turning very difficult or it needs more manoeuvres, but it has a good stability in high-speed turns.

Controllability: Controllability and manoeuvrability don't work well together. As example, a Swedish wheel uses free rollers along the diameter of the wheel, which provide an extra slippage. This will result in a reduction of accuracy and an increase in complexity for controlling.

To summarise, there are many different wheel configurations where there has to be found a good as possible compromise between manoeuvrability and controllability. In table 5 the most common wheel arrangements are listed.



Table 2: Wheel configurations [14]


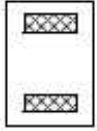
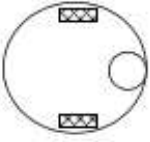
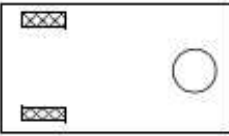
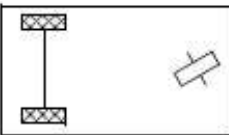
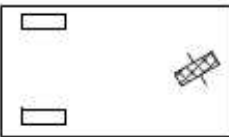

# of wheels	Arrangement	Description	Typical examples
2		One steering wheel in the front, one traction wheel in the rear	Bicycle, motorcycle
		Two-wheel differential drive with the center of mass (COM) below the axle	Cye personal robot
3		Two-wheel centered differential drive with a third point of contact	Nomad Scout, smartRob EPFL
		Two independently driven wheels in the rear/front, one unpowered omnidirectional wheel in the front/rear	Many indoor robots, including the EPFL robots Pygmalion and Alice
		Two connected traction wheels (differential) in rear, one steered free wheel in front	Piaggio minitrucks
		Two free wheels in rear, one steered traction wheel in front	Neptune (Carnegie Mellon University), Hero-1
		Three motorized Swedish or spherical wheels arranged in a triangle; omnidirectional movement is possible	Stanford wheel Tribolo EPFL, Palm Pilot Robot Kit (CMU)

Table 2: Wheel arrangements (continuation)

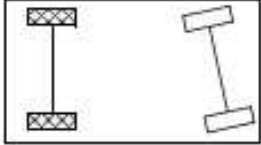
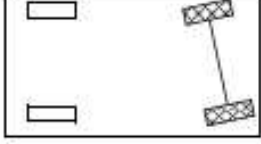
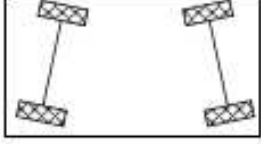
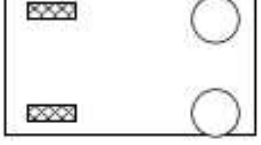
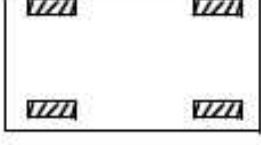

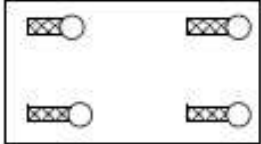
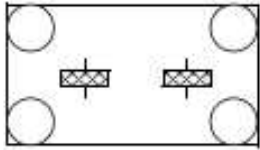
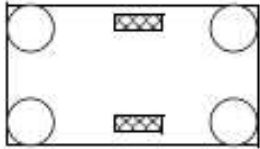

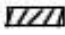



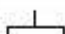

# of wheels	Arrangement	Description	Typical examples
4		Two motorized wheels in the rear, two steered wheels in the front; steering has to be different for the two wheels to avoid slipping/skidding.	Car with rear-wheel drive
		Two motorized and steered wheels in the front, two free wheels in the rear; steering has to be different for the two wheels to avoid slipping/skidding.	Car with front-wheel drive
		Four steered and motorized wheels	Four-wheel drive, four-wheel steering Hyperion (CMU)
		Two traction wheels (differential) in rear/front, two omnidirectional wheels in the front/rear	Charlie (DMT-EPFL)
		Four omnidirectional wheels	Carnegie Mellon Uranus
		Two-wheel differential drive with two additional points of contact	EPFL Khepera, Hyperbot Chip
		Four motorized and steered castor wheels	Nomad XR4000

Table 2: Wheel arrangements (continuation)

# of wheels	Arrangement	Description	Typical examples
6		Two motorized and steered wheels aligned in center, one omnidirectional wheel at each corner	First
		Two traction wheels (differential) in center, one omnidirectional wheel at each corner	Terregator (Carnegie Mellon University)
Icons for the each wheel type are as follows:			
	unpowered omnidirectional wheel (spherical, castor, Swedish)		
	motorized Swedish wheel (Stanford wheel)		
	unpowered standard wheel		
	motorized standard wheel		
	motorized and steered castor wheel		
	steered standard wheel		
	connected wheels		

### 2.3.1.3 Suspension

Most industrial AGV's drive on smooth solid flat surfaces and therefore they do not need a suspension. The operation environment of this thesis' AGV varies, causing the need for a suspension. A suspension is to allow motion between the tires and the chassis, with the general goal to make the ride as comfortable as possible. In the course of time different kind of suspensions are developed, these are examined in this chapter. It will also be discussed where to pay attention to when choosing or designing a kind of suspension.

The most common suspensions come from the automotive sector. Leaf springs were used for the first spring-suspension vehicle (Figure 9a). In 1901 the first car with a shock absorber was made, the shock absorber added a big advantage over the leaf springs due to its damping. The next step in the history of car suspensions was the

coil springs which are easier to install, lighter and have a more travel [15]. For very heavy vehicles, leaf springs remain better due to the load distribution. 19 years later, in 1920, the torsion bar was used for a suspension system. Yet this solution is not used on cars anymore. Most present-day suspensions use a spring and a damper combined (Figure 9b). Yet there are still a lot of different solutions for a suspension, whether or not it is with a spring and damper. [16]

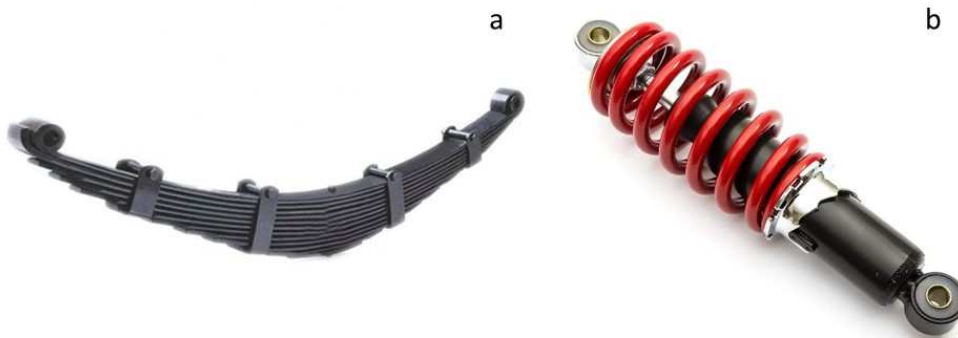


Figure 9: (a) Leaf spring [17], (b) Shock absorber with coil spring

### Properties [16]

When choosing a suspension there are a lot of factors to take into account. Some of the most important ones will be discussed here.

Spring rate: the ride height of the vehicle is an important for the handling of the vehicle. The spring rate is how resistant the spring is during deflection. For a compression spring this means when a high load is applied, the spring will compress more when the spring rate is low. This relation is stated by Hooke's Law:

$$F = -kx$$

Where:

- F applied (axial) force [N]
- k spring rate [N/m]
- x deflection of the spring from its original state [m]
- $C_{rr}$  coefficient of rolling resistance [/]

Damping: damping is the parameter which ensures comfort through controlling the oscillation.

Weight transfer: this is, as the name states, the transfer of weight during acceleration, braking or cornering. It is most of the time calculated per wheel and compared with the static weight of the same wheel.

This parameter is affected by four aspects: the height of the centre of gravity, distance between wheel centres, acceleration, and the mass of the vehicle. When braking:

$$\Delta W = a * \frac{h}{b} * m$$

Where:  $\Delta W$  change of load on front wheels [N/m]  
 $a$  acceleration [ $m/s^2$ ]  
 $h$  height of centre of mass [m]  
 $b_w$  distance between wheel centres [m]  
 $m$  mass of the vehicle [kg]

As stated before, industrial AGV mostly do not need a suspension, therefore there won't be much information to find. But in the agriculture sector nevertheless, suspensions are needed for most of its applications. In Figure 10 the suspension of the Thorvald II from Saga Robotics' is showed. It contains a gas spring, oil dampened shock absorber and allows trough two rotation arm travel in the vertical direction [18].



*Figure 10: Saga Robotics' Thorvald II AGV suspension [19]*

Another agriculture robot is the AgBott II from QUT (Figure 11). This suspension looks more like a rear suspension of a motorcycle with a coil spring, hydraulic shock absorber and a rotation arm.



*Figure 11: Suspension of the Agbott II [20]*

In the next chapter, 3. design concept, there will be gone deeper in some concepts for the suspension which will bring out the pros and cons of some solutions

### **2.3.2 Power supply [5]**

Obviously the vehicle needs to be powered by some energy source for driving, steering, the sensors, etc. For this, batteries will be used. All motors that will be used will be DC motors, so no conversion to AC or an AC generator is needed. But there are still some different kind of batteries available on the market. Therefore it will be reviewed which has what advantages and or disadvantages.

#### *2.3.2.1 AGM and gel cell*

Absorbent Glass Mat (AGM) and gel cell batteries are not the same but have some very similar characteristics. Both fall on the category of valve regulated lead-acid batteries (VRLA) or also known as sealed lead-acid batteries (SLA). But in AGM and gel cell batteries, the electrolyte is not a fluid. In AGM it is a fiberglass mat, in gel cells it is in a form of paste.

Some characteristics of these batteries:

- Sealed and non-spillable
- Maintenance-free
- Discharge up to 50%
- Low self-discharge rate
- Very robust
- Recharging time around 5 hours
- Not good for opportunity charging
- Low to no gas emissions
- Recharge cycles at 50% DoD<sup>1</sup>:  $\pm 1500$  cycles

#### *2.3.2.2 Lithium-ion*

In these batteries, lithium is the material of the positive electrode (anode when charging). The lithium-ion battery will be compared to the AGM and gel cell batteries.

Advantages for lithium-ion:

- Longer cycle time, at 50% DoD:  $\pm 5000$  cycles.  
This is on average 3 times more.
- Deeper DoD, excellent battery life at 80%
- Higher efficiency: near 95% instead of the 80-85% from the VRLA
- Faster charge rate: around 2 hours

<sup>1</sup> DoD is the Depth of Discharge of a battery. A DoD of 80% means that the battery is discharged for 80% of its capacity and will be charged after that. The DoD-rate has an impact on the cycle life of the battery, the lower rate the longer the life time of the battery. This is a non-linear relation.

- Higher energy density: this means less volume and weight for the same power.

Disadvantages for lithium-ion:

- Require electronic protection against overcharging due to instability of the battery.
- Transport limitations for air transportation
- More expensive, can be up to four times more.

### 2.3.2.3 Flooded Lead-Acid

In a lot of forklift application flooded Lead-Acid batteries (FLA, Figure 12a) are found. Which work on the same principle of the SLA (Figure 12b) batteries.

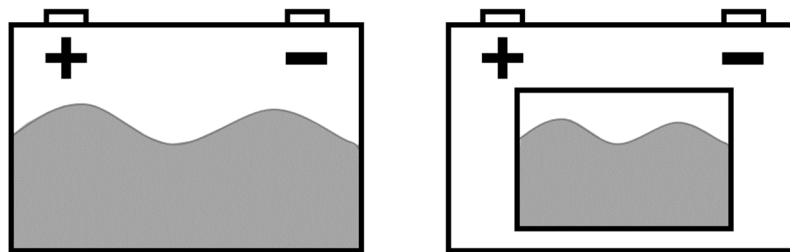


Figure 12: (a) Flooded Lead-acid battery, (b) Sealed Lead-Acid battery

The main advantage of the FLA batteries is that they are the cheapest batteries on the market. But it comes with a few disadvantages:

- Maintenance required: refill with ionized water, check for leakage,...
- The low DoD of 50%
- Heavy batteries
- Only mounting straight, due to leakage possibilities.
- Releases gasses

So, a lot more disadvantages than advantages, but still this type of battery is used often in heavy outdoor applications.

Table 3: Overview batteries

	AMG and gel	Lithium-ion	Flooded lead-acid
Low maintenance	+	+	-
Depth of charge	-	+	-
Weight	+	++	-
Gas emission	+	+	-
Recharge time	-	+	-
Transport	+	-	-
Price	-	--	+

### 2.3.3 Navigation system [5]

AGV's for indoor application have many different ways to navigate: laser-guided, magnetic, natural, magnetic spot, wire, optical and vision navigation. But, a lot of these navigation types are not suitable for outside environments, because of the different circumstances: weather situations, uneven terrain, random objects, etc.

So, in this chapter the navigation systems that do work in outdoor systems will be discussed.

#### 2.3.3.1 Magnetic

Magnetic navigation is in theory a very easy system. A magnetic sensor on the vehicle follows a magnetic tape on or in the ground. A great advantage of this system is that it is weather independent, the weather doesn't have an effect on the magnetic forces.

Nevertheless, there are some disadvantages. This makes the vehicle not fully free to move, it has to follow the magnetic line. If you want to make adaptations to the track, the magnetic line has to be moved, which in the case of outside applications is a tough job. In Figure 13 the preparation for laying a magnetic tape is shown. First a track has to be milled where the tapes lies in, then the tape and the resin is put on top. As can be seen, this is an outdoor application, but still not the environment which is aimed for. In loose earth applications, this kind of navigation will also not be possible.



Figure 13: Preparation for magnetic navigation [5]

#### 2.3.3.2 LiDAR

LiDAR is an acronym for Light Detection And Ranging. The system sends a laser light and measures the distance to a target by measuring the reflected light from the target



(Figure 14). The differences in feedback (timing, wavelengths, etc.) are used to make a digital 2D or 3D-illustration of the target.

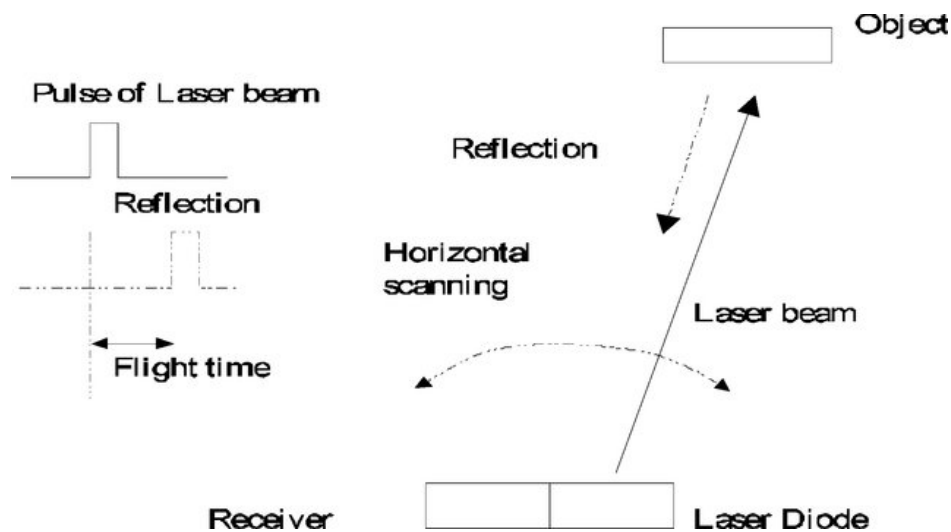


Figure 14: Scheme working LiDAR sensor [21]

The LiDAR is commonly used with a SLAM system. SLAM stands for Simultaneous Localization And Mapping. It uses the data from the LiDAR sensor to create a map of the environment so it can later localize itself in that map. Very large open fields with minimal reflection points can give difficulties for the sensor, therefore a GPS can be added. And on the other hand, very chaotic changing environments can create problems for the SLAM system.

A big advantage of this navigation technique is that the vehicle easy to install and relatively not too expensive. The AGV is also not restricted to tracks, they can be easily modified. When selecting a LiDAR sensor there are some things to take in consideration.

- Resistance to ambient light. The sunlight could interfere with the sensor, making it unable to identify it owns laser beam. Therefore it should resist around 70 000 lumens.
- Resistance to environmental noise. Raindrops could give wrong signals which could create navigation problems. This can be prevented by Multi-echo technology.
- Ingress Protection (IP). LiDAR sensor should be at least IP65 or IP67 to protect the sensor from dust and water.
- Temperature operation range.

### 2.3.3.3 GPS

A GPS (Global Positioning System) will provide position and speed, even in harsh weather conditions. Indoor application are less suitable for this system because of bad or no signal situations.

#### 2.3.3.4 Combination of navigation systems

As seen before, almost no navigation system is ideal for indoor and outdoor applications, therefore a combinations of two or more systems can be used. A widely used combination for agriculture AGV's is the LiDAR sensor with GPS, the 'BoniRob' uses this [22].

#### 2.3.4 Safety system [5]

Safety is very important in every industry, machine and environment. And it surely is also from the upmost importance for AGV's. The operatorless vehicle needs to meet some standards, in Europe these are the EN 1525: 1997: Safety of Industrial Trucks - Driverless Trucks and Their Systems. America has ANSI B45.5 – 2012: Safety Standard for Driverless, Automatic Guided Industrial Vehicles and Automated Functions of Manned Industrial Vehicles. Both are very similar and define safety requirements relating to the elements of design, operation and maintenance of AGV's.

##### Vehicle safety and emergency controls and devices

*Vehicle safety and emergency controls and devices are those which automatically and rapidly stop propulsion, stop moving components, and apply full braking power. To prevent contact between the load and any possible obstructions, AGV's should include sensors pointing in the direction of travel and covering the maximum moving width and/or length provided. [5]*

##### Stopping distance:

*Braking systems in conjunction with the object detection system and the response time of the safety control system are built to cause the vehicle to stop prior to impact between the vehicle's structure and other equipment, including its intended load or an observed obstruction in front of the moving vehicle. [5]*

##### Guidance system:

*Deviation of travel from the intended path shall also require an emergency stop. [5]*

Safety elements can be categorized in two, active safety elements and passive safety elements.

#### 2.3.4.1 Active safety devices or sensors

Active safety systems are systems that can change the status of the AGV. This can be an emergency stop, slow braking,...

##### **Safety laser scanner or collision avoidance system**

If safety lasers are used as the main sensing device, it should be fail-safe in its operation. On top of that, when sensing an object or people in its path at a distance that is smaller than the leading edge of the sensing field, the AGV should make a safety stop before any contact between the vehicle and the

object or people.

The laser makes a safety fields which is divided in two safety fields, a warning field and a protective field. When an object or person is detected in the warning field, the vehicle decelerates. When this happens in the protective field, the vehicle stops. Both area's together are called the safety area.

A safety area of an AGV needs to be variable, it depends on the AGV's speed, surrounding area, load of the vehicle, and floor conditions. This means that every point on the vehicles trajectory has its own safety area. In Figure 15 different safety areas for high, low speed and turning are shown.

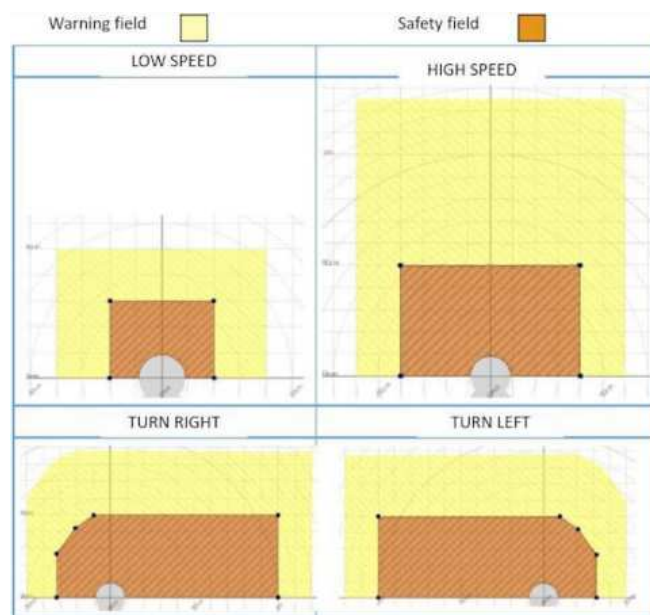


Figure 15: Safety areas [5]

### Contact bumper

It is not obliged to cover all 360° of the AGV with a safety laser. They are mainly for the direction of movement. To reduce the cost contact bumper can be placed where only low speed contact is possible. Bumper can come in many forms and sizes depending on the vehicle and the object that could possibly hit it. The principle is very simple, if the vehicle touches something/ someone, it may not damage the obstacle or itself. EN 1525: 1997 and ANSI B45.5 -2012 state both that if the speed is less than 0,3 m/s, a collision avoidance system is not needed.

### Emergency Stop Buttons

Emergency stops are obliged on each AGV. They must be visible and easy to reach from every side. When activated, the vehicle enters an emergency stop state and all motion will be shut down.

### Safety control

The AGV needs an element that manages these safety elements. This can be

done by a safety PLC or safety relays. It has one main function, ensuring that the vehicle stops when needed.

#### 2.3.4.2 *Passive safety devices*

Passive safety devices do not change the state of the vehicle but are more to warn bystanders to prevent collisions. This can be done in different ways.

##### **Warning lights**

AGV's can have turn indicator lights in applications where a lot of people are in the same area of the AGV. It can also have warning lights for different statuses of the vehicle: driving, emergency stop, restart after stop, etc. When warning lights are used, they have to be visible from every side of the vehicle.

##### **Audible warning/ Alarm signals**

As with the warning lights, the sound signals an AGV can emit can be used for different statuses of the vehicle. A direct citation:

*Prior to initiation of the vehicles movement or remote reactivation from a sleep or inactive state, a warning device (on or off the vehicle) shall be activated, to be either audible, visual, or a combination thereof, indicating the imminent movement of the vehicle under automatic control. [5]*

##### **Signs and Symbols**

The AGV must have signs and symbols showing hazard zones. All signs must be in accordance with the local legislation and shall be durable.

#### 2.3.4.3 *Exception*

The safety scanner is designed to detect objects and people and avoid collisions with it/them. But there is an exception stated in the standard of ANSI B56.5-2012:

*Although the vehicle braking system may be performing correctly and as designed, it cannot be expected to function as designed should an object suddenly appear in the path of the vehicle and within the designed safe stopping distance. Examples include, but are not limited to, an object falling from overhead or a pedestrian stepping into the path of a vehicle at the last instant. [5]*

### 3 DESIGN CONCEPTS

In this section different concepts are explained for four different designing problems. The concepts will be rated on several topics and in the next chapter there will be picked a solution for the actual prototype.

#### 3.1 WHEEL GEOMETRY

In the literature review a list of different wheel geometries was shown. Out of this list three are picked to look closer into. The configurations with two and three wheels are thrown out of the equation because the high load capacity. This would result in bigger motors, higher power, higher current and bigger cables. Also options where the vehicle isn't omnidirectional, due to a steering radius, are not suitable for this thesis' AGV.

##### 3.1.1 Concept 1

The first concept is a geometry of four identical Swedish wheels. How these wheels can make the AGV steer without a rotation around the wheels' z-axis is shown Figure 16.

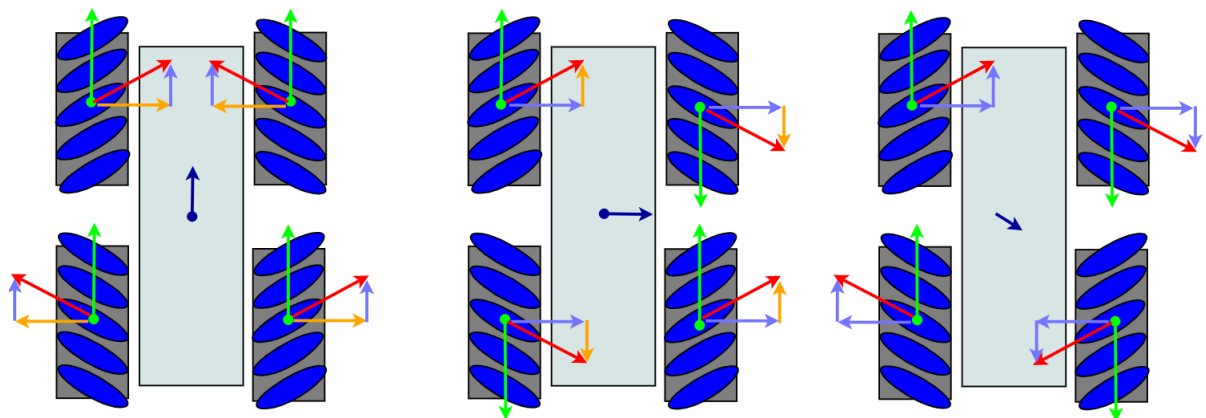


Figure 16: Swedish omniwheel steering [23]

The left situation is where all four wheels are rotating in the same direction to move the vehicle forward. Due to the angle of the rollers, there are also axial forces, but because the wheels are mirrored to each other, these force cancel each other out. In the middle situation the diagonal pairs move in opposite direction. This time the radial forces are cancelled out and the axial forces make the vehicle move sideways. At the right the vehicle will turn around it centre point.

This kind of wheels have a great advantage that with only four motors you have a four wheel drive with omnidirectional steering. But this makes the speed control much more important. The application of this thesis' AGV can be in sandy conditions, which means very low friction with the rollers. This could easily result in slippage and as can be seen in the figure, this would result in a change of direction of the AGV. Therefore are these wheels more used in indoor application with good surface circumstances.

### 3.1.2 Concept 2

The second concept is also a four wheel bases solution. Here the Swedish wheels are changed by standard wheels which can pivot around their own z-axis. All four wheels will also be driven. Figure 17 shows that turning the vehicle around it's z-axis is possible is the diagonal pair of wheels are steered at the same angle but are driving in the other direction. Of course the omnidirectional movement is a great advantage, but this applies for all three concepts. But this configuration is better for outdoor applications than the previous concept due to superior friction. A disadvantage is that four motor angles need to be monitored and controlled for accurate steering.

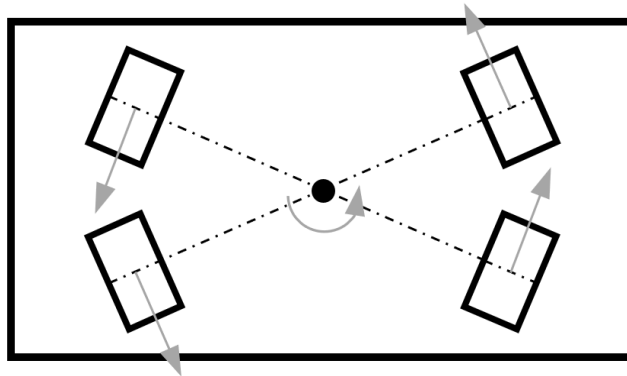


Figure 17: Four steering and driving wheels geometry

### 3.1.3 Concept 3

The last concept is a six wheel configuration with two driving wheels and four castor wheels. This will distribute the load over even more wheels, which increase also the stability of the vehicle. Yet the driving motors need to be more powerful because there are only two.

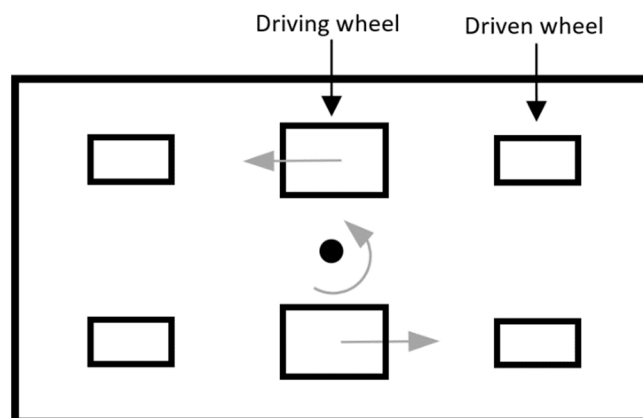


Figure 18: Six wheel configuration

The steering can be done by varying the speed and rotation of the two driving wheels. If they rotate in the same speed but in the opposite direction, the AGV will turn around its centre. In the contrary of previous two concepts, the orientation of the frame not be kept. Which means that driving forward will always have the same front end of the

frame. For some applications this can be a problem, but in general this is neglectable. The suspension of this concept also needs to be well configured, because if one of the driving wheels is not connected to the ground the vehicle will be stuck.

### 3.1.4 Overview

Table 4: Overview wheel geometry concepts

	Swedish wheels	Four wheel drive & steering	Six wheels
Easy steering	--	-	+
Omnidirectional	++	++	+
All surfaces	-	++	+

## 3.2 DRIVE

Here different concepts of how the wheels will be driven will be discussed.

### 3.2.1 Concept 1: on axle

The first concept is that the motor (probably with gearbox) will be installed on straight on the wheel with a flange. In this way the motor energy is transferred in the most efficient way, only the efficiency of the gearbox needs to be taken in to account. A disadvantage is that the width of the wheel module will increase because the motor and gearbox will come next to it.

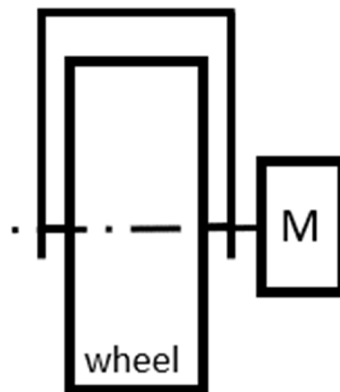


Figure 19: Drive concept, motor on axle

### 3.2.2 Concept 2: drive belt

The second concept is where the motor will transfer its energy to the wheel through a drive belt (Figure 20). The main advantage of this concept is that it is smaller than the previous concept. A disadvantage is that even though there can be used a reduction through different sizes of pulleys, there probably is still needed a reduction by a gearbox. This will decrease the efficiency of the system. Another disadvantage is that the tensioning of the belt will need to be checked and adapted after a while which increases maintenance.

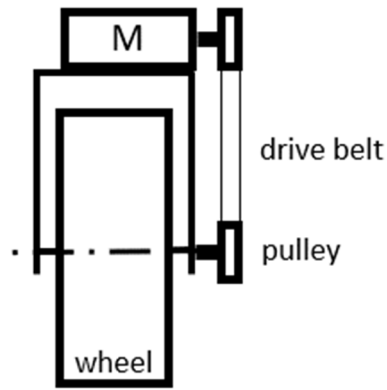


Figure 20: Drive concept, drive belt

### 3.2.3 Concept 3: mechanical chain

The 3th and last concept is one where the drive belt from the previous concept is changed by a mechanical chain (Figure 21)

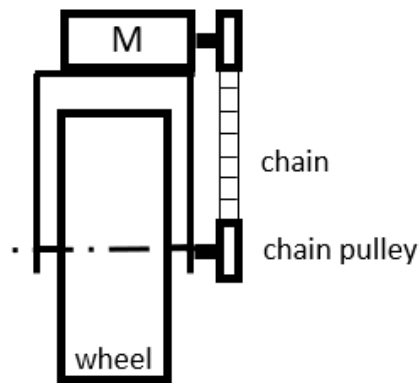


Figure 21: Drive concept, mechanical chain

The efficiency of a chain transmission is very high (around 98%). And, in comparison with the drive belt, the pre tension is less which result in less force on the axles of the pulleys. Also chains are better for harsh environments with high temperatures, dirt and moist. But they have also disadvantages, like they are more expensive and need lubrication. [24]

### 3.2.4 Overview

Table 5: Overview drive concepts

	Drive belt	On axle	Mechanical chain
Efficiency	++	-	+
Low maintenance	+	-	--
Space needed	-	+	+
Price	+	-	--



### 3.3 BACKLASH STEERING

For the steering a slewing gear and a regular spur gear are meshed together to create a speed reduction and to put the full load of the motor axis. To get a high precision steering, this gear mesh is crucial. When changing the direction of the motor it is the goal that the wheel instantly turns also, any delay will result in a non-accurate steering. Enter, the term backlash:

*“The maximum distance or angle through which any part of a mechanical system may be moved in one direction without applying appreciable force or motion to the next part in mechanical sequence.” (Bagard, 2003, p.1-8) [25]*

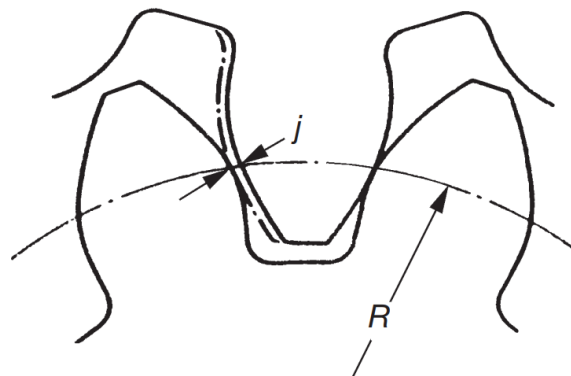


Figure 22: Backlash between gears [26]

In a perfect world where gears are made on the perfect size, they will make contact perfect on the point where the both pitch circles  $R$  collide. There are multiple origins possible for backlash, yet most are due to the machining process. In Figure 22 the upper gear has a smaller teeth than expected, if the lower gear now turns to the right, it will move a distance of  $j$  (the backlash) before it touches the upper gear again. In a certain degree backlash is preferred because it prevents gears from jamming and it leaves space for lubrication. But as said before, too much backlash is detrimental for the accuracy of the steering.

#### 3.3.1 Concept 1

The first concept for this problem is high precision gears. These gears are manufactured with very high standards and low tolerances. The advantage of this is pretty clear, low tolerance finishing results in low backlash. The disadvantage is the cost price, the more accurate something needs to be made, the more accurate the machine which makes the product needs to be and this drives the cost up. Another disadvantage is that the slewing gear can come from another manufacturer, if this is not finished with the same tolerance it will undo all the work on this gear.

### 3.3.2 Concept 2

The second concept is changing the centre distance between the gears.

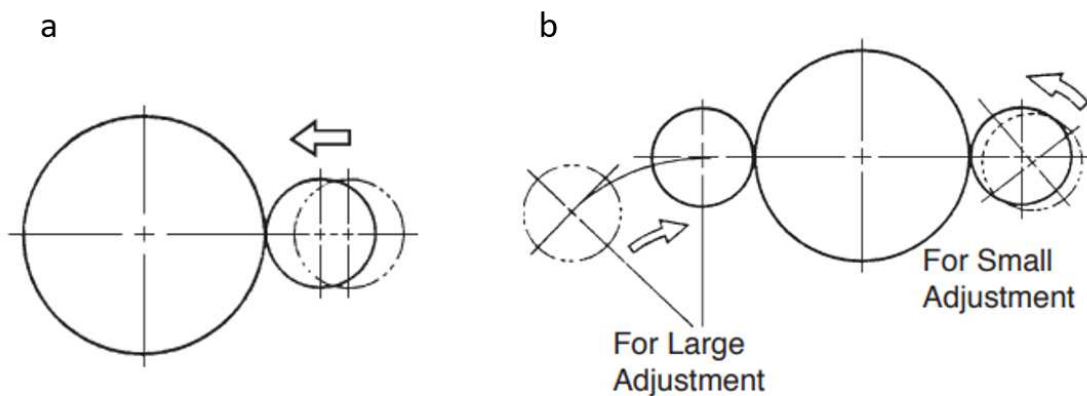


Figure 23: Backlash, adjustment of centre distance [26]

In Figure 23 two methods are shown, method a is a parallel movement and method b is a rotary movement. Both will result in the same process. Luckily in our application the steering motor will not be a big motor, which makes this a suitable solution which would be relatively easy to perform. Yet the slewing gear makes this a difficult option. The slewing gear has a positive profile shift, which results in a wider tooth width. When moving the centre distance closer to each other, this could result in undercutting of the gear. This is when the bottom of the smaller gear gets cut out by the top of the bigger gear.

### 3.3.3 Concept 3

The last concept is an anti-backlash gear. This is a gear that exist of two gear, which have the same number of teeth but can rotate from each other (Figure 24).

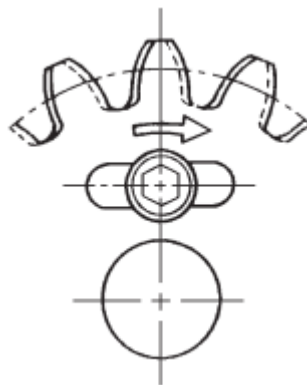


Figure 24: Backlash, anti-backlash gear [26]

To set the backlash to zero one gear of the anti-backlash gear is put against a tooth of the slewing gear, the other gear is moved to the other tooth from the same cavity. In this way if the motor changes direction, the gear is always connected to the slewing gear. A downside of this concept is that more parts are needed, thus increases the maintenance.

### 3.3.4 Overview

Table 6: Overview backlash steering

	High precision	Centre distance	Anti-backlash
Easy (not complex)	-	++	+
Maintenance	+	+	-
Price	--	++	+
Risk of undercut	++	--	+

### 3.4 SUSPENSION

Before going to the concept, there has to be taken in account one major item: the placement of the suspension. The suspension in this sketch is shown as a compression spring and a damper, but it doesn't have to be these two objects which make the suspension. The situations are sketched in Figure 25. In situation A, the frame is attached to the steering module, which steers the suspension and the driving wheel. Situation B is the other way around, where the suspension is attached to the frame and only thereafter the wheel is steered.

The advantage of situation A is that the steering motor and the steering components will be damped and therefore will endure less shocks, which is good for the life cycle and maintenance for these components. On the downside there has to be found a way to transfer the steering torque through the suspension so the wheel can turn.

Situation B on the other hand has the advantage that there is more unsprung weight, so the suspension needs to damp less weight. But it comes with the logical disadvantages that the steering module is not damped.

Considering the pros and cons, situation A is more preferable mainly because of the damper steering module. The extra weight is disadvantage that doesn't weigh through as hard.

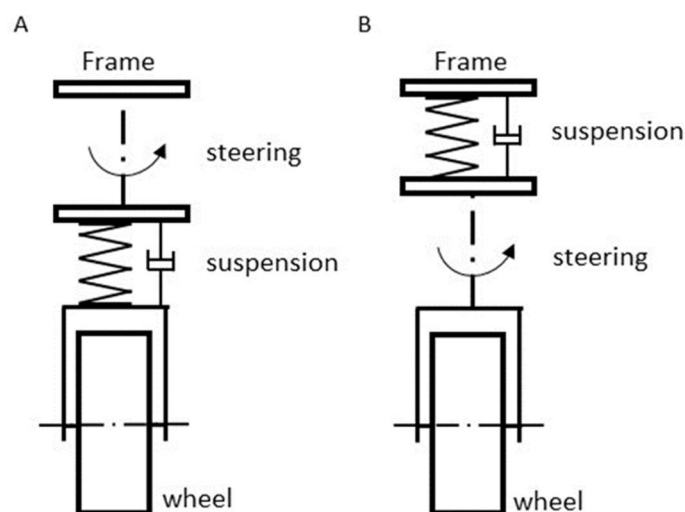


Figure 25: Suspension placement sketch

### 3.4.1 Concept 1

In the literature review some examples where already seen, under which the Thorvald II. A sketch is made to explain how this suspension works (Figure 26).

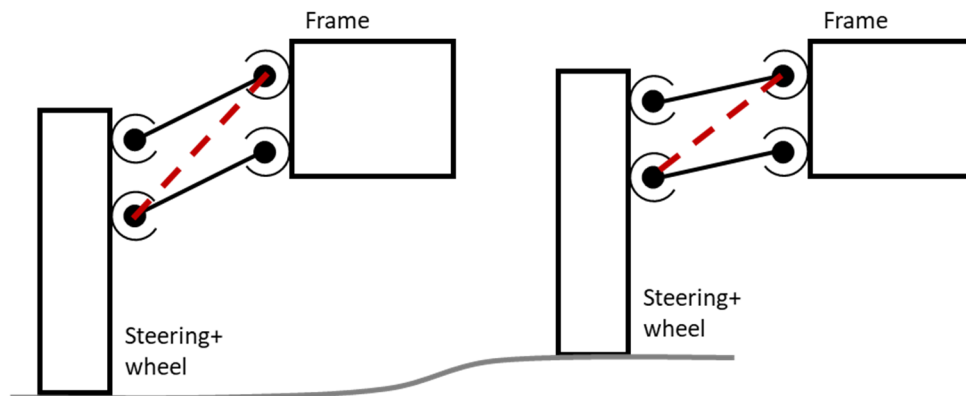


Figure 26: Suspension: concept 1

The steering module and the wheel are connected to the frame by 2 parallel bars. They are connected by hinges so that the two parts can in relation to each other. The red dotted line which goes diagonal between the hinges is the representation of the shock damper. This method is also used in some cars and is named the double wishbone suspension.

This concept it can get a big vertical movement with a small movement for the shock damper, which means you don't need a big shock damper. Yet this concept makes it that the wheels are outside of the frame and makes the vehicle wider. This is also a method of situation B, which means the steering unit is undamped.

### 3.4.2 Concept 2

The second concept is pretty straight forward, it is situation A as stated before and can be seen in Figure 25. Where the suspension is put below the steering unit. And the suspension contains of one shock absorber and one compression spring. This is one of the most basic and common suspension in the car industry which makes it hard to ignore. Due to the Ackerman steering in cars, the suspension of the AGV will be different put it works on the same principals.

A good advantage of this suspension is that the wheels are beneath the frame and don't take extra space. On the other hand, the ride height is higher because using the whole length of the compression spring is not good because the limit elasticity can be reached [27]. This means that if, for example, a vertical height of 100 mm needs to be overcome, the spring needs a least more than this 100 mm as travel. The increase in height is detrimental for the stability of the load.

### 3.4.3 Concept 3

A disadvantage of previous two concepts is that when a load is not centred, the load on each wheel and suspension will be different, this will make the vehicle lean to side where the load is the highest. To overcome this problem an air suspension or an hydropneumatics suspension can be used, which are also called self-levelling suspensions.

These suspension's characteristics are shown in the figure below. When the mass of the load increases, the spring rate will linearly increase also. This results in a static deflection for each load. The increasing spring rate is obtained by compression of air in the chamber of the air suspension.

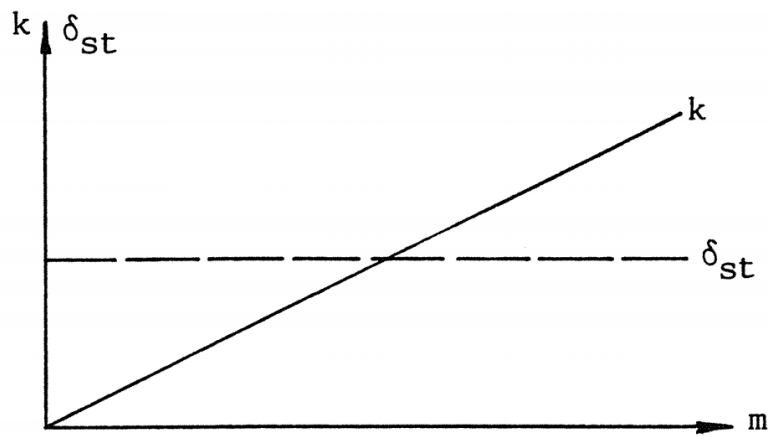


Figure 27: Spring rate of an air suspension [27]

The disadvantage of this kind of system is that there is a compressor needed to put the air on a pre-set value of pressure.

### 3.4.4 Overview

Table 7: Overview suspension concepts

	Double wishbone	Straight compr. spring	Air suspension
Easy (not complex)	+	++	-
Width	-	+	+
Damping steering	-	+	+
Self-levelling	-	-	+



## 4 DESIGN

The time of options has come to an end, in previous chapters research was done to have options for the prototype's design. Now it is time to make responsible decisions to create the best prototype possible within the set boundaries. An important factor in the design is the material choice. When picking a material there are some factors that are taking into account: weight, strength, corrosion, price and environment of application.

Table 8: Design table

Topic	Option 1	Option 2	Option 3
Type AGV	Unit	Towing	Forklift
Frame	Monobloc	Sheet metal	Profiles
Wheel geometry	Swedish wheels	Four wheel drive	Six wheels
Drive	On axle	Drive belt	Chain belt
Backlash steering	Precision gear	Adapt centre distance	Anti-backlash
Suspension	Double wishbone	Straight compression spring	Air suspension
Power supply	AMG and gel	Lithium-ion	Flooded lead-acid
Navigation system	Magnetic	LiDAR	GPS

From the start it was chosen to make a unit AGV prototype. The other types were addressed to get an overview, also at KU Leuven there will be a similar project but with a forklift AGV. For the frame there is opted for the structure with aluminium ITEM-profiles (Figure 28). The adaptability with easy assembly possibilities tipped the scale in its favour. The aluminum (3.3206.72, EN AW-6082 [AlSi0,5Mg-F25]) has yield strength of 195 N/mm<sup>2</sup> which is almost as high as regular construction steel (235 N/mm<sup>2</sup>). But the big advantage is that aluminum weighs three times less (2700 kg/m<sup>3</sup> to 8050 kg/m<sup>3</sup>). Also to be more resistant to scratching and corrosion, the profiles are natural anodized.

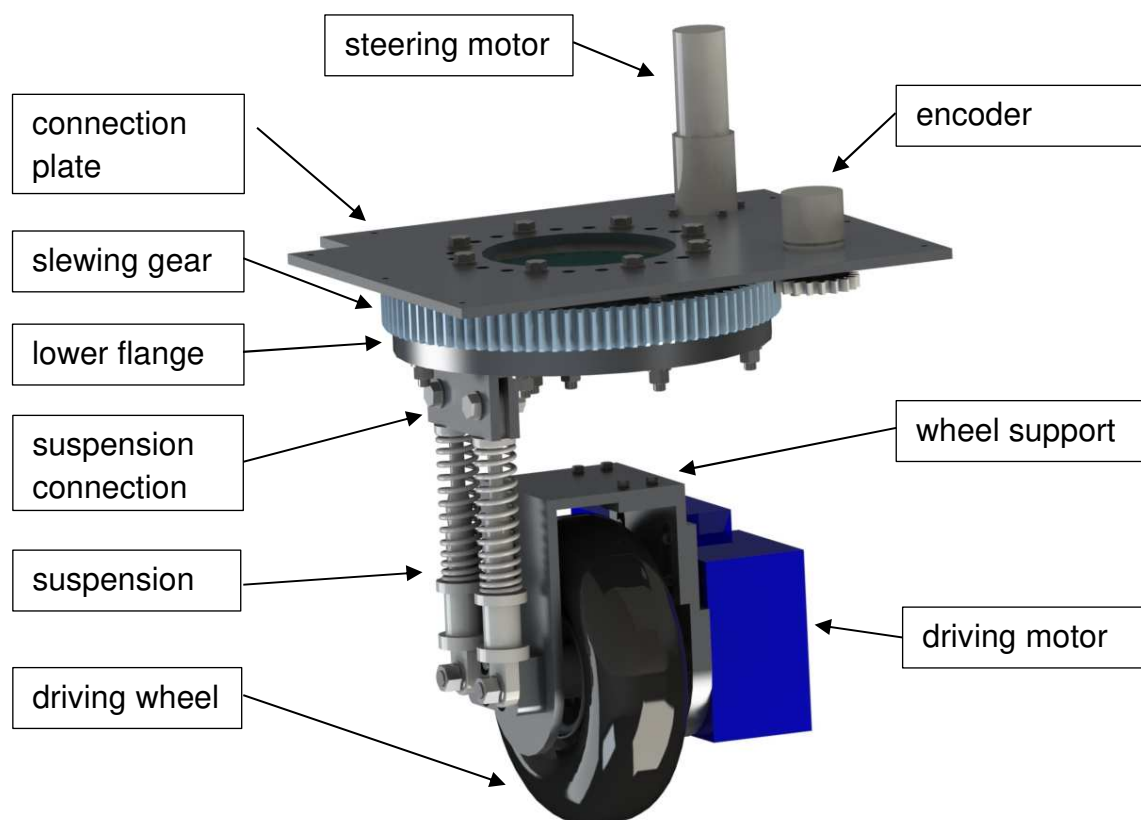


Figure 28: Frame

There is designed a wheel geometry with four driving and steered wheels. The extra effort needed for controllability doesn't outplay the benefits of having a full

omnidirectional vehicle which can operate in many environments. In the renders of the design the tire is pictured as a slick tire, so with no profile on it. This 3D-model fault. The actual tire will have the needed profile.

The solutions for the drive, backlash of the steering and suspension come all together in what is called now, the suspension unit. This is a module which is used four times, for the four driving wheels (Figure 29). The driving motor is bolted to wheel support and the motor axle is attached to a wheel flange which is attached to the wheel rim. This was concept 1 for the driving movement. The wheel support holds the wheel, driving motor and the bottom of the suspension together. The support (Figure 30) is not a fixed set of plates, the plates have slots so the motor axle can be accurately aligned. The motor attach plate and secondary L make vertical alignment possible and the Main and secondary L horizontal alignment.



*Figure 29: Suspension unit*

The whole wheel support, the connection plate, slewing gear flanges, suspension connections are made of aluminium alloys, in particular EN AW-6082-T6 [AlSi1MgMn]. This alloy had great corrosion and strength characteristics, the strength comes for annealing and warm hardening (implied by the T6 at the end) and results in tensile strength of minimum 260 N/mm<sup>2</sup>. It is not the ideal material for machining, but is still acceptable. To make an aluminium alloy more machinable, there is copper added. But, this makes the material much more corrosion sensitive. Because of this, the compromise was made to take the EN-AW 6082-T6 alloy.



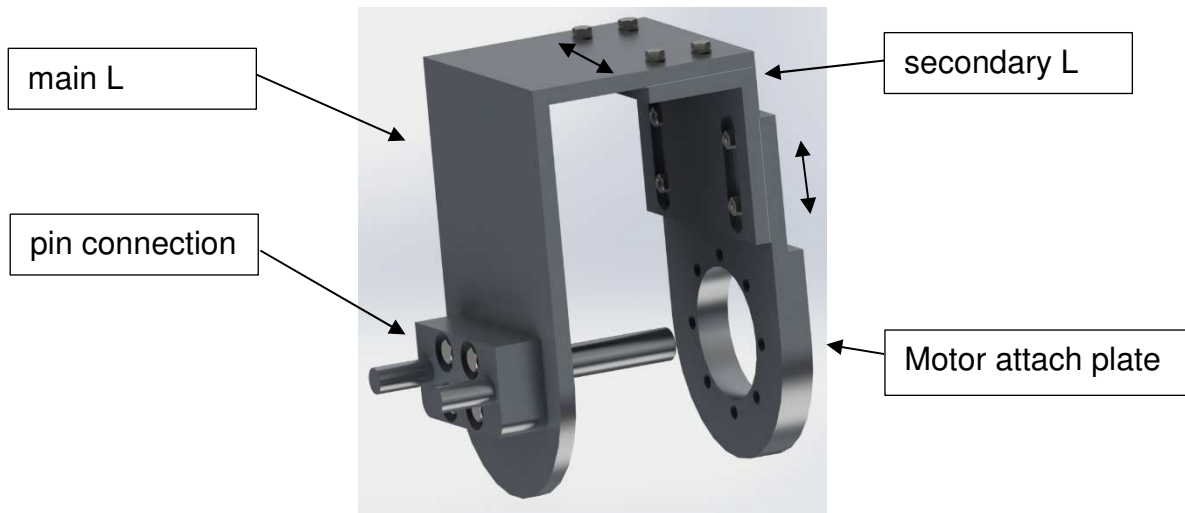


Figure 30: Wheel support

The next topic is the backlash of the steering. In Figure 31b the bottom of the suspension unit is shown, there the solution with the anti-backlash gear is situated. The gears are coloured red (inner gear) and blue (outer gear) to see better the difference. The slewing gear itself is made of steel, therefore the anti-backlash gear is also made of wear resistant steel (C45).

To explain the steering principle a little more, the steering motor drives the anti-backlash gear, which is meshed with the slewing gear. The inner ring of the slewing gear is fixed to the connection plate, the outer ring to the lower flange. On this lower flange the suspension connection is assembled, this connection is out of the centre of the slewing gear. The suspension connection is linked to the wheel support through the suspension itself. Everything is lined out so the middle of the wheel is in line with the centre of the slewing gear, so the wheel turn around its z-axis.

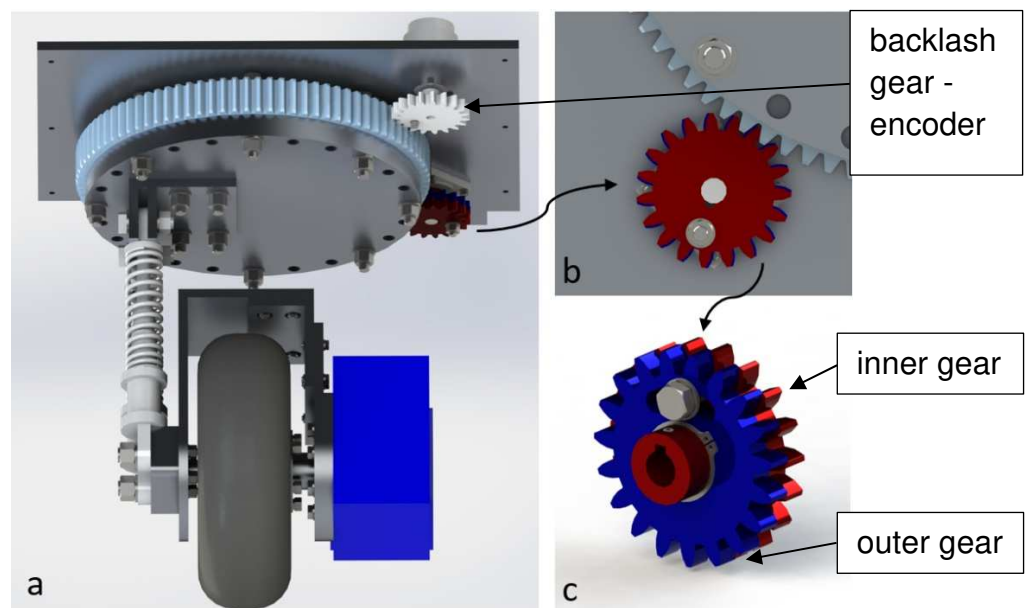
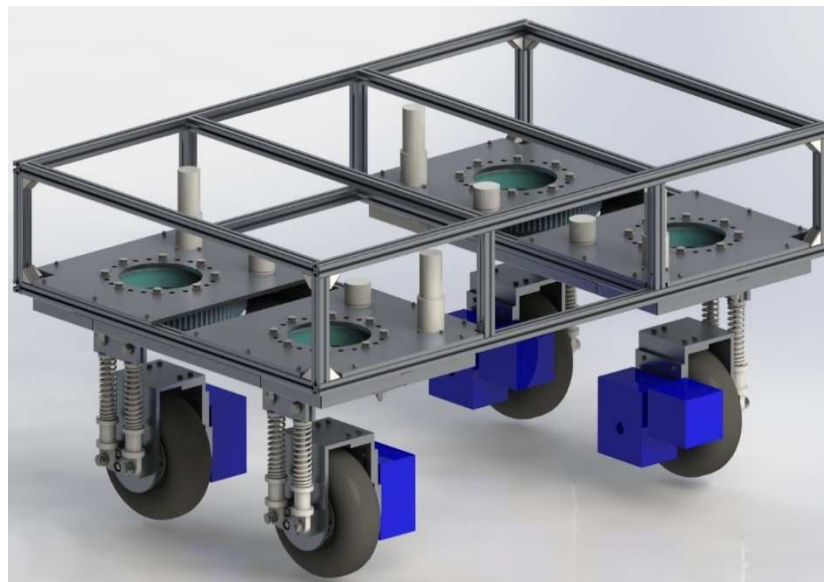


Figure 31: (a) Suspension unit, (b) bottom view mesh between slewing gear and anti-backlash gear, (c) anti-backlash gear

The positioning of the steering wheel will be measured by an encoder. The encoder is a multiturn absolute encoder. This means that the encoder knows its positioning for more than one turn, even when the voltage supply cuts out and comes back, the encoder knows its current situation. To ensure the accuracy the encoder is also provided with an anti-backlash gear (Figure 29a). But this one is made out of ABS plastic, this because the encoder cannot handle great forces.

The suspension is made on base of the principal of concept 2, where the steering unit is damped also. But instead of one shock absorber and compression spring, there are used two. This because the rotation moment has to go through the rod of the shock absorber, which is detrimental for its life cycle. To reduce this torsion on the rod, a second shock absorber is put parallel next to it. The idea came first from a mountain bike's front suspension where also two shock absorbers are used, one on each side of the wheel. But because on one side of the wheel the driving motor is already installed, this was not an option. So, a new system was made where both suspensions are put on the same side.

The connection plate is bolted to the frame, four times in the four outer corners of the frame on the lowest profiles. As a safety measure the gears will be shielded to the outside so nobody can get hurt there. The shielding plates don't have to endure big forces, therefore a lesser strong aluminium can be chosen, EN AW 5754 [AlMg3] is ideal for sheet metal bending and has very good corrosion characteristics. This all results in following vehicle (Figure 32)



*Figure 32: Frame with suspension unit*

Next on the agenda where the decisions of the more electrical parts. For the power supply Lithium-Ion batteries are chosen, mainly because of the low weight to energy ratio and the high depth of recharge percentage. The needed capacity is calculated in chapter 5.3. Although Lithium-Ion batteries are light in comparison to lead-acid batteries, doesn't mean they aren't heavy. Especially for this application where a lot of

energy is needed. When the battery needs to be recharged a person needs to pick the battery up and replace it. If the battery is located in the middle of the AGV it is bad for this persons back. Therefore a drawer is made so the battery can slide out of the AGV and person can take the battery ergonomically (Figure 33). The drawer slides are telescopic slides with a travel of 900 mm, the width of the AGV is 1 m. They are made of EN AW-6082-T6 and can hold a load of 80 kg. It has space for two batteries, one 24 V battery for the steering motor and control circuit components, the 48 V battery is for the driving motors. In front of these battery there is some available space for the control circuit elements. Because the drawer moves up to 950 mm, the cables need to be able to travel also. Therefore the cable carriers are added at both sides. The drawer door itself is made from an 10 mm acrylic plate (also known as plexiglass or PMMA) and is connected to the slides through the door connector. The door can be locked by a simple key lock.



Figure 33: (a) Top view drawer, (b) 3D-view drawer

Navigation is not the main goal of this thesis, this will be for the follow-up. Yet there has been looked into the different types and for the applications of this AGV, the best solution is probably a combination of LiDAR and GPS. The LiDAR is ideal for detection of object indoor and outdoor, and the GPS adds the advantage of location determination in big open fields. Because of the easy montage system of the ITEM-profiles these can be easily installed on the preferred places.

All sides of the frame are shielded with plexiglass plates so there can be visual control during testing. The safety devices are described in chapter 7.



## 5 CALCULATIONS

In this chapter the formulas and the methodology of most calculations are described.

### 5.1 DRIVING MOTOR

The driving motor, as the name says it, is the motor which makes the AGV move. The vehicle is four wheel drive, so there will be needed four (equal) driving motors. In the department of mechanical engineering (DEMec) at UFSCar, there are brushed motor with a worm gearbox motors available. These motors are from the company Imobras and the type number is 100502112 (Attachment A.1). So, it's important to calculate if this motor is powerful enough to drive this AGV.

As stated before, the AGV must be able to operate in different environments. For the motor calculations there is chosen for these 4 situations: empty on concrete, loaded on concrete, empty on sand and loaded on sand. These for situations can be on a flat terrain or on a slope. Throughout the calculations the impact of the different conditions will be revealed.

#### 5.1.1 Rolling resistance

First and foremost, the rolling resistance is calculated. This is the force resisting the motion when the wheel rolls on a surface.

$$F_{Rf} = m' * g * C_{rr}$$

where:  $F_{Rf}$  rolling resistance [N], on a flat surface  
 $m'$  mass on each driving tire [kg]  
 $g$  gravitational acceleration [m/s<sup>2</sup>]  
 $C_{rr}$  coefficient of rolling resistance [/]

The mass of the AGV itself is estimated at 200 kg and when loaded 700 kg (500 kg load). Because the AGV is four wheel drive, the mass per motor is the total mass divided by four. It is assumed that the total weight of the AGV is evenly distributed. An empty AGV has a mass of 50 kg per wheel and a loaded one, 175 kg.

The AGV's applications are targeted to be on earth, so the gravitational acceleration  $g$  is the standard 9,81 m/s<sup>2</sup>.

The coefficient of rolling resistance  $C_{rr}$  is the force needed to push (or tow) a wheeled vehicle forward per unit force of weight [28]. This coefficient can be found in tables for different contact surfaces (ex. railroad steel wheel on steel rail). The coefficient for rubber on concrete is 0,001 and for rubber on sand, 0,3 [28].

$C_{rr}$  can also be calculated with the formula:

$$C_{rr} = \frac{b_f}{r}$$

where:  $b_f$  arm of the rolling friction [m]  
 $r$  radius of the wheel [m]

The explanation of this formula gives us more insight of what this coefficient means. The arm of the rolling friction  $b_f$  is the horizontal distance between the centre of the wheel and the place where the reaction force  $R$  takes in (Figure 34). When driving the force in the tyre will not be distributed symmetrical. So, when a wheel is driving on sand, the wheel will have a greater contact surface with the sand than it would have when driving on concrete. The greater the deformation of the surface (wheel or road), the greater the distance of  $b$ . [29]

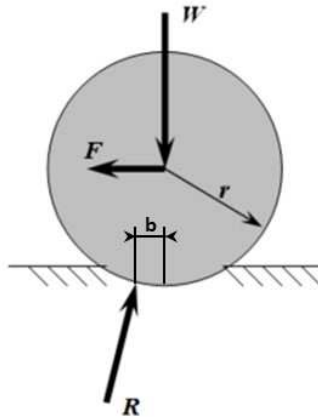


Figure 34: Rolling resistance with arm of rolling friction [28]

When driving up a slope, the resistance is higher. Therefore, to know the most challenging situation, this must also be included. The maximum slope  $\gamma$  is set on  $20^\circ$  or 36%. The formula for rolling resistance on the slope will be explained based on Figure 35.

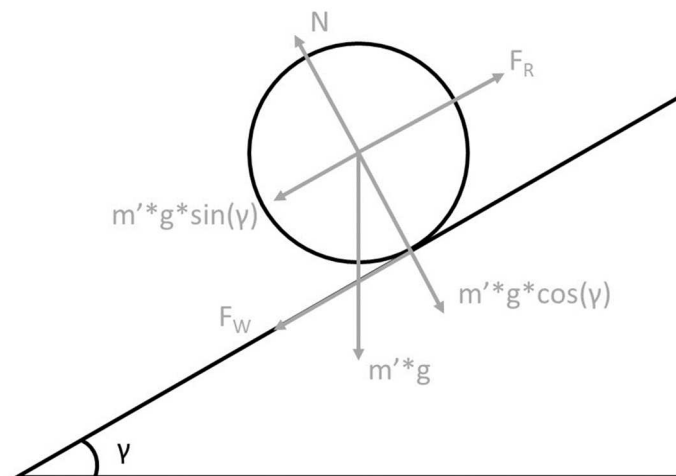


Figure 35: Forces on a slope with decomposed gravity force

The normal force stands always perpendicular on the surface. This means it isn't in the same direction of the gravity force. The normal force is now equal to  $m' * g * \cos(\gamma)$ . The force to move the object uphill does now not only need to overcome the friction force  $F_W$  but also an addition force that comes from the gravity. This force is equal to  $m' * g * \sin(\gamma)$ .

Now the rolling resistance force is calculated as followed:

$$F_R = F_W + m' * g * \sin(\gamma) = m' * g * \cos(\gamma) * C_{rr} + m' * g * \sin(\gamma)$$

This formula can be simplified, index s is added to show that it's the rolling resistance on a slope:

$$F_{RS} = m' * g * (\sin(\gamma) + C_{rr} * \cos(\gamma))$$

Table 9: Rolling resistance

		Car tires on concrete		Car tires on sand		
Driving resistance	Formula	Empty	Loaded	Empty	Loaded	Unit
Flat	$F_{Rf} = m' * g * C_{rr}$	4,91	17,17	147,15	515,03	N
On slope (20°)	$F_{RS} = m' * g * (\sin(\gamma) + C_{rr} * \cos(\gamma))$	172,37	603,30	306,04	1071,13	N

### 5.1.2 Static power

To check whether the motor is suitable for our application, the power required to overcome the rolling resistance is calculated.

$$P_S = \frac{F_F * v}{\eta}$$

where:  $P_S$  static power [W], extra index f for flat and s for slope surface  
 $v$  speed of the vehicle [m/s]  
 $\eta$  efficiency gearbox [/]

The speed of the vehicle is set on average walking speed, 5 km/h or 1,39 m/s [30]. On this speed researchers/ bystanders can follow the prototype and if necessary, avoid collisions by going away quick enough and or use the emergency stops. A higher speed would also mean a higher stopping distance.

The efficiency of the gearbox depends on a lot of things. Which kind of gears, the gear ratio, accuracy in finish, etc. The efficiency is set at 80% and will be reviewed after calculating the reduction and choosing the gearbox.

Table 10: Static power

Static power	Formula	Car tires on concrete		Car tires on sand		Unit
		Empty	Loaded	Empty	Loaded	
Flat	$P_{Sf} = \frac{F_{FF} * v}{\eta}$	8,52	29,80	255,47	894,14	W
On slope (20°)	$P_{Ss} = \frac{F_{FS} * v}{\eta}$	299,25	1047,39	531,31	1859,60	W

### 5.1.3 Dynamic power

Not only is there a power required to start the AGV, but also a power to accelerate the AGV to its required speed. This is the dynamic power and is calculated as followed:

$$P_D = \frac{m' * a * v}{\eta}$$

where:  $P_D$  dynamic power of the load [W]  
 $a$  acceleration [m/s<sup>2</sup>]

The acceleration is limited because when the acceleration is too high, the wheels would slip.

$$F_U = m * a = F_R = 4 * m' * g * \mu_0 * \cos(\gamma)$$

where:  $F_U$  peripheral force [N]  
 $F_R$  static friction force [N]  
 $\mu_0$  static friction coefficient [/]

When the peripheral force – the tangential force on the wheel as a result of the torque of the motor – is lower or equal to the friction force, the wheel doesn't slip. The peripheral force is calculated by the second law of Newton. The static friction force is calculated with its well know formula. But there are some things to be considered.

Because one motor takes only ¼ of the mass,  $m'$  is used. But on the other hand, the AGV is four wheel drive, which means there is four times a friction force. These two factors eliminate each other. The static friction coefficient of rubber on sand is nowhere to be found, so the coefficient of Polytetrafluoroethylene (Teflon) on snow is used. This is guessed to be the best comparison because it has also a very low friction coefficient, the value is 0,15. For rubber on concrete it's 0,9. [31]

Now the only unknown factor in the equation is the acceleration. This means that the maximum acceleration before the wheel start to slip can be found.



Table 11: Maximum acceleration

	Formula	Car tires on concrete		Car tires on sand		Unit
		Empty	Loaded	Empty	Loaded	
Maximum acceleration without slip	$a_p = g * \mu_0 * \cos(\gamma)$	8,3	8,3	1,38	1,38	m/s <sup>2</sup>

The maximum acceleration before the wheels start to slip when driving on loose sand is 1,38 m/s<sup>2</sup>. This would mean that the AGV be would its maximum speed of 1,39 m/s in 1 s. This acceleration is considered too fast. The acceleration will be reduced to 0,7 m/s<sup>2</sup> so the maximum speed is reached in around 2 s. In further calculations the reduced acceleration a will be used.

Table 12: Dynamic power

	Formula	Car tires on concrete		Car tires on sand		Unit
		Empty	Loaded	Empty	Loaded	
Dynamic power	$P_D = \frac{m' * a * v}{\eta}$	60,76	212,67	60,76	212,67	W

#### 5.1.4 Motor choice

The total needed power of the motor is the sum of the static and dynamic power.

Table 13: Total power

Total power	Formula	Car tires on concrete		Car tires on sand		Unit
		Empty	Loaded	Empty	Loaded	
Flat	$P_{Tf} = PSf + PD$	69,28	242,48	316,23	1106,82	W
On Slope (20°)	$P_{Ts} = PSs + PD$	360,02	1260,06	592,08	2072,27	W

The available motor at the department is not even close to being strong enough for this application. The company also doesn't provide models which come close to our needs. In the search for another company, ATO was found. The company has a wide range of industrial automation products. Which also contains high torque BLDC motors.

The situation where most power is needed, is the situation where the AGV drives on a slope of sand. But this situation is not the standard. When it occurs, it will only be briefly. The AGV will not drive 8 hours a day uphill. That is why a motor of 1,5 kW will be chosen. 1 kW looks also doable for most situations, but the maximum needed

power is double, which would result in a doubling of current.

ATO-D110BLD1500 48V is chosen. The whole datasheet is included at attachment A.3. But in Figure 36, the basic specifications, which are needed for the calculations, are shown.

#### 1.5 KW BLDC MOTOR SPECIFICATION

Model	ATO-D110BLD1500 (Click it to see more motor specs)	
Matched Controller Model	ATO-BLD100 (Click it to see more controller specs)	
Square Flange Size	110 mm	
Motor Weight	5.5 kg	
Phase	3 phase	
Number of Pole	4 pairs of poles (8 poles)	
Rated Voltage	36V DC	48V DC
Rated Current	52.08 A	39.06 A
Rated Power	1500W	
Maximum Power	4.5 kW	
Holding Torque	4.78 Nm	
Peak Torque	14.33 Nm	
Rated Speed	3000 rpm	
No-load Speed	4200 rpm	
Efficiency	85%	

Figure 36: Specifications driving motor

#### 5.1.5 Gear ratio

The nominal speed of the motor is 3000 rpm, this speed is probably too high to get a horizontal velocity of 1,39 m/s. Therefore, a reduction is needed. But with the worm gearbox of ATO, the rated speed of the BLCD motor is 2000 rpm.

$$n = \frac{v * 60}{\pi * D_w} = \frac{1.39 \frac{m}{s} * 60}{\pi * 0.3 m} = 88,42 \text{ rpm}$$

With a wheel with diameter  $D_w$  0,3 m, there are only 88,42 rpm needed. Where the motor has 2000 rpm.

$$i = \frac{n_m}{n} = \frac{2000 \text{ rpm}}{88,42 \text{ rpm}} = 22,62$$

Therefore, a reduction of 22,62 is needed. This reduction is not a standard number. The closest gearbox ratios are 20 and 25 (Figure 37)

(Note: The rated speed of BLDC motor is 2000rpm if matches the worm gearbox.)

<b>Gear Ratio</b>	7.5	10	15	20	25	30	40	50
<b>Rated Output Speed (rpm)</b>	267	200	133	100	80	67	50	40
<b>Rated Output Torque (Nm)</b>	28.7	38.2	57.3	74.5	90.7	106	133.7	124

Figure 37: Gear ratios ATO worm gearbox

Gear ratio 20 will be chosen so the AGV speed of 1,39 m/s will be reached. The 100 rpm output speed will give the vehicle a speed  $v$  of 1,57 m/s.

Now the gearbox is picked, the efficiency used before must be reviewed (chapter 4.1.2). The efficiency was set on 80%, this looks to be a good estimation. The efficiency is not given by the producer but there are plenty of producer which do provide it. With a reduction of 20, the value is between 78 and 82%. Also an independent research of Ghent University shows that the actual efficiency of worm gearboxes in this range of ratio, are close to the given efficiency [32]. Therefore, the calculation is accurate.

<b>Reduction Ratio</b>	<b>% Efficiency</b>
1/10	82~85%
1/20	78~82%
1/30	73~76%
1/40	69~75%
1/50	67~72%
1/60	65~70%

Figure 38: Efficiency worm gearbox [33]

### 5.1.6 Torque

The torque of the motor depends on the situation of the AGV, accelerating on a sandy slope will require much more torque than driving at a constant speed on a flat concrete surface. The heavy-duty situations can make the motor go above its rated torque. But this situation may not be constant, due to overheating. Therefore, the RMS torque is calculated.

$$T_{RMS} = \sqrt{\frac{T_1^2 * t_1 + T_2^2 * t_2 + T_n^2 * t_n}{t_{total}}}$$

This formula considers not only the varying amounts of torque that are needed during operation, but also the amount of time for which each torque must be produced. The  $T_{RMS}$  value is the torque that, if produced continuously, will have the same amount of motor heating as all the different torque situations in its duty cycle. [34]

Because the cycle of the AGV is not known, there will be picked one which potentially could be a cycle for this AGV.

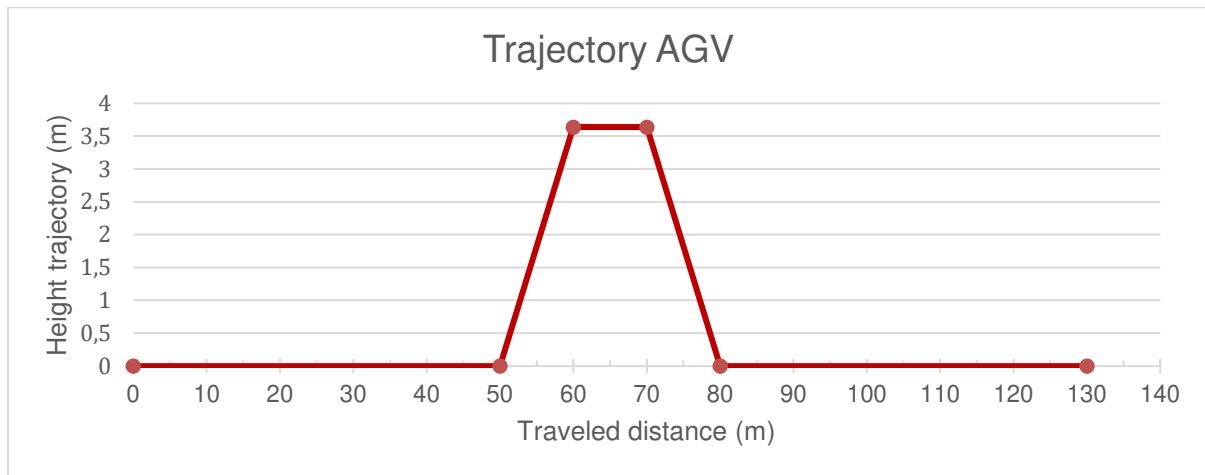


Figure 39: Trajectory AGV

The trajectory (Figure 39) goes as followed:

- 50 m driving on a flat sandy surface, loaded.
- 10 m driving on a sandy slope (20°), loaded
- 10 m driving on a flat sandy surface, loaded
- 30 s stand still, unloading
- 10 m driving on a flat sandy surface, empty
- 10 m driving on a sandy downhill slope (20°), empty
- 50 m driving on a flat sandy surface, empty
- 30 s stand still, loading

Next to the trajectory, the speed of the AGV in function of the time is important. Hereby the acceleration and constant speed is visible.

$$v = \frac{s}{t} \text{ and } a = \frac{v}{t}$$

With these standard formulas for linear motion, the v-t diagram (Figure 40) is created.

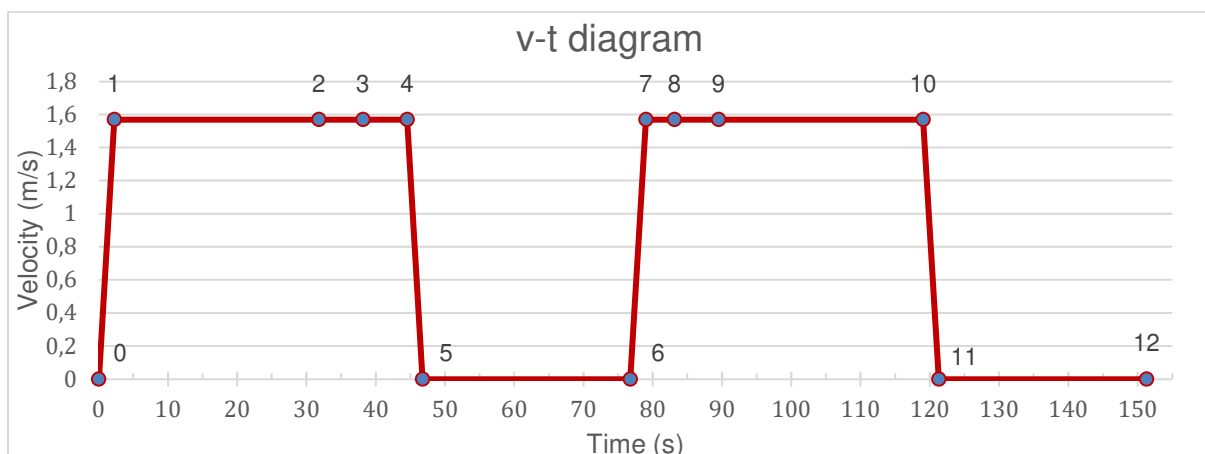


Figure 40: v-t diagram motor cycle

The numbers on the graphic are points in the cycle where the situation changes. In Table 14 the situations and the associated duration and velocity is stated.

Table 14: Cycle situations v-t

Period	Situation (on a sand surface)	Duration (s)	Time cum. (s)	Velocity (m/s)
0	start cycle	0	0	0
0 - 1	acceleration, loaded	2,24	2,24	0 - 1,57
1 - 2	constant speed, loaded	29,55	31,79	1,57
2 - 3	uphill slope, constant speed	6,37	38,16	1,57
3 - 4	constant speed loaded	6,37	44,53	1,57
4 - 5	deceleration	2,24	46,77	1,57 - 0
5 - 6	stand still	30,00	76,77	0
6 - 7	acceleration, flat, empty	2,24	79,01	0 - 1,57
7 - 8	constant speed flat, empty	4,13	83,14	1,57
8 - 9	constant speed downhill, empty	6,37	89,51	1,57
9 - 10	constant speed flat, empty	29,55	119,06	1,57
10 - 11	deceleration	2,24	121,30	0
11 - 12	stand still	30,00	151,30	0

The nominal torque of these situations are different, therefore these torques are all calculated (Table 15).

Table 15: Nominal torque driving motor

Nominal torque	Formula	Car tires on sand		Unit
		Empty	Loaded	
Flat	$T_{nom,f} = \frac{60 * P_{Tf}}{2 * \pi * n_m}$	1,22	4,27	Nm
Slope	$T_{nom,s} = \frac{60 * P_{Ts}}{2 * \pi * n_m}$	2,54	8,88	Nm

Now only the acceleration torque is needed for an empty or loaded vehicle.

To get the moment of inertia J to calculate the dynamic torque, the law of conservation of energy is used. The rotational kinetic energy needs to be equal to the translational kinetic energy. In this formulas  $\omega$  is used, this is the angular velocity.

$$E_{rot} = E_{trans} \Rightarrow \frac{1}{2} * J * \omega^2 = \frac{1}{2} * m * v_t^2$$

$$J = \frac{m' * v_t^2}{\omega^2}$$

$$\omega = \frac{n}{9,55} = \frac{100 \text{ rpm}}{9,55} = 10,47 \frac{\text{rad}}{\text{s}}$$

So, for the empty and loaded AGV the moment of inertia is respectively 1,13 kgm<sup>2</sup> and

3,93 kgm<sup>2</sup>. Due to the reduction, the moment of inertia the motor needs to overcome is much smaller. In inertia calculations the ratio is quadrated.

$$J^* = \frac{J}{i^2 * \eta}$$

At a gearbox efficiency of 90%, the inertia on the motor is 0,0035 kgm<sup>2</sup> for an empty vehicle and 0,012 kgm<sup>2</sup> for a loaded one.

The angular acceleration  $\alpha$  of the motor is the relation between the acceleration and the radius of the wheel  $r$ .

$$\alpha_m = \frac{a}{r} * i = \frac{0,7 \frac{m}{s}}{0,15 m} * 20 = 93,33 \frac{rad}{s^2}$$

The acceleration torque of the motor is the product of the angular acceleration and the moment of inertia of the motor.

$$T_{acc} = \alpha_m * J^*$$

$T_{acc}$  for an empty AGV, 0,33 Nm and for a loaded, 1,15 Nm.

So, for the RMS torque the torque for every situation needs to be calculated. For example, the first situation is accelerating on a flat sandy surface with a loaded AGV. This means a nominal torque of 4,27 Nm (found in Table 15) and an additional acceleration torque of 1,15 Nm. A total of 5,42 Nm. The torque for every situation is found in the next table.

*Table 16: total torque per situation*

Situation (on sand surface)	T (Nm)	time (s)	T <sup>2</sup> *t (Nm <sup>2</sup> s)
acceleration, loaded	5,42	2,24	65,81
constant speed flat, loaded	4,27	29,55	538,58
uphill slope, constant speed	8,88	6,37	502,14
constant speed flat, loaded	4,27	6,37	116,08
deceleration	-1,15	2,24	2,95
stand still	0,00	30,00	0,00
acceleration, flat, empty	1,55	2,24	5,37
constant speed flat, empty	1,22	4,13	6,14
constant speed downhill, empty	0,78	6,37	3,88
constant speed flat, empty	1,22	29,55	43,97
deceleration	-0,33	2,24	0,24
stand still	0,00	30,00	0,00
Total		151,30	1285,15

At last the  $T_{RMS}$  is calculated by taking the square root of the total of the last column and dividing it by the total time. This results in a RMS torque of 2,91 Nm. This torque is lower than the rated torque of the motor (Figure 41, also found in attachment A.2). Which means that the motor will not overheat during this cycle, and this motor is

suitable for this application.

SPEED-TORQUE CURVE

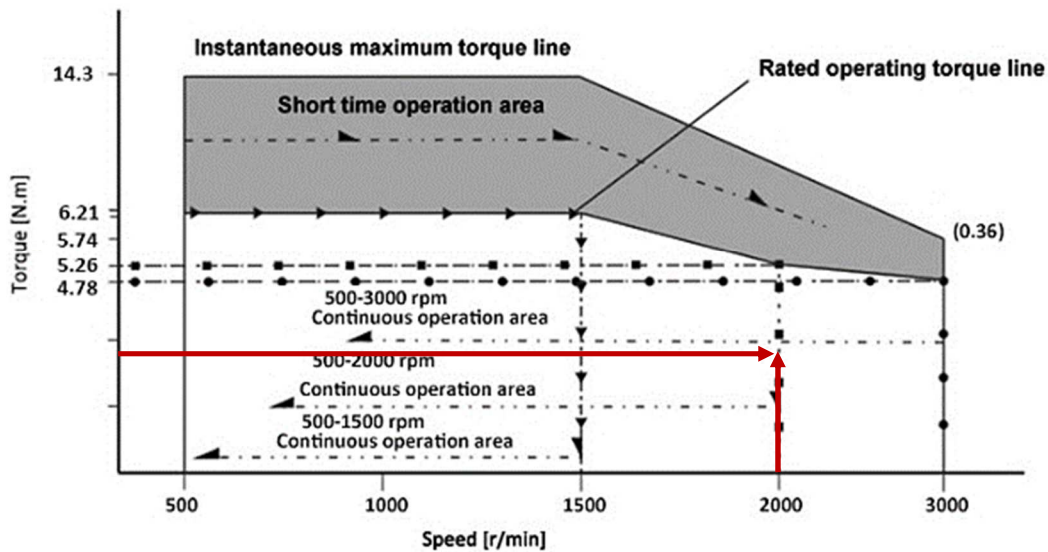


Figure 41: Speed-Torque diagram, driving motor

## 5.2 STEERING MOTOR

The four driving wheels will all be able to steer independently. Therefore, there are also four steering motors needed which will need enough power to steer in difficult circumstances. In the previous calculations it was obtained that the loaded AGV driving on a sand surface is the most challenging situation for driving. Yet for steering, the static friction coefficient is the biggest parameter. Therefore, the steering will be calculated in the situation where the loaded AGV is on a concrete surface.

### 5.2.1 Static friction resistance

Turning the wheel will be opposed by the static friction resistance.

$$F_W = m' * g * \mu_0 = 175 \text{ kg} * 9,81 \frac{\text{m}}{\text{s}^2} * 0,9 = 1545,08 \text{ N}$$

The needed torque to overcome this resistance force is calculated as followed:

$$T_W = F_W * \frac{b_w}{2} = 1545,08 \text{ N} * \frac{0,1 \text{ m}}{2} = 77,25 \text{ Nm}$$

Where  $b_w$  is the width of the tire in meters.

### 5.2.2 Static Power

To steer, the wheels will be rotated around their z-axis'. The steering angle  $\theta$  is displayed in Figure 42.

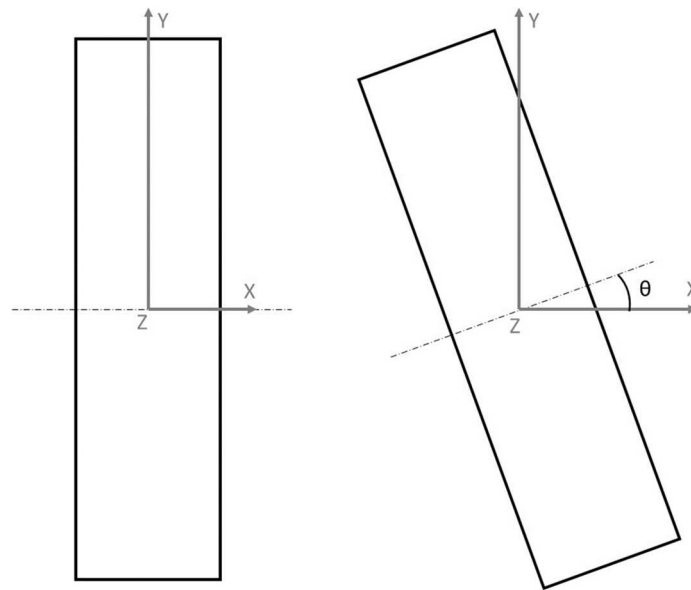


Figure 42: Steering angle wheel, top view

For this calculation an angle of  $45^\circ$  is used. This steering angle needs to be reached in one second. So, the average angular velocity  $\omega$  will be:

$$\omega = \frac{\theta}{t} = \frac{0,79 \text{ rad}}{1 \text{ s}} = 0,79 \text{ rad/s}$$

Now the needed static torque and the angular velocity are obtained, the static power can be calculated.

$$P_s = \omega * T_W = 0,79 \text{ rad/s} * 77,25 \text{ Nm} = 60,67 \text{ W}$$

### 5.2.3 Dynamic power

Due to the small time in which the angular velocity is reached, the angular acceleration  $\alpha$  will needed to be reached even faster. This time is set at 0,2 s.

$$\alpha = \frac{\omega}{t} = \frac{0,79 \text{ rad/s}}{0,2 \text{ s}} = 3,93 \text{ rad/s}^2$$

$$v_t = \omega * \frac{D_{sg}}{2} = 0,79 \text{ rad/s} * \frac{0,276 \text{ m}}{2} = 0,11 \frac{\text{m}}{\text{s}}$$

$D_{sg}$  is the outer diameter of the slewing gear, where the wheel turns around. This results in a tangential velocity  $v_t$  of 0,11 m/s.

The moment of inertia is calculated the same way as previously with the driving motor.



$$E_{rot} = E_{trans} \Rightarrow \frac{1}{2} * J * \omega^2 = \frac{1}{2} * m' * v_t^2$$

$$J = \frac{m' * v_t^2}{\omega^2} = \frac{175 \text{ kg} * 0,11^2 \frac{\text{m}}{\text{s}}}{0,79^2 \frac{\text{rad}}{\text{s}}} = 3,33 \text{ kgm}^2$$

Now all parameters for the dynamic and acceleration power are figured out. The dynamic power is the product of the angular acceleration and the moment of inertia.

$$P_d = J * \alpha = 3,33 \text{ kgm}^2 * 3,93 \frac{\text{rad}}{\text{s}^2} = 13,09 \text{ W}$$

#### 5.2.4 Motor choice

The maximum needed power of the motor is the sum of the static and dynamic power.

$$P_{max} = P_s + P_d = 60,67 \text{ W} + 13,087 \text{ W} = 73,76 \text{ W}$$

The transmission efficiency is the product of the efficiency of the slewing gear and the gear box. Both are set on 0,9 which makes the total efficiency 81% of 0,81.

$$P_n = \frac{P_s}{\eta} = \frac{43,34 \text{ W}}{0,81} = 74,91 \text{ W}$$

$$P_{tot} = \frac{P_{max}}{\eta} = \frac{52,69 \text{ W}}{0,81} = 91,06 \text{ W}$$

Again, the motors which are available at the department have not enough power. Therefore, there will be searched for other motors. Because it's easy to buy all the motors at the same company, the catalogue of ATO will be checked again. The lowest power in the BLDC series is 100 W, which is ideal for this application.

#### 100W 12V/24V BLDC MOTOR SPECIFICATION

Model	ATO-D2BLD100-30S	
Matched Controller Model	ATO-BLD750 (Click it to see the controller specs)	
Square Flange Size	60 mm	
Weight	2.5 kg	
Rated Voltage	12V DC	24V DC
Rated Current	10.42 A	5.21A
Rated Power	100 W	
Phase	3 phase	
Number of Pole	4 pairs of poles (8 poles)	
Holding Torque	0.32 Nm	
Peak Torque	0.96 Nm	
Rated Speed	3000 rpm	
No-load Speed	3300 rpm	
Efficiency	85%	

Figure 43: Specifications steering motor

### 5.2.5 Gear ratio

The chosen motor has a nominal 3000 rpm, this can be converted to an angular velocity  $\omega_n$  in rad/s.

$$3000 \text{ rpm} = \frac{3000 \text{ rpm} * 180}{\pi} \frac{\text{rad}}{\text{min}} * \frac{1}{60} = 314,14 \frac{\text{rad}}{\text{s}}$$

The ratio is the factor between the motor's angular velocity and the needed angular velocity on the wheel.

$$i = \frac{\omega_n}{\omega} = \frac{314,14 \frac{\text{rad}}{\text{s}}}{0,79 \frac{\text{rad}}{\text{s}}} = 400$$

This is the total ratio. Yet there is already a ratio due to the slewing gear. The slewing gear has 92 teeth the gear on the outer motor shaft has 19 teeth. This gives already a ratio  $i_{sg}$  of 4,84. Therefore, the needed gearbox ratio  $i_g$  on the motor will not need to be 400.

$$i_g = \frac{i}{i_{sg}} = \frac{400}{4,84} = 82,6$$

ALLOWABLE TORQUE BEING WITH GEARBOX

<b>Gear Ratio</b>	4	5	7	10	16	20	25	28	35	40	50	70	80	100
<b>Rated Output Speed (rpm)</b>	750	600	429	300	188	150	120	107	86	75	60	43	38	30
<b>Rated Output Torque (Nm)</b>	1.2	1.5	2.1	3.1	4.8	6	7.5	8.4	10.5	12	14.9	20.9	22.9	28.7
<b>Peak Output Torque (Nm)</b>	3.7	4.6	6.4	9.2	14.3	17.9	22.4	10.5	31.4	35.9	44.8	62.8	68.8	75

Figure 44: Gear ratios steering motor

The closest gearbox ratio available is 80 (Figure 44). This is acceptable.

### 5.2.6 Torque

The nominal needed torque of the motor can be calculated by dividing the nominal power by the nominal angular velocity.

$$T_n = \frac{P_n}{\omega_n} = \frac{74,91 \text{ W}}{314,14 \frac{\text{rad}}{\text{s}}} = 0,24 \text{ Nm}$$

The maximum torque occurs when accelerating (includes nominal torque), therefore the moment of inertia is calculated.

$$J^* = \frac{J}{i^2 * \eta} = \frac{3,33 \text{ kgm}^2}{400^2 * 0,81} = 2,57 * 10^{-5} \text{ kgm}^2$$

The gear ratio affects the angular acceleration of the motor.

$$\alpha_{motor} = \alpha * i = 3,93 \frac{\text{rad}}{\text{s}^2} * 400 = 1570,68 \frac{\text{rad}}{\text{s}^2}$$

The acceleration torque of the motor is the product of the angular acceleration and the moment of inertia of the motor.

$$T_{acc} = \alpha_{motor} * J^* = 1570,68 \frac{\text{rad}}{\text{s}^2} * 2,57 * 10^{-5} \text{ kgm}^2 = 0,040 \text{ Nm}$$

$$T_{tot} = T_n + T_{acc} = 0,24 \text{ Nm} + 0,040 \text{ Nm} = 0,28 \text{ Nm}$$

In Figure 43 is given that the nominal torque of the motor is 0,32 Nm, which is good enough.

### 5.3 BATTERY CAPACITY

All the motors on the AGV will be provided from energy by a battery. Bearing in mind that the driving motor requires 48 V and the steering motor 24 V, there will be at least 2 batteries needed. The capacity of a battery is expressed in Amps hour (Ah). This means that if a battery has a capacity of 10 Ah, the battery can provide energy for 1 hour if the current is 10 A.

$$Q = I * t$$

To calculate the needed capacity Q, the same cycle as the calculation of the driving motor is used. The current I and time t per situation of the cycle are the main parameters that are needed. The duration of the situations is already known. The current can be found from the motor power.

$$P_{nom} = U * I_{nom} \Rightarrow I_{nom} = \frac{P_{nom}}{U}$$

The nominal power differs at each situation. The values are previously calculated and can be found in Table 10.

Another important value for comparing batteries is the stored energy. The SI unit of energy is J, which is Ws. For high power applications like this, the number of Joules would be too big of a number, therefore it is converted to kWh. Because the charge capacity of a battery doesn't take the voltage in account, it can give a false implication. The batteries have a current limit due to overheating. So, a 10 Ah battery can most of the time not provide 10 A for 1 hour due to this limitation. This is where the energy comes in to play, because energy is power times time and takes the voltages in account.

$$E = P_{nom} * t$$

In the table below the current, needed capacity and energy for each situation are calculated.

Table 17: Battery capacity calculations

MOTOR	Distance (m)	Time (s)	Situation (all on sand)	Power (W)	Current (A)	Capacity (Ah)	Energy (kwh)
Driving	50	31,85	Loaded, flat	894,14	18,63	0,16479	0,007910
Steering		10,00		74,91	3,12	0,00867	0,000208
Driving	10	6,37	Loaded, uphill sand slope	1859,60	38,74	0,06854	0,003290
Steering		2,00		74,91	3,12	0,00173	0,000042
Driving	10	6,37	Loaded, sand, flat	894,14	18,63	0,03296	0,001582
Steering		4,00		74,91	3,12	0,00347	0,000083
	0	30,00	Unload	0,00	0,00	0,00000	0,000000
Driving	10	6,37	Empty, sand, flat	255,47	5,32	0,00942	0,000452
Steering		4,00		30,00	1,25	0,00139	0,000033
Driving	10	6,37	Empty, downhill sand slope	200,00	4,17	0,00737	0,000354
Steering		2,00		30,00	1,25	0,00069	0,000017
Driving	50	31,85	Empty, sand flat	255,47	5,32	0,04708	0,002260
Steering		10,00		30,00	1,25	0,00347	0,000083
	0	30,00	Loading	0,00	0,00	0,00000	0,000000
Total cycle time		149,17					
Total per cycle: Driving	140	89,17		4358,82	90,81	0,33	0,0158
Total per cycle: steering		36,00		314,72	13,11	0,019	0,00047

In every situation the calculation is divided by the driving motor and the steering motor. The time of steering is an assumption, when driving a distance of 50 m, the AGV will have set it direction quite well and will not have to steer constantly. But before unloading, the AGV will have to manoeuvre to the unloading spot. This will increase the time of needed steering.

Now all parameters for 1 cycle are calculated, the calculation progresses to a full AGV working up to 8 hours a day. 8 hours a day are 28800 seconds. The total cycle takes 149,17 s, which results in 193 cycles a day. The vehicle is four wheel drive, which makes that all calculations need to be multiplied by four. Also, the motor power, which is used in the calculations, is the mechanical output power. The motors have an efficiency of 85 %, which makes the electrical input higher.

$$Q_{total} = Q_{per\ cycle,per\ wheel} * 193\ cycles * 4\ wheels * 0,85$$

This results in:

*Table 18: Total capacity and energy required for batteries*

	Capacity (Ah)	Energy (kwh)
Total for driving	299,97	14,40
Total for steering	17,65	0,42

The battery for driving needs to have a capacity of 300 Ah to drive the AGV for a day (8 hours). The battery for the steering motor needs only 18 Ah. The driving battery needs a really high capacity, which on this voltage, not a lot of batteries have.

48 V batteries are less common than 24 V or 12 V batteries for this amount of capacity. But 48 V are made more compact than two times 24 V batteries, this because there is only one casing and energy management system. Both options are looked into when choosing the right battery/batteries.

The chosen battery for the driving motors is a Lithium-Ion battery 48V – 105Ah – 5.38kWh from the company Powertech (attachment A.7). This battery has only a third of the calculated capacity. So, if this cycle occurs, the battery will be needed to switched 2 times. Yet this calculation was made for a sand track with a steep hill. So probably in most applications the battery will not be as heavily loaded and will not be needed to charge as much. Also in the continuation of this project there should be looked into regenerative braking, which will recharge the battery during braking. Due to dimension restrictions a second parallel battery is not possible.

For the battery which will provide energy for the steering, there will be searched for a bigger capacity than 15 Ah. This because the drives, PLC and sensors also will be connected to this battery. Therefore the Lithium-Ion Battery 24V – 50Ah – 1.28kWh – PowerBrick+ from the same company Powertech is chosen (attachment A.8).

#### 5.4 SUSPENSION

The objective of a suspension is to make the ride as comfortable and as efficient as possible. Yet these two parameters conflict with each other. Finding the right suspension is all about compromising [27]. The AGV has different operation field, it will need to ride as good as possible in all the different situations.

A vehicle's suspension can be simplified to tree main parts. The mass of the vehicle, the suspension itself and the unsprung mass (Figure 45).

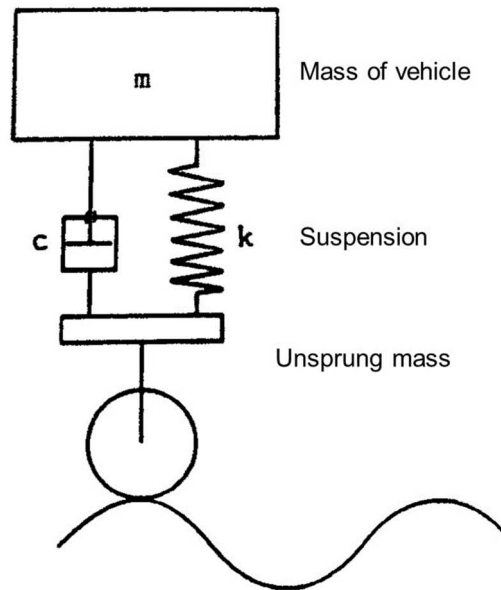


Figure 45: Schematic diagram of a vehicle's suspension [27]

The mass of the vehicle is the total mass which will be damped from the vibrations. The suspension consists out of two parts: a compression spring and a damper. Beneath the suspension there is still a mass which will not be damped from vibrations, this is called the unsprung mass.

The AGV has a mass of 650 kg, when loaded. This means that there is an unsprung mass of 50 kg. Calculating the stiffness and damping will be done per wheel. So, the mass per wheel is 162,5 kg. The preserved value of the deflection for a loaded AGV is 0,05m.

When excluding the damper, the system's equation of motion is as followed. With  $k$  being the stiffness of the spring and  $x$  the deflection of the mass out of the state of equilibrium.

$$m\ddot{x} + kx = 0$$

The solution of this equation, when solving to  $x$ , is:

$$x(t) = X * \cos(\omega_0 t - \vartheta)$$

This gives a harmonic sinusoidally equation where the amplitude  $X$  and the phase angle  $\theta$  are integral constants. And where the natural oscillation  $\omega_0$  is found as followed.

$$\omega_0 = \sqrt{\frac{k}{m}}$$

The natural frequency  $f_0$  follows from:

$$f_0 = \frac{\omega_0}{2\pi} \quad \Rightarrow \quad f_0 = \frac{1}{2\pi} * \sqrt{\frac{k}{m}}$$

Hooke's law states that the displacement of the spring is linearly proportional to the applied force.

$$F = -kx \quad \Rightarrow \quad \frac{k}{m} = \frac{g}{x}$$

Last two equations can be put together so the natural frequency is written in function of the displacement. The displacement  $x$  will from this point on be written as  $\delta_{st}$  because this is the static displacement.

$$f_0 = \frac{0,5}{\sqrt{\delta_{st}}} = \frac{0,5}{\sqrt{0,05 \text{ m}}} = 2,24 \text{ Hz}$$

The natural frequency for the AGV with a static displacement of 0,05m is 2,24 Hz. By manipulating the formula for natural frequency, the stiffness of the spring can be found. The suspension on each wheel contains 2 shock absorbers which stand parallel of each other. Therefore, the spring stiffness will be divided by two.

$$k = \frac{(2 * \pi * f_0)^2 * m}{2} = \frac{(2 * \pi * 2,24 \text{ Hz})^2 * 162,5 \text{ kg}}{2} = 16038,11 \frac{\text{N}}{\text{m}}$$

When implementing a damping in the system, the system's equation changes.

$$kx + c\dot{x} + m\ddot{x} = 0$$

Where  $c$  is the damping coefficient in  $\frac{\text{Ns}}{\text{m}}$ .

When solving the system's equation, there are again some parameters found. The natural oscillation  $\omega_0$  stays the same as found before. A new term is the critical damping coefficient  $c_c$  also in  $\frac{\text{Ns}}{\text{m}}$ .

$$c_c = 2 * \sqrt{k * m} = 2 * \sqrt{32076,21 \frac{\text{N}}{\text{m}} * 162,5 \text{ kg}} = 4566,13 \frac{\text{Ns}}{\text{m}}$$

The ratio between the actual damping and the critical damping is called the damping ratio  $D$ .

$$D = \frac{c}{c_c}$$

The behaviour of a system is in function of the damping ratio. There are 3 types of damping (Figure 46).

- Overdamped  $D > 1$ : After a disturbance of the system the mass return exponentially to the state of equilibrium after the disturbance is gone.
- Critical damped  $D = 1$ : The system will return to its original state exponentially but at the fastest way as possible after a disturbance of the state of equilibrium.
- Underdamped  $D < 1$ : The oscillation will decay exponential combined with an oscillatory portion.

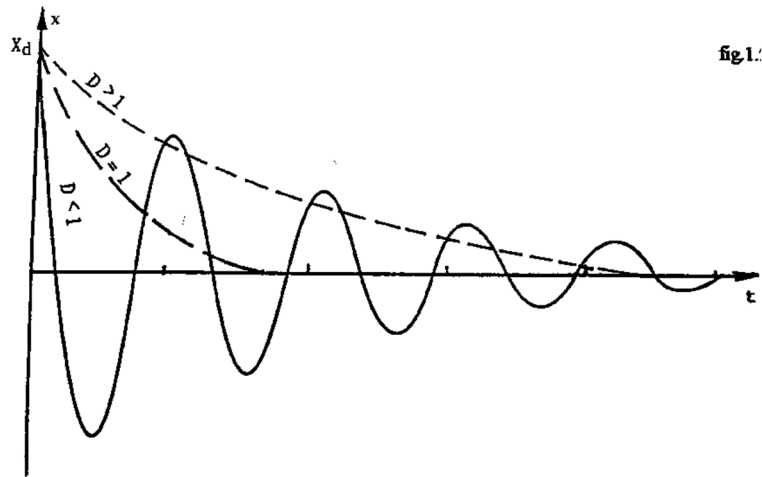


Figure 46: Influence of different damping ratio's [27]

This is where the compromising kicks in. The choice of the right damping ratio is an estimated guess. There is not a ratio which is good for every situation. For the AGV there is a very big difference in weight between loaded and empty. The calculations until now are done with the loaded weight. This is because it is chosen that comfort during the loaded ride is prioritized.

$$D = \frac{c}{2 * \sqrt{k * m}}$$

From the formula of the damping ratio there can be seen that the ratio increases if the mass decreases. So, imagen the calculation where made with an empty AGV, then the load would make the damping ratio decrease a lot. Which results in a very undamped system. This would mean a lot of oscillations and an unstable platform. Therefore, everything is calculated with load. The downside of this is the opposite, when driving empty, the damping will be high so there is a stiff suspension. But because of the lower weight, this is less important.

The damping ratio of a regular car is mostly taken at 0,25 à 0,3 and for a sportscar around 1. This because traction is very important for a sportscar and for a regular can, comfort is prioritized [27]. For the AGV it's important that all four wheels keep connected to the ground but also that load doesn't bounce off the AGV. Therefore, a model of the AGV will be made in ABAQUS where the reaction of the AGV on different damping ratios can be monitored. Table 19 shows the different damping coefficients for different ratios. Because the suspension on each wheel contains two shock dampers, the damping coefficient is divided by two.

Table 19: Damping coefficient for different damping ratios

D	c (Ns/m)	D	c (Ns/m)
0,2	456,61	0,7	1598,15
0,3	684,92	0,8	1826,45
0,4	913,23	0,9	2054,76
0,5	1141,53	1	2283,06
0,6	1369,84		



## 6 DYNAMIC SIMULATION

With the dynamic simulation the answers to two questions are searched: Is the frame with ITEM-profiles strong enough to hold the load and endure the dynamic responses? And what is the best damping coefficient for the suspension?

### 6.1 STRUCTURE STATIC MODEL

The model is made in the Finite Elements Method (FEM) based programme Abaqus CAE. The goal in FEM is to get the most accurate result in the lowest possible time. This can be done by making simplifications to the model, unnecessary parts lead to additional calculation time.

The frame of the vehicle is directly imported in an IGES structure from SolidWorks. In this way the frame can be made out of 2D-beam elements. These elements are ideal for elements: where the length is much greater than the width or depth, with constant cross-sectional properties, which must be able to transfer moments and which must be able to handle a load distributed across its length [35]. If a 3D-solid model was used, there would be result over the whole cross-section, which is certainly not necessary.

But to get the right bending results, there still has to be added a cross-section of the profiles. Because the ITEM-profiles aren't standard profiles, they have to be added in a different way. Abaqus has a feature 'generalized profiles' where you can add profiles by adding some parameters (Figure 47). The parameters of the ITEM-profile are found in the product sheet of the profile (attachment A.3). All parameters are put in SI-units.

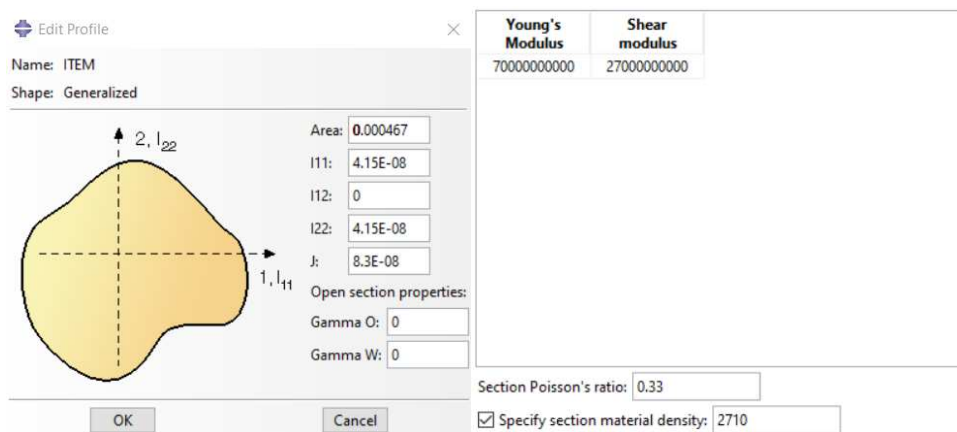


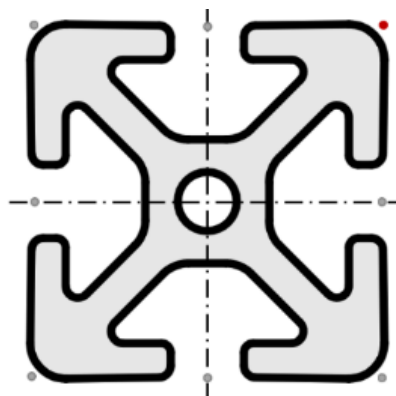
Figure 47: Adding generalized profile in Abaqus

Where:

Area	Cross-section	0,000467	m <sup>2</sup>
I11	Area moment of inertia around x-axis	4,15E-08	m <sup>4</sup>
I12	Product moment of area	0,41E-08	m <sup>4</sup>
I22	Area moment of inertia around y-axis	4,15E-08	m <sup>4</sup>
J	Polar moment of area	8,3E-08	m <sup>4</sup>

E	Young's modulus	70E09	N/m <sup>2</sup>
G	Shear modulus	27E09	N/m <sup>2</sup>
$\nu$	Poisson ratio	0,33	[/]
$\rho$	Density	2710	kg/m <sup>2</sup>

Stress is calculated in the elements, displacement in the nodes. But because a generalized profile is used, the program doesn't know the geometry of the beam. This way it doesn't know where to calculate the stress. Therefore calculation points need to be defined. The stress is always the biggest the furthest from the neutral line, this is why mostly the points on the edges of the profile are used. Yet, as seen on Figure 48, these points don't fall on the profile edge because of its geometry. But for the simulation still a corner point will be picked (red dot with coordinates 0,015;0,015).



*Figure 48: Cross-section of ITEM-profile with stress calculation points*

A 'step' is made in the model, this is the timestamp and sort of simulation where everything is put. First step is a static step from 1 second. After that the constraints and boundary conditions are put on the model. To simulate the connection plate of the suspension unit (see Figure 29), a constraint is used. The rotation centre of the wheel and slewing gear is used as a reference point (RP), each suspension unit has one (RP-1 to RP-4, Figure 49). The RP is constrained to the profiles where the connection plate actually is bolted to. In this way we simulate that the profiles are connected to the connection plate without actually having to simulate the plate. Next step is adding the suspension, this is done by connecting the RP's to the ground with a spring and dashpot. The ground is here simulated as fixed RP's (RP-5 to RP-8). For the simulation only one suspension per wheel is used. Therefore the damping ratio's from Table 19 in chapter 0 are doubled.

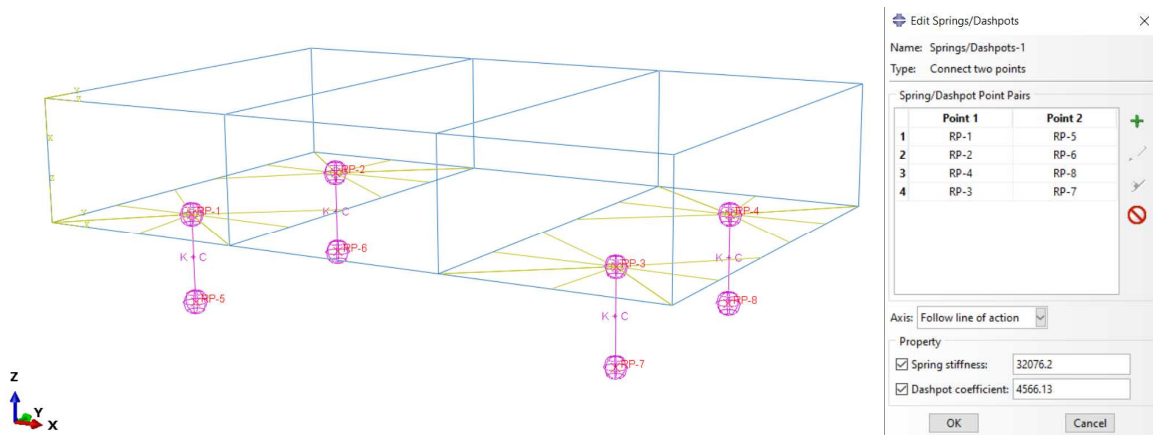


Figure 49: Model with constraints, spring and dashpot

Thereafter the boundary conditions are added. The AGV has only 4 points of contact to the ground, the four wheels. These points (RP-5 to RP-8) can't move up or down (z-direction). To keep the model static, the x and y direction are also set fixed.

The weight of the frame and the extra components, like batteries, shielding plates, suspension unit (the undamped mass) is put as a concentrated force on the RP's of the connection plate (RP-1 to RP-4). In this way the mass is divided equally over the bottom profiles of the frame. This load is -400N in the z-direction (160 kg unsprung mass). The spring stiffness and damping coefficient are calculated with a loaded vehicle, which mean the load also needs to be added. This is done by a line load all over the top profiles of the frame (Figure 50). The load is 500 kg ( 5000 N), and the length of all profiles on the top is 7 m. This results in a line load of 714,3 N.

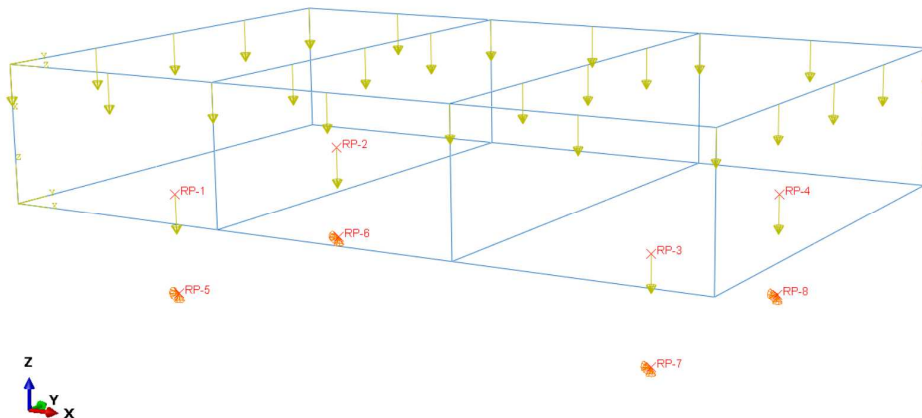


Figure 50: Load and boundary conditions

The final part is meshing the frame. For the element type, B31: a 2-node linear beam in space, is chosen. Using Quadratic elements would be overkill for this application, where only the stress in the frame is needed. The size of the elements is set at 0,01 m, which results in 1580 elements in total.

With this set-up the model is just a static simulation where the stress in the frame can be simulated and the static displacement of the suspension. But the most important part of this modelling is making a dynamic model. Therefore some adaptations need to

be made. To see how the suspension react, a kind of situation needs to be created.

Situation:

- Vehicle drives over a bump of 0,05 m.
- Load removed at the end.

First an extra step needs to be made, an implicit dynamic step. This step will be 5 seconds so everything can be monitored and the time increments are set on 0,005 s which will allow to get the values of quick oscillations.

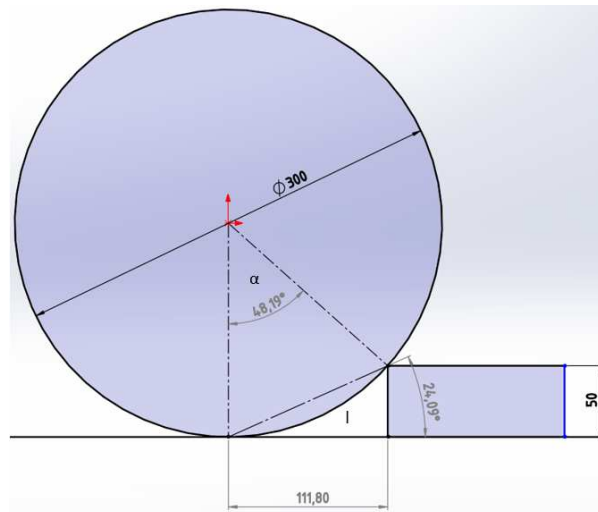


Figure 51: Sketch bump

In Figure 51 a sketch of the wheel with the bump is shown, dimensions are in mm. The time in which the wheel goes over the bump has to be known. The angle between the corner of the bump and where the wheel touches the ground allows this ( $\alpha$ ).

$$\frac{\alpha}{\text{full circle}} = \frac{\text{length arc sector}}{\text{circumference}} \Rightarrow \frac{48,19^\circ}{360^\circ} = \frac{l}{0,3 * \pi}$$

Which gives a length of 0,126 m for the arc of the sector. This distance has to be traveled to overcome the bump. With a speed of 1,57 m/s this will be done in 0,078 s. If the front wheels go over the bump, the back wheels will probably too. The wheels have a distance of 1,04 m between them, again with a speed of 1,57 m/s, results this in a time of 0,66 s between when the wheels hitting the bump.

So, now the model has to be modified to this parameters. Instead of fully fixing the wheels, the z-axis will be set flexible in the boundary conditions. In Table 20 the time and displacement is shown. So the front wheels (RP-5 and RP-6) will starting to go up at 0,92 s in the dynamic step (this is 1,92 in total time, 1 s static added).

*Table 20: Amplitudes wheels on bump*

Front wheels		Back wheels	
Time (s)	Displacement (m)	Time (s)	Displacement (m)
0	0	0	0
0,92	0	1,58	0
1	0,05	1,66	0,05
2,92	0,05	3,58	0,05
3	0	3,66	0

At last the load has to be removed. This can be done by modifying the line load in the dynamic step, again with using an amplitude. The load will be removed at 4,5 s in the dynamic step (5,5 s total time) and it is set to be done in 0,01 s. Which is very fast, but it will show even better the effect of the damping.

For finding the right suspension every damping ratio from 0,1 to 1 will be run through. The damping coefficients for a one suspension per wheel are:

*Table 21: Damping coefficients for dynamic simulation*

D	$c_e$ (Ns/m)	D	$c_e$ (Ns/m)
0,1	456,613	0,6	2739,68
0,2	913,2259	0,7	3196,29
0,3	1369,839	0,8	3652,90
0,4	1826,452	0,9	4109,52
0,5	2283,065	1	4566,13

## 6.2 RESULTS

So the first objective is finding the maximum stress in the frame, to see if the 30x30 ITEM-profiles are strong enough to hold the load in dynamic circumstances. The spring stiffness and damping coefficient are respectively set at: 32076,21 N/m and 456,61 Ns/m ( $D=0,1$ ).

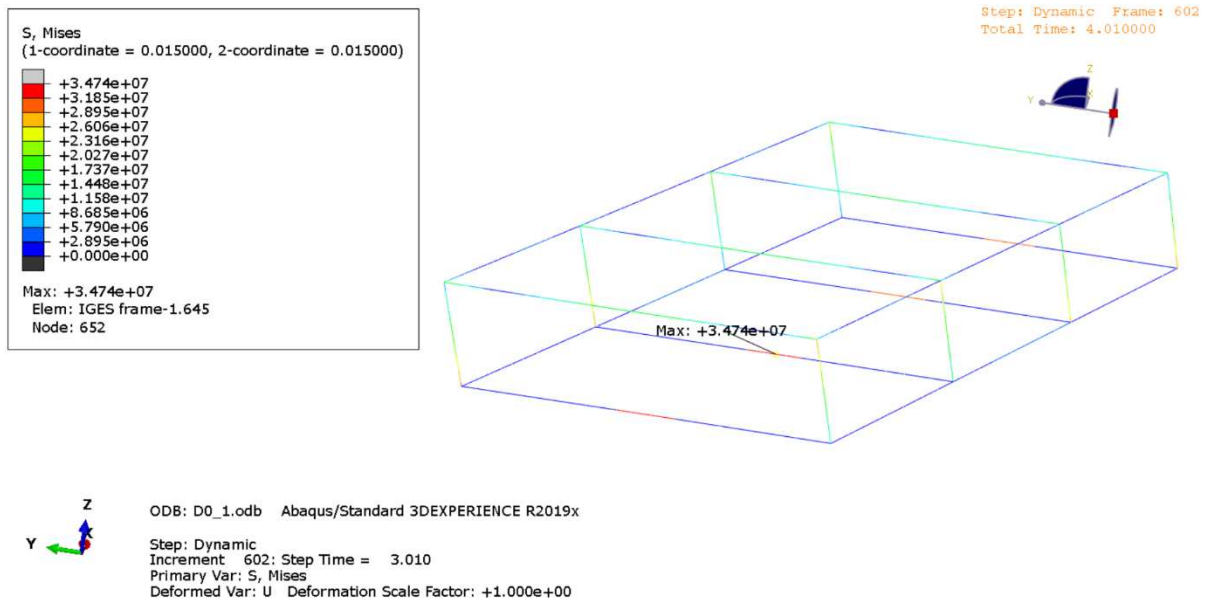


Figure 52: Maximum stress in frame with  $D=0,1$

It is found that the maximum stress Von Mises (SVM) in the frame is  $3,47E07 \text{ N/m}^2$ , which is  $34,7 \text{ N/mm}^2$ . This happens at  $4,01 \text{ s}$  in the cycle, the moment that the front wheels hit the ground again after leaving the bump. The location of the maximum stress is in the middle of the lower profiles as seen in Figure 52. This makes sense because the outside of this profile is constrained by the connection plate and thus has very low stress. SVM is a multidimensional stress which is calculated by a combination of one dimensional normal and shear stresses. [36] If the SVM is lower than the yield strength, the material will not deform plastic. The minimum yield strength of the profiles is  $195 \text{ N/mm}^2$ , but it is a dynamic load, a safety factor of four is used [37]. This means the stress in the profile may not exceed  $48,88 \text{ N/mm}^2$  or  $4.88E07 \text{ N/m}$ .

When applying all the loads, before any dynamic step, the maximum displacement of the frame is  $51,96 \text{ mm}$  (Figure 53). This maximum displacement is found on the middle top cross beams, here is the load the biggest and the unsupported length of the beam the longest. But this is not the deformation of the frame alone, the displacement of the spring is also included. The deformation of the spring is  $50,44 \text{ mm}$  (suspension was calculated at a displacement of  $50 \text{ mm}$ ), this result is a maximum deformation of the frame of  $1,52 \text{ mm}$ .

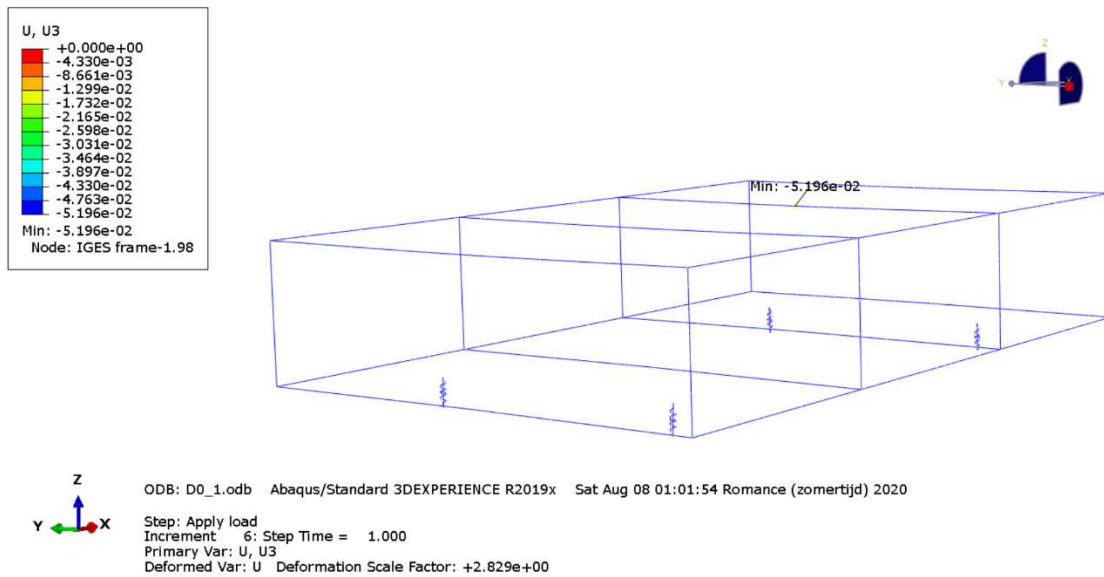


Figure 53: Displacement frame in static step

Next on the list is putting the stress and displacement on the same graph to see how they influence each other (Figure 54). The black line is the stress in the element the maximum stress was measured (element 644), the displacement is measured in RP-2 (red line) and RP-4 (blue line). In this way the effect of only the spring is shown.

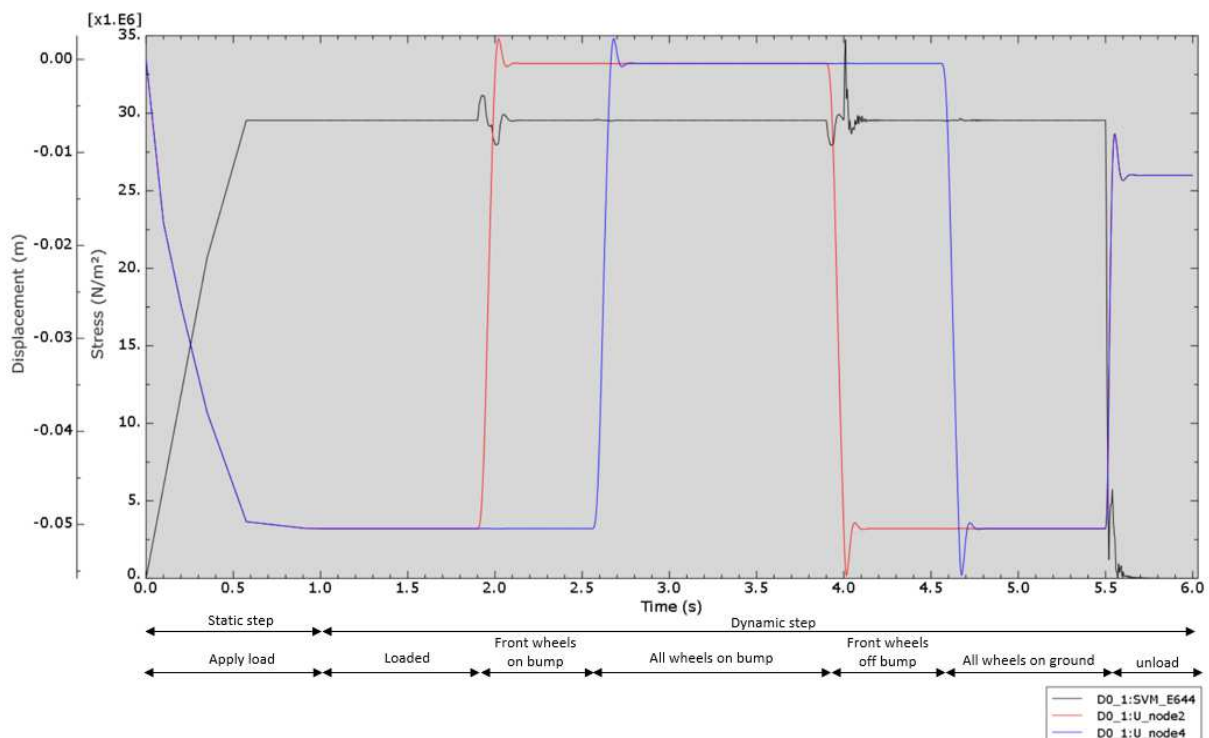


Figure 54: Stress in frame and displacement from compression spring with  $D=0,1$

The first second is as stated before, just applying the load. The vehicle will get lower to -0,05 m and the stress will rise to 2,95E07 N/m<sup>2</sup>. At 1,9 s the front wheels will hit the

bump and the wheels will start to go upwards, this give a small peak in the stress curve. The suspension will have a small amount of overshoot of 2,69 mm, detail in Figure 55, and it will take 0,22 s to get stabilized.

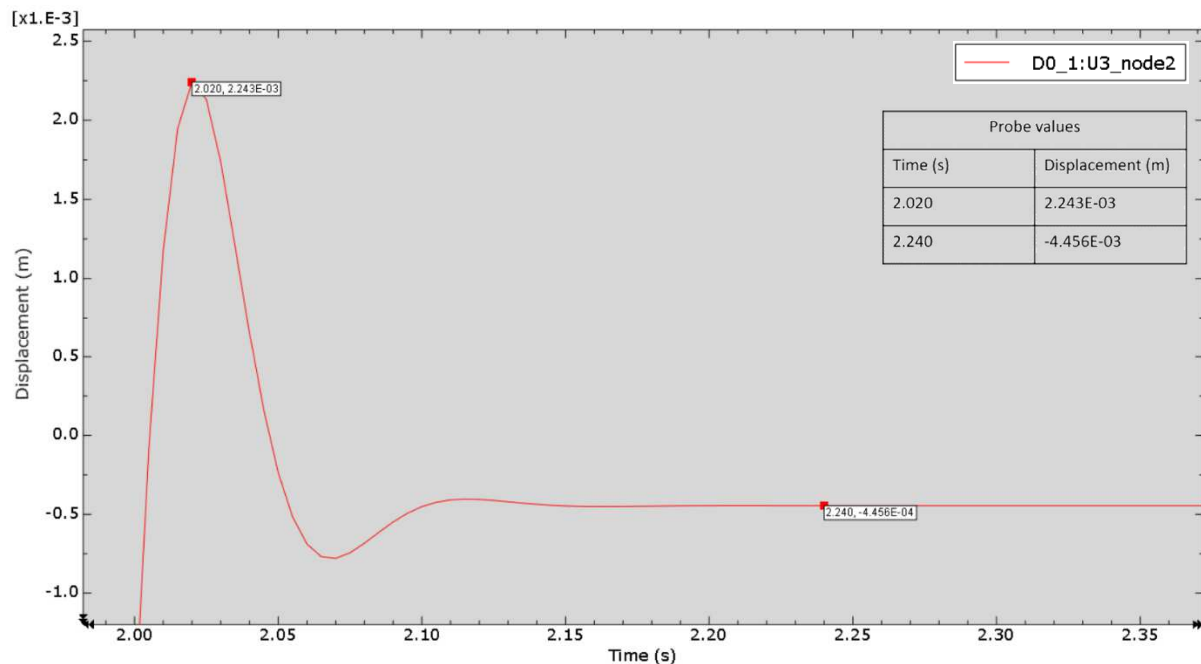


Figure 55: Detail overshoot front suspension with  $D=0.1$

Next is the back wheels that hit the bump, the same will happen to the back wheels suspension. This doesn't affect the stress curve of element 644 much because it is in a profile of the front side of the vehicle. At 3,9 s the front wheels of the vehicle have reached the end of the bump and will go down to the ground again. This is where the big oscillation and peak in the stress curve is seen. The peak is the maximum stress in the frame, as simulated in Figure 52. It takes 0,4 s until the stress is stabilized with the wheel back on the ground.

At last at 5,5 s the load is removed, which makes the stress in the frame fall to only 182 N/m<sup>2</sup>. The release of load will let the coil spring expand and the frame of the vehicle will go up. Because of the very fast unload, the overshoot of the spring is bigger, 2,05 mm.

Next the different damping ratios are being applied to see which effect they have on the stress and the overshoot of the compression spring. In Figure 56 the stresses are plotted, the plot is zoomed in on where the peak stress is. With all the oscillations it is difficult to see what happens, but it is obvious that the peak stress for the highest damping ratio is higher than the peak stress of the lowest damping ratio. Even though the peak stress is higher, it still doesn't exceed the maximum allowed stress.



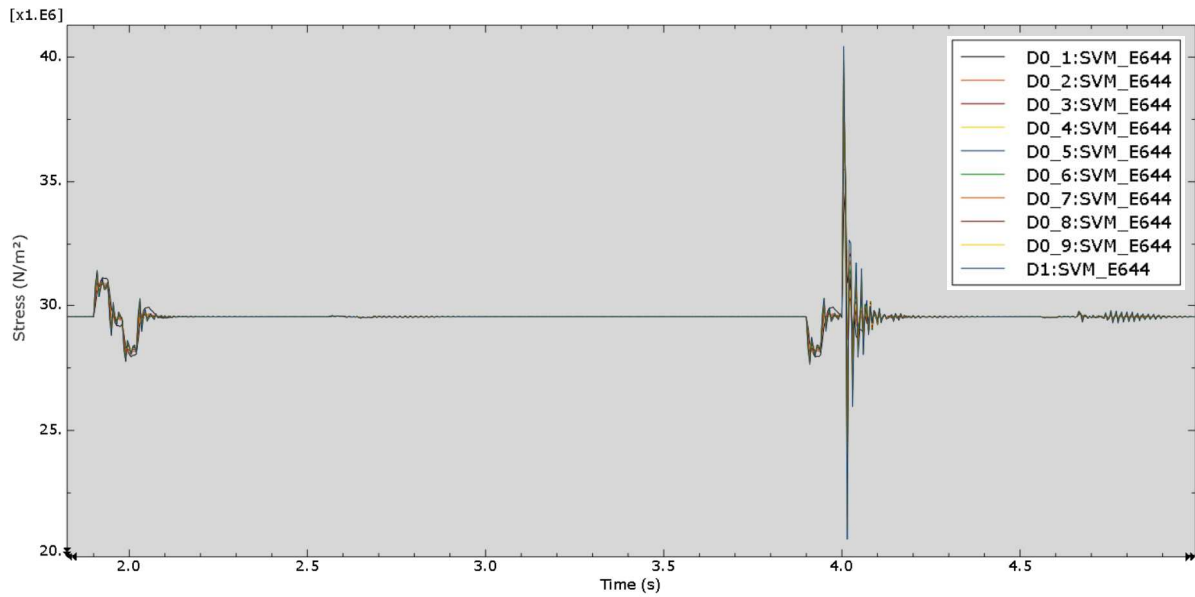


Figure 56: Peak stress for different damping ratios

To see the difference better, there is zoomed in to the centre of the oscillation, but only the stress for D=0,1, D=0,2,D=0,6 and D=1 are plotted (Figure 57). It can be concluded that a higher damping ratio results in a higher frequency of oscillation and amplitude.

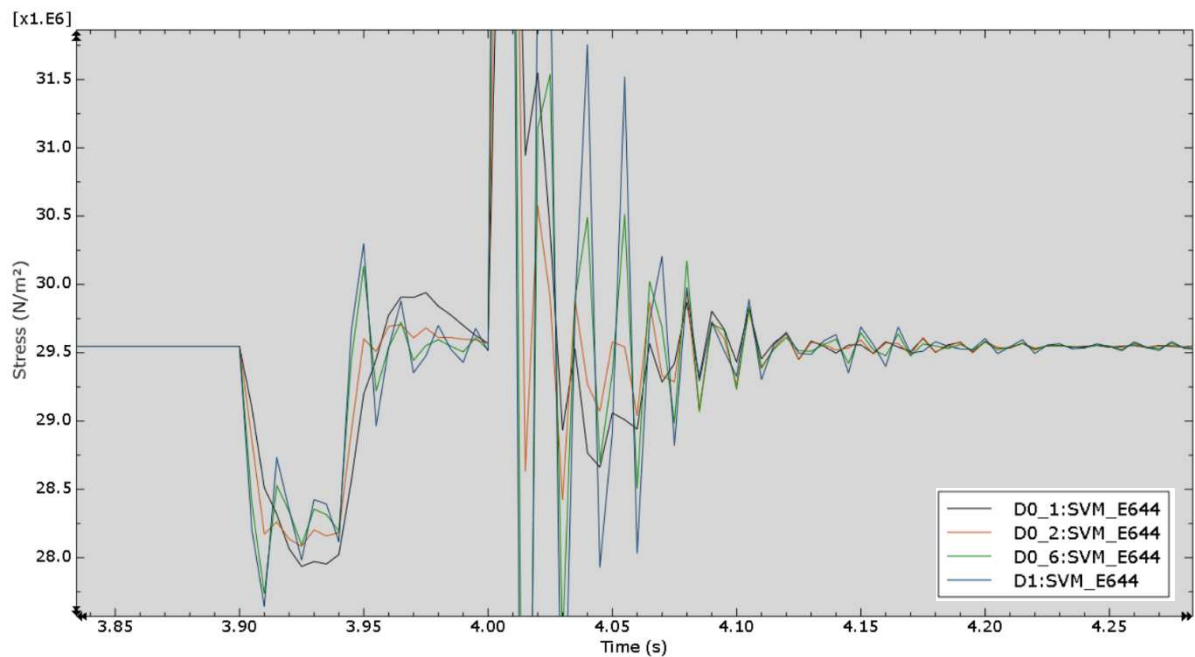


Figure 57: Detail oscillation with a few damping ratios

The reaction of the compression springs differs also due to the different damping ratios (Figure 58). A higher damping ratio, damps the overshoot more, as expected. At a damping ratio of 0,1 a second overshoot is formed. This is something that will be tried to avoid, in Figure 59 the same can be concluded. Therefore a damping ratio of 0,2 or 0,3 looks better. Higher ratios than this damp too much which will make the settling take too long and it creates bigger stress peaks as stated before.

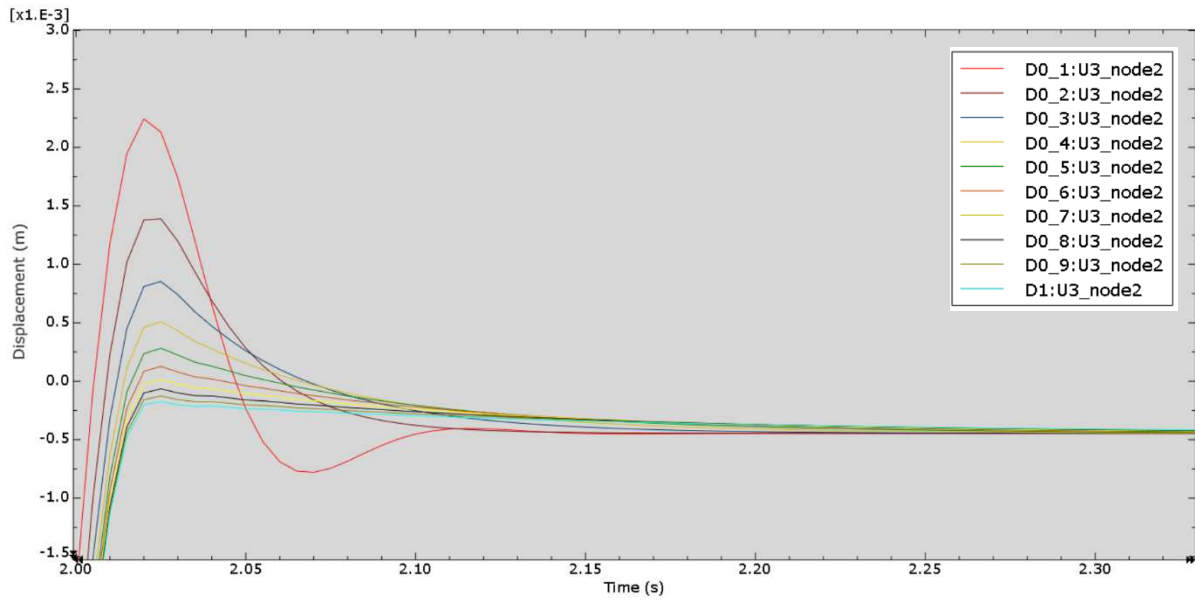


Figure 58: Detail overshoot front wheels with different damping ratios

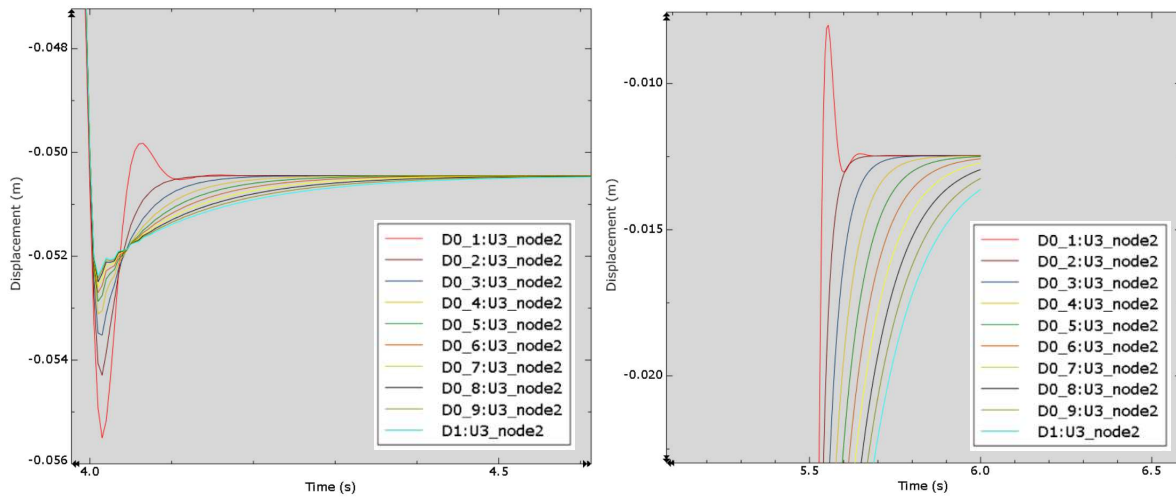


Figure 59: Detail front wheels come down (left), detail unload (Right)

So to conclude, the frame is strong enough for the dynamic circumstances and a damping ratio of 0,2 looks ideal. This makes that the damping is also not too stiff when the vehicle is not loaded.

## 7 SAFETY MEASURES

In the chapter 2.3.4, there was an overview, based on EN 1525: 1997 and ANSI B45.5 -2012, about which measures should be taken to have a safe AGV. In this chapter the implementation of these measures will be discussed.

### 7.1 ACTIVE SAFETY DEVICES

Before any devices are installed, any risks should be avoided before. Therefore some measures are made in the design of the AGV itself. The gears are shielded by plates so nobody can get stuck in between. Also the whole outside of the frame is shielded with plexiglass so everything in the frame can't be touched or something could be stuck at.

The braking on the driving wheels, which allows the vehicle to stop, is performed by electromagnetic brakes. They are designed that if the power supply of the motor is accidentally or intentionally cut off, the brakes automatically are put on.

The safety laser scanner will be the main sensing device of the vehicle. Because the vehicle is omnidirectional, it should be protected on every side. Therefore four safety laser scanner will be used and not one safety bumper. The safety scanner should be placed so there is 360° of protection. A safety scanner has most of the time a scan angle of 275° [38]. In Figure 60 the positioning of the safety laser scanners is shown. The scan angle will be limited to 180° because activating an emergency stop because the wheels turn is by all means not wanted. These scanner have a safety zone of 3 to 4 m and a warning zone up to 40m. The length of the safety and warning zone depends on the speed, underground and load of the vehicle. This means that for every application the zones needs to be defined in advance. In general safety scanners have a Performance level d (PLd, EN ISO 13849) and Safety Integrity Level 2 (SIL2, IEC 61508).

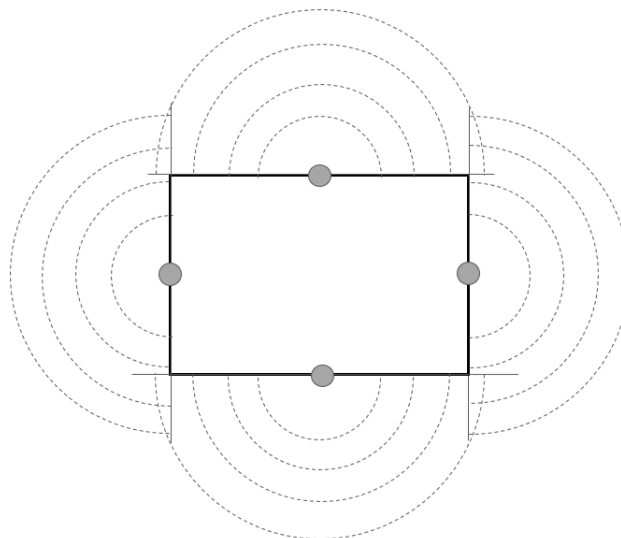


Figure 60: Positioning safety laser scanners, top view

There will be also four emergency stop buttons on the vehicle, they will be placed on the same positioning of the safety scanners, but a little higher which makes them better reachable. Because of this placement an emergency stop button can be reached from every side of the vehicle.

On the drawer door an extra safety device is placed. This because when the vehicle is driving, in no circumstances the drawer should be opened. A non-contact safety switch is used (Figure 61), when the door is opened (when the vehicle is driving) the emergency safety procedure should be activated. This means that it has the same consequences as hitting an emergency stop button or an object in the safety zone.



*Figure 61: A non-contact safety switch from Pilz [39]*

## 7.2 PASSIVE SAFETY DEVICES

As stated before, passive safety devices do not change the state of the vehicle, it are just warnings. For this prototype the passive safety devices are not installed/ placed. The goal of this prototype is to evaluate the working of the suspension and the navigation. These passive safety devices do not change anything in this. But for the completeness of this thesis, the elements that should be places when going on the market will be determined.

Warning lights and warning sounds should be visible/hearable from all around the vehicle. Therefore the warning light should be placed above the vehicle.

In indoor application warning sign should be placed around the path of the vehicle, so the pedestrians know they should watch out. Also loading places where the size of the gap less is than the safety clearance, and hazard zone should be marked, preferably on the floor



*Figure 62: Hazard zone marked on the floor [40]*

### 7.3 EXCEPTION

The exception that the safety braking cannot be expected to work as designed due to an instant change in the safety zone, can be a tricky element. Yet there can be a solution for people. If people would wear a RFID tag, the vehicle could sense the person's presence by the tag and wouldn't have to rely only on the laser scanner.



## 8 ELECTRICAL DIAGRAM

In this chapter the general electrical circuit is described. The electrical part of the AGV is for the continuation of this project but is interesting to know what the build-up looks like.

The AGV can be controlled wireless by an offboard controller, this can be for example a touchscreen panel. The controller will be connected through Wi-Fi from the WLAN access point that's on the vehicle. When programming the vehicle, a laptop will be connected to the access point and the switch. The switch is able to connect network segments to one network and it can control which packet of information is send and received by which segment [41].

The onboard controller is the brains of the vehicle. Directly on the controller connected are, an inclinometer/ IMU (Inertial Measurement Unit), the absolute encoders, warning siren and warning lights. On top the LiDAR scanner is also connected to the switch so it can send it's information to the controller. The type of cables which are used for connection/communication depends on which connection type the controller has.

At the bottom of the schematic the motor drives are drafted. They control the DC-motors with speed and torque control. If sized correctly, a drive is able to control two motors. But if the programmer prefers one drive per motor, this is also possible.

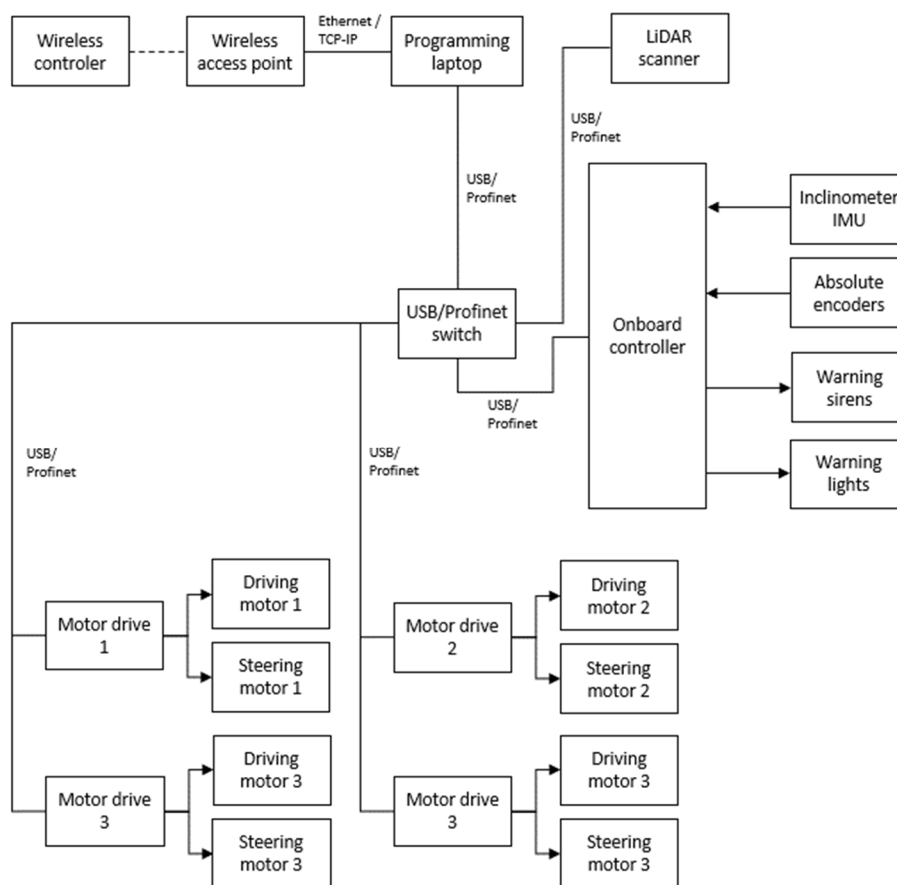


Figure 63: Electrical diagram





## 9 PRICE ESTIMATION

Price quotations are included in attachment B. Some prices are estimated because some parts are not chosen yet, like the safety laser scanners, control system etc. The estimation is made so there is an objective value to find funding for the project. The price is calculated in euros and Brazilian reais (Table 22).

Conversion: dollar to euro: x0,85, euro to real: x6,6, dollar to real: x5,58

Table 22: Price estimation

Part	Price per part	Quantity	Total price	EURO	REAIS
Steering motor with gearbox and brake	\$ 660,21	4	\$ 2.640,84	€ 2.244,71	R\$ 14.735,89
Driving motor with gearbox and brake	\$ 856,53	4	\$ 3.426,12	€ 2.912,20	R\$ 19.117,75
ITEM products	€ 632,87	1	€ 632,87	€ 632,87	R\$ 4.176,94
Slewing gear	\$ 100,00	4	\$ 400,00	€ 340,00	R\$ 2.232,00
Drawer slider	€ 135,61	2	€ 271,22	€ 271,22	R\$ 1.790,05
48 V battery	€ 3.840,00	1	€ 3.840,00	€ 3.840,00	R\$ 25.344,00
24 V battery	€ 1.260,00	1	€ 1.260,00	€ 1.260,00	R\$ 8.316,00
Cable carrier	€ 16,80	2	€ 33,60	€ 33,60	R\$ 221,76
Encoder	€ 419,00	4	€ 1.676,00	€ 1.676,00	R\$ 11.061,60
Compression spring	\$ 42,77	8	\$ 342,16	€ 290,84	R\$ 1.919,52
Wheel	€ 49,00	4	€ 196,00	€ 196,00	R\$ 1293,6
Fasteners	€ 400,00	1	€ 400,00	€ 400,00	R\$ 2.640,00
Aluminium sheets and solids	€ 1.000,00	1	€ 1.000,00	€ 1.000,00	R\$ 6.600,00
Plastics	€ 21,27	13,5	€ 287,15	€ 287,15	R\$ 1.895,16
Safety scanners	€ 1.000,00	4	€ 4.000,00	€ 4.000,00	R\$ 26.400,00
Control system	€ 500,00	1	€ 500,00	€ 500,00	R\$ 3.300,00
<b>Total</b>				<b>€ 13.697,44</b>	<b>R\$ 89.109,52</b>



## 10 CONCLUSIONS

The objective of this thesis was to design a prototype of an autonomous guided vehicle which could work in indoor and outdoor environments and different surfaces types of floors. Current vehicles are usually for indoor or outdoor applications, not both, this is detrimental for its deployability.

The start of the project was spent on searching information about already existing AGV's: which components they have, what are the possibilities and which safety measures are needed? The literature review provided the answers and it is the solid base where the project is built on. Based on the literature review, different design concepts were evaluated. There are many solutions to one problem, and here these solutions were rated on different aspects. Next these concepts were made into an actual design. Although the concepts were rated, it was difficult to choose the right one. There are always negative points for a certain aspect, so it was all about compromise to choose the best solution as possible.

The driving and steering motors were calculated on the toughest outdoor environment (sandy surface with a slope of  $20^\circ$ ). Based on these calculations the BLDC motors were chosen and the batteries, which provide the motors from energy, were calculated. The main solution for overcoming the problems with the outdoor environment, is a suspension. This suspension consists of two compression springs and shock absorbers per wheel. The spring stiffness is calculated on the basis of a basic diagram of the vehicle.

To see if the frame of the AGV is strong enough and to see how the suspension reacts to disturbance a dynamic model of the vehicle is made. The dynamic model is solved with finite element method in the program Abaqus and the disturbance is simulated by a bump of 0,5 m. Out of the simulations could be concluded that the frame was strong enough and a damping ratio of 0,2 is ideal for the loaded vehicle.

At last the electrical diagram, safety measures and price estimation were made and described. These chapters give already some extra information and insight for the continuation project.

The goal of this thesis is achieved, there is a design of a prototype which meets the initial parameters. Yet, there is still some work for the whole project to have a completely working AGV that is ready for the market. In continuation project(s) the prototype will need to be built. Also the electrical part will be realized, this includes: controlling the motors, navigation, emergency safety procedure, battery management, etc. The calculations showed that a lot of energy is needed to power the motors, therefore it is advised that in the continuation project there will be looked into regenerative braking. With this process the battery can recharge during braking, it will allow the vehicle to drive more hours with the same battery. At last the vehicle will need to be tested in different environments, including safety and navigation tests. If the tests are positive, a new AGV will be on the market.



## REFERENCE LIST

- [1] R. E. Osborn, Forbes, 1945.
- [2] UFSCar, "About UFSCar," [Online]. Available: <https://www2.ufscar.br/foreign-visitor/about-ufscar>. [Accessed August 2020].
- [3] KU Leuven, "Geschiedenis," [Online]. Available: <https://www.kuleuven.be/over-kuleuven/geschiedenis>. [Accessed August 2020].
- [4] Wikipedia, "Amazon Robotics," [Online]. Available: [https://en.wikipedia.org/wiki/Amazon\\_Robotics](https://en.wikipedia.org/wiki/Amazon_Robotics). [Accessed 2020 February].
- [5] K. SRLS, What the heck is an automated guided vehicle?, AGV Network, 2019.
- [6] Scott, "Conveyor/Unit Load AGV," [Online]. Available: <https://www.scottautomation.com/products/conveyor-unit-load/>. [Accessed February 2020].
- [7] jbtc, "towing agvs," [Online]. Available: <https://www.jbtc.com/en/south-america/automated-systems/products-and-applications/products/towing-agvs>.
- [8] Hyster-Yale Group, "LO5.0T - LO7.0T," [Online]. Available: <https://www.hyster.com/north-america/en-us/products/overview/tow-tractors/lo5.0t-lo7.0t/>. [Accessed February 2020].
- [9] BA Systèmes, "Horizontal Reel AGV," [Online]. Available: <https://www.basystemes.com/en/agvs/range/gbh/>. [Accessed February 2020].
- [10] Robohub, "Meet the drone that already delivers your packages, kiva robot teardown," [Online]. Available: <https://robohub.org/meet-the-drone-that-already-delivers-your-packages-kiva-robot-teardown/>. [Accessed February 2020].
- [11] Contour Group bvba, "Machineframe uit plaatwerk," [Online]. Available: <http://www.contour.eu/portfolio-items/machineframe-uit-plaatwerk/>. [Accessed February 2020].
- [12] MND BILIMS, "Concept of construction," [Online]. Available: [www.bilims.com/home](http://www.bilims.com/home). [Accessed February 2020].
- [13] item Industrietechnik GmbH, "Item profiles," [Online]. Available: <https://pt.item24.com/en/productworld/building-kit-system/item-profiles/>.
- [14] I. R. N. D. S. Roland Siegart, "Wheeled Mobile Robots," in *Introduction to Autonomous Mobile Robots*, Cambridge, Massachusetts, The MIT Press, 2011, pp. 35-49.

- [15] Sanderson Leaf Springs, "Leaf springs vs coil springs," [Online]. Available: <https://sandersonleafsprings.co.uk/leaf-springs-vs-coil-springs>. [Accessed February 2020].
- [16] Wikipedia, "Car suspension," [Online]. Available: [https://en.wikipedia.org/wiki/Car\\_suspension](https://en.wikipedia.org/wiki/Car_suspension). [Accessed February 2020].
- [17] J. P. k. Karthik, Artist, *Fatigue life prediction of a parabolic spring under non-constant amplitude proportional loading using finite element method*. [Art]. RVR&JC Engineering College, 2012.
- [18] L. Grimstad and P. J. From, "The Thorvald II Agricultural Robotic System," Faculty of Science and Technology, Norwegian University of Life Sciences, Ås, Norway, 2017.
- [19] Saga Robotics, "Thorvald platform," [Online]. Available: <https://sagarobotics.com/pages/thorvald-platform>. [Accessed February 2020].
- [20] C. McCool, Artist, *Case study: Agbott II*. [Art]. QUT: the university for the real world, 2015.
- [21] M. Tomizuka, "LIDAR Sensing for Vehicle Lateral Guidance: Algorithm and Experimental Study," *Transactions on mechatronics*, vol. 11, no. 6, pp. 653-660, 2006.
- [22] P. Biber and M. D. A. A. Ulrich Weis, "Navigation System of the Autonomous Agricultural Robot "BoniRob"," Corporate Sector Research and Advance Engineering, Stuttgart, Germany, 2012.
- [23] J. McGough, "Introduction to Mobile Robotics- Chapter Locomotion," Sphinx, South Dakota, 2018.
- [24] Wikipedia, "Kettingaandrijving," [Online]. Available: <https://nl.wikipedia.org/wiki/Kettingaandrijving>. [Accessed march 2020].
- [25] V. S. Bagad, "Introduction to Mechatronics," in *Mechatronics*, Pune, India, Technical Publications Pune, 2004, revision 2008, pp. 1-8.
- [26] SDPSI, "Elements-of-metric-gear-technology," Designatronics, Hicksville, NY, 2018.
- [27] S. Debruyne, *Cursus trillingen (Dutch)*, Gent: KU Leuven, 2020.
- [28] Wikipedia, "Rolling resistance," [Online]. Available: [https://en.wikipedia.org/wiki/Rolling\\_resistance](https://en.wikipedia.org/wiki/Rolling_resistance). [Accessed February 2020].
- [29] Elessa S.p.A., "Rolling friction," 2020. [Online]. Available: <https://www.elesa.com/en/CatalogoDatiTecniciOC/42-rolling-friction>. [Accessed

March 2020].

- [30] "Walking in robotics," [Online]. Available: [https://en.wikipedia.org/wiki/Walking#In\\_robotics](https://en.wikipedia.org/wiki/Walking#In_robotics). [Accessed february 2020].
- [31] Engineering ToolBox, "Friction and friction coefficients," 2014. [Online]. Available: [https://www.engineeringtoolbox.com/friction-coefficients-d\\_778.html](https://www.engineeringtoolbox.com/friction-coefficients-d_778.html). [Accessed February 2020].
- [32] P. D. E. A. S. D. K. S. Steve Deryne, "Efficiency measurement campaign on gearboxes," Ghent University, Kortrijk, 2015.
- [33] Varitron Drive Technology, "Worm Gearbox Efficiency," 2014. [Online]. Available: [https://www.c-var.com/faq\\_show.asp?seq=65&title=Worm-Gearbox-Efficiency](https://www.c-var.com/faq_show.asp?seq=65&title=Worm-Gearbox-Efficiency). [Accessed July 2020].
- [34] D. Collins, "Why RMS torque is important for motor sizing," Linear motion tips, July 2015. [Online]. Available: <https://www.linearmotiontips.com/why-rms-torque-is-important-for-motor-sizing/>. [Accessed July 2020].
- [35] Autodesk, "Beam elements," [Online]. Available: [http://download.autodesk.com/us/algor/userguides/mergedProjects/setting\\_up\\_the\\_analysis/linear/Elements/Beam\\_Elements.htm](http://download.autodesk.com/us/algor/userguides/mergedProjects/setting_up_the_analysis/linear/Elements/Beam_Elements.htm). [Accessed august 2020].
- [36] Wikipedia, "von Mises yield criterion," [Online]. Available: [https://en.wikipedia.org/wiki/Von\\_Mises\\_yield\\_criterion](https://en.wikipedia.org/wiki/Von_Mises_yield_criterion). [Accessed August 2020].
- [37] W. D. Clippeleer and B. Wellekens, "Sterkteleer-dynamische belastingen," in *Tabellenboek voor metaaltechniek*, Mechelen, Plantyn, 2012, p. 39.
- [38] Pilz, "Safety laser scanner PSENscan," [Online]. Available: <https://www.pilz.com/en-GB/eshop/00106002197131/PSENscan-Safety-Laser-Scanner>. [Accessed Augustus 2020].
- [39] Pilz, "Coded, non-contact safety switch PSENcode," [Online]. Available: <https://www.pilz.com/en-BE/eshop/00106002217046/PSENcode-non-contact-coded-safety-switches>. [Accessed August 2020].
- [40] Rocla, "Safety guidelines Rocla AGV," 2019. [Online]. Available: [https://www.rocla-agv.com/sites/default/files/downloadable-files/safety\\_guidelines\\_5.pdf](https://www.rocla-agv.com/sites/default/files/downloadable-files/safety_guidelines_5.pdf). [Accessed 2020 August].
- [41] Wikipedia, "Switch (hardware)," [Online]. Available: [https://nl.wikipedia.org/wiki/Switch\\_\(hardware\)](https://nl.wikipedia.org/wiki/Switch_(hardware)). [Accessed August 2020].





## APPENDIX A – List of drawings

Number	Name	Size	Type
	3D-assembly	A3	3D-Assembly
0.0	Assembly	A0	Assembly
0.1	Assembly A-A	A0	Assembly
0.2	Assembly B-B	A0	Assembly
	Suspension unit-3D	A2	3D-Assembly
1	Suspension unit-3D	A0	Assembly
1.1	Connection plate slewing gear	A2	Part
1.2	Anti-backlash gear	A3	Assembly
1.2.3	Inner gear	A3	Part
1.2.4	Outer gear	A3	Part
1.6	Anti-backlash gear - encoder	A3	Assembly
1.6.3	Inner gear - encoder	A3	Part
1.6.4	Outer gear - encoder	A3	Part
1.7	Lower flange slewing gear	A3	Part
1.9	Damper connection	A3	Part
1.10	Upper flange slewing gear	A3	Part
1.14	Motor attach plate	A3	Part
1.18	Secondary L	A3	Part
1.30	Main L	A3	Part
1.31	Pin connection	A3	Part
1.38	Wheel flange	A3	Part
1.39	Big washer	A3	Part
1.45	End cap driving motor	A3	Part
1.47	Driving motor axle	A3	Part
2	Shielding plate - left	A3	Part
3	Frame	A2	Assembly
4	Side plexi plate	A3	Part
6	Shielding plate	A3	Part
7	Shielding plate center	A2	Part
9	Top plate	A3	Part
14	Short plexi plate	A3	Part
22	Connection cable carrier	A2	Part
24	Drawer door	A2	Part
31	Door connector	A2	Part
28	Slider support	A2	Part
39	Drawer support	A3	Part
41	Extra plate	A3	Part
43	Drawer bottom	A2	Welding assembly
43a	Bottom plate	A2	Part
43b	Corner battery	A3	Part
45	Moveable corner battery	A3	Part
48	Long plexi plate	A3	Part

## ATTACHMENT A – Datasheets

### ATTACHMENT A.1 – IMOBRAS BRUSHED DC-MOTOR



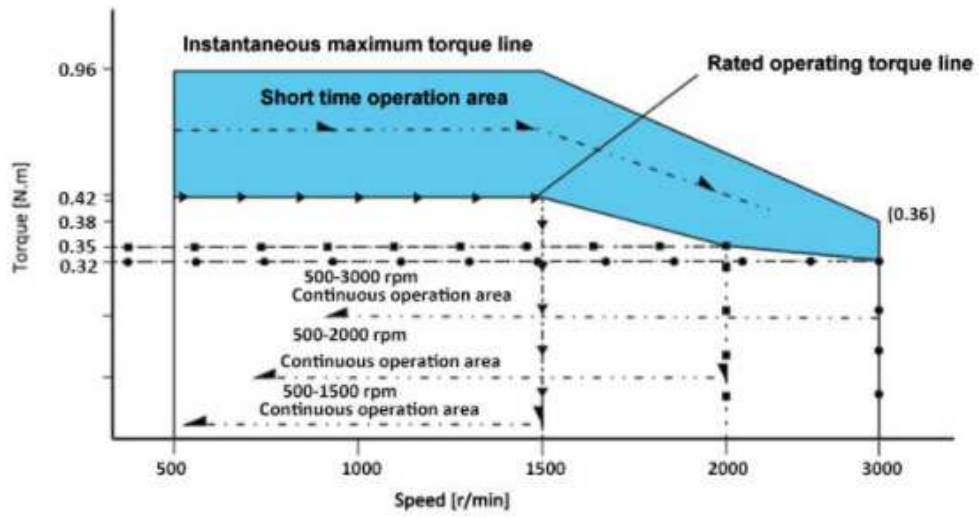
### ATTACHMENT A.2 – STEERING MOTOR WITH GEARBOX

#### 100W 12V/24V BLDC MOTOR SPECIFICATION

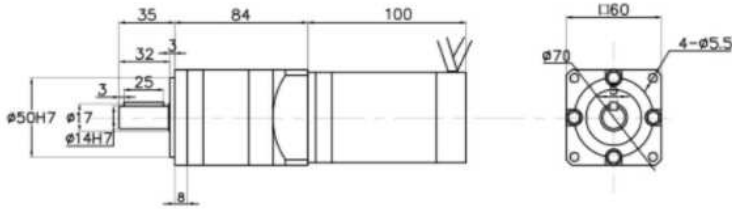
Model	ATO-D2BLD100-30S	
Matched Controller Model	ATO-BLD750 (Click it to see the controller specs)	
Square Flange Size	60 mm	
Weight	2.5 kg	
Rated Voltage	12V DC	24V DC
Rated Current	10.42 A	5.21A
Rated Power	100 W	
Phase	3 phase	
Number of Pole	4 pairs of poles (8 poles)	
Holding Torque	0.32 Nm	
Peak Torque	0.96 Nm	
Rated Speed	3000 rpm	
No-load Speed	3300 rpm	
Efficiency	85%	
Brake Apparatus Voltage	24V DC, (Electromagnetic brake will trigger when the DC supply cuts off) Brake size: Ø56*32mm	
No-load Current	< 1.2A	< 0.8A
Insulation Rank	F	
Protection Rank	IP 54	
Motor Lead Length by Default	100 cm	
Warranty Time	12 months	
Certificate	CE, ROHS, ISO/TS16949	
Temperature	0~50°C	
Humidity	<90%RH (no dewing)	

**NOTE:** Tell us your application needs, we can customize the BLDC motor to meet your precise power, speed, voltage and current requirements.

SPEED-TORQUE CURVE



BLDC MOTOR WITH PLANETARY GEARBOX DIMENSION (Unit:mm)



ALLOWABLE TORQUE BEING WITH GEARBOX

Gear Ratio	4	5	7	10	16	20	25	28	35	40	50	70	80	100	125	140	175	200
Rated Output Speed (rpm)	750	600	429	300	188	150	120	107	86	75	60	43	38	30	24	21	17	15
Rated Output Torque (Nm)	1.2	1.5	2.1	3.1	4.8	6	7.5	8.4	10.5	12	14.9	20.9	22.9	28.7	35.8	37.5	41	37.5

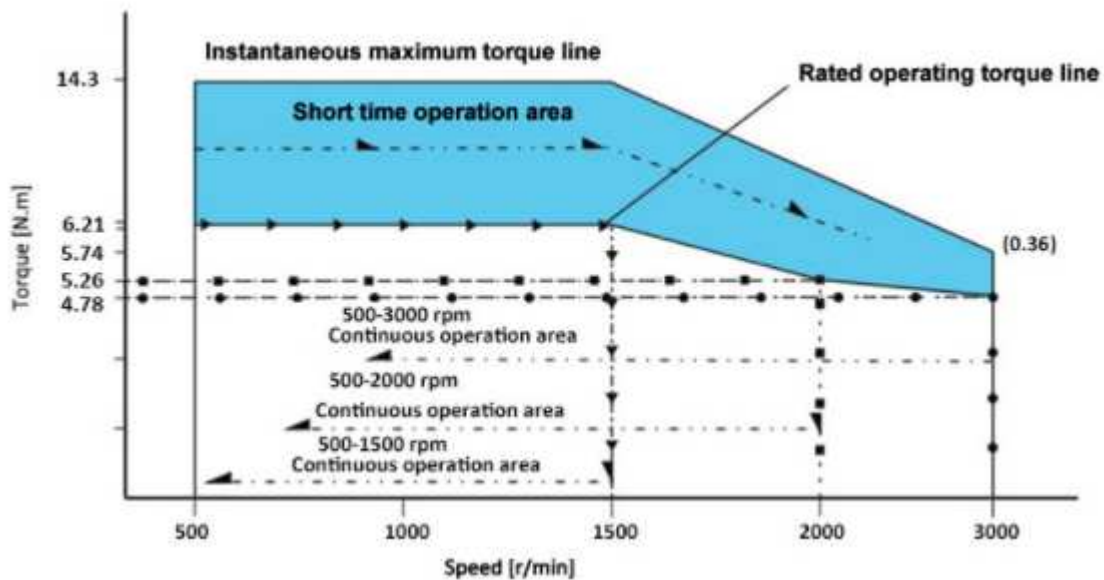
## ATTACHMENT A.3 – Driving motor with gearbox

### 1.5 KW BLDC MOTOR SPECIFICATION

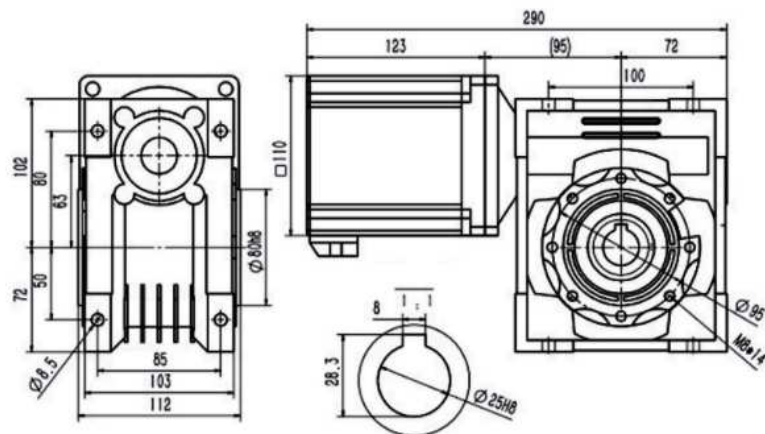
Model	ATO-D110BLD1500 (Click it to see more motor specs)	
Matched Controller Model	ATO-BLD100 (Click it to see more controller specs)	
Square Flange Size	110 mm	
Motor Weight	5.5 kg	
Phase	3 phase	
Number of Pole	4 pairs of poles (8 poles)	
Rated Voltage	36V DC	48V DC
Rated Current	52.08 A	39.06 A
Rated Power	1500W	
Maximum Power	4.5 kW	
Holding Torque	4.78 Nm	
Peak Torque	14.33 Nm	
Rated Speed	3000 rpm	
No-load Speed	4200 rpm	
Efficiency	85%	
Brake Apparatus Voltage	24V DC, (Electromagnetic brake will trigger when the DC supply cuts off) Brake size: $\phi 76.8 \times 27.7$ mm	
Electric Potential	20 V/Krpm	
Insulation Rank	F	
Protection Rank	IP54	
Motor Lead Length by Default	100 cm	
Warranty Time	12 months	
Certificate	CE, ROHs, ISO/TS16949	
Environment	Temperature	-20~55°C
	Humidity	<90%RH (no dewing)

*NOTE: Tell us your application needs, we can customize the BLDC motor to meet your precise power, speed, voltage and current requirements.*

### SPEED-TORQUE CURVE



BLDC MOTOR WITH WORM GEARBOX DIMENSION (Unit=mm)



ALLOWABLE TORQUE BEING WITH GEARBOX

(Note: The rated speed of BLDC motor is 2000rpm if matches the worm gearbox.)

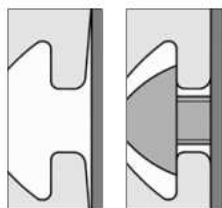
Gear Ratio	7.5	10	15	20	25	30	40	50	60	80	100
Rated Output Speed (rpm)	267	200	133	100	80	67	50	40	33	25	20
Rated Output Torque (Nm)	28.7	38.2	57.3	74.5	90.7	106	133.7	124	94	115	87

ATTACHMENT A.4 – item profiles



TECHNICAL DATA

Technical Data for Profiles



Extruded Profile

Symbol Al Mg Si 0.5 F 25  
Material number 3.3206.72  
Status: artificially aged

Mechanical values (apply only in pressing direction)

Tensile strength R<sub>m</sub> min. 245 N/mm<sup>2</sup>  
Yield point R<sub>p0.2</sub> min. 195 N/mm<sup>2</sup>  
Density 2.7 kg/dm<sup>3</sup>  
Ductile yield A<sub>5</sub> min. 10 %  
Ductile yield A<sub>10</sub> min. 8 %  
Linear coefficient of expansion 23.6x10<sup>-6</sup> 1/K  
Modulus of elasticity E approx. 70,000 N/mm<sup>2</sup>  
Modulus of rigidity G approx. 25,000 N/mm<sup>2</sup>  
Hardness approx. 75 HB - 2.5/187.5

Tolerances

Deformations such as straightness and flatness tolerance to DIN EN 12020 Part 2.  
Profiles not cut to size may be up to 100 mm longer than specified, due to manufacturing methods.

Surface

The aluminium profiles are natural (C0) or black (C35) anodized and are therefore permanently resistant to scratching and corrosion. Surface with matt finish (E 6), compressed with anodic oxidation. Minimum layer thickness 10 µm, layer hardness 250 - 350 HV. The all-round hard anodized surface covering makes saw cuts virtually burr-free, thereby eliminating the need for remachining.

All standard Profiles and Profiles "light" and Profiles "E" feature defined points of support on the Profile exterior and inclined groove flanks. These ensure a firm and stable connection with other components. Thanks to controlled elastic deformation in the groove flanks, the fastening screw creates a vibration-free connection.

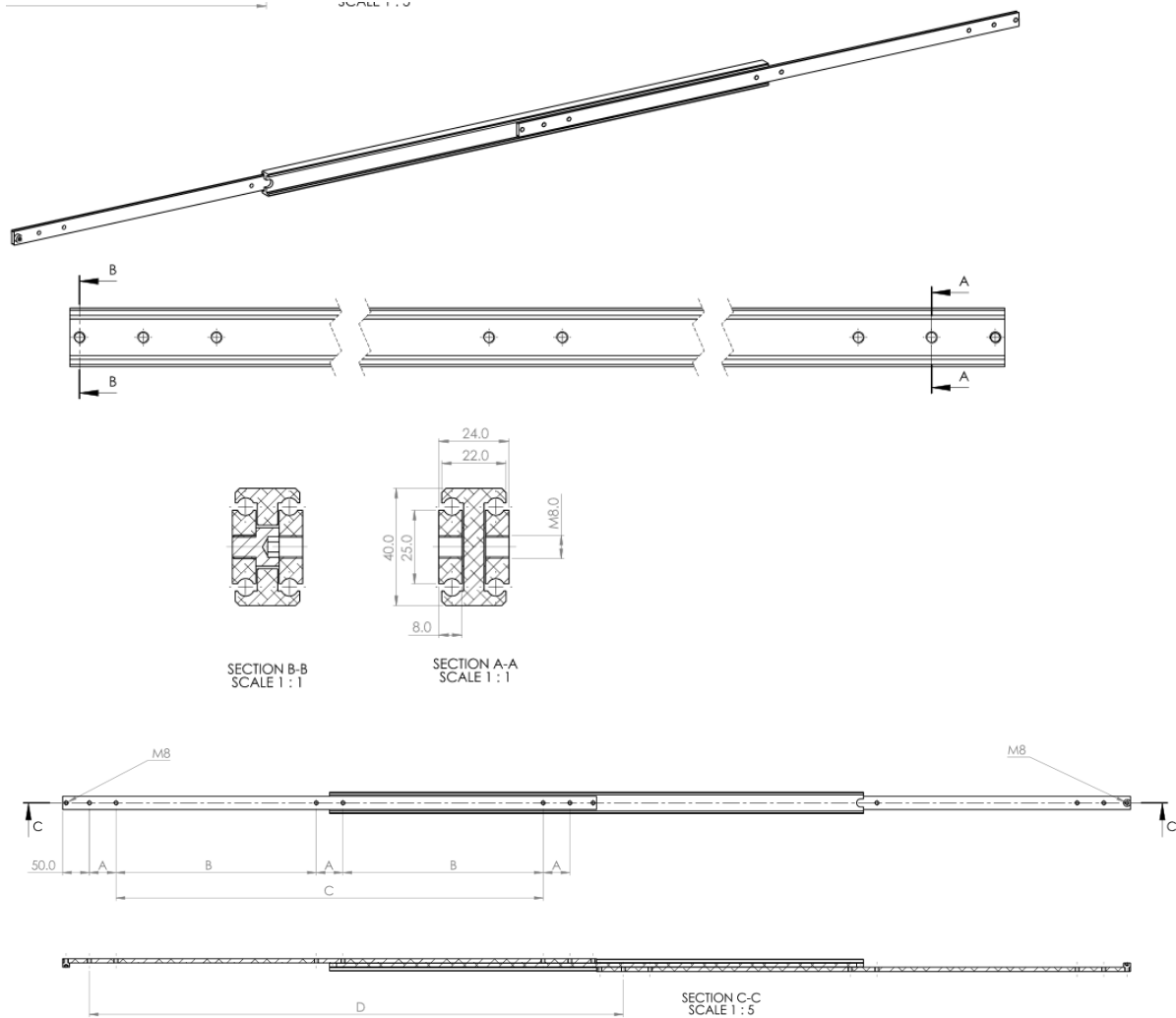
# ATTACHMENT A.5 – Slewing gear

Implantation suivant A  
Implantation according to A  
Ansicht nach A

<p><b>Droite</b> - Gear - Verzahnung</p> <p>Modèle - Model 4</p> <p>Angle de pression - Pressure angle 20°</p> <p>Engrenage - Gear 92</p> <p>Nombre de dents - Number of teeth 92</p> <p>Troncature - Truncature 368</p> <p>Profondeur de la dent - Tooth depth 4</p> <p>Module - Module 4</p> <p>Profil de la dent - Tooth profile 130,314</p> <p>Angle de la dent - Tooth angle 130,194</p> <p>Troncature - Truncature 130,194</p> <p>Four rond au diamètre pmt - Run out on P.D. Roughness 0.32</p> <p>General 0.42</p>		<p>Tolérances géométriques suivant l'ETB 061 Geometric tolerances according to ETB 061</p> <p>BE 24 Tous les bords A.K. Pour les bords B.1. Bélişingünönlügen B.2. Tous de bélişingünönlügen B.3. Bélişingünönlügen B.E. Tous de grazevats A.K. Şablonlar B.1. Tous de grazevats B.2. Grazevats B.3. Şablonlar</p> <p>equil. gl. Abst. equil. gl. Abst. equil. gl. Abst. equil. gl. Abst. equil. gl. Abst. equil. gl. Abst. equil. gl. Abst.</p> <p>Position approximative du bouchon et du raccord de temps Rflr plug and handring connection of trackway ca Şaplan - und Handringşaplan - position</p> <p>Ind Date A 15/11/1996 Industrialisation Nature - Change - Art Via 1</p>	
<p>Masse estimée 20 kg Estimated weight lbs</p> <p>Cette coovone brevetees D.U.O.R.O.L.L.I.X. est une coovone brevetees D.U.O.R.O.L.L.I.X. et est reservee au fabricant. Toute utilisation non autorisee est interdite. This patent is a trademark of ROLLIX. Any use of this patent without the written consent of ROLLIX is prohibited.</p> <p>Imprimé en France Printed in France</p> <p>Indice A</p>		<p>N° 01-0289-06</p> <p>Logo ROLLIX GROUPE DEFONTAINE</p> <p>Siège social : 3 rue Louis Reraull B.P. 339 - 48503 ST HERBLAIN CEDEX Tel. 02.40.67.89.89 Télécopie 02.40.67.89.03</p> <p>ETB 061.ind.03.3</p>	

# ATTACHMENT A.6 – Drawer slider

Configuration Table						
Part Number	Installation Length "L"	Extension Length "D"	Load Per Pair (kg)	Drill Table		
				"A"	"B"	"C"
4015.ADTS040.0200	200	200	70	50		
4015.ADTS040.0250	250	250	75	50		50
4015.ADTS040.0300	300	300	80	50		100
4015.ADTS040.0350	350	350	85	50		150
4015.ADTS040.0400	400	400	90	50		200
4015.ADTS040.0450	450	450	95	50		250
4015.ADTS040.0500	500	500	100	50		300
4015.ADTS040.0550	550	550	105	50	150	
4015.ADTS040.0600	600	600	110	50	175	
4015.ADTS040.0650	650	650	105	50	200	
4015.ADTS040.0700	700	700	100	50	225	
4015.ADTS040.0750	750	750	95	50	250	
4015.ADTS040.0800	800	800	90	50	275	
4015.ADTS040.0850	850	850	85	50	300	
4015.ADTS040.0900	900	900	80	50	325	
4015.ADTS040.0950	950	950	75	50	350	
4015.ADTS040.1000	1000	1000	70	50	375	
4015.ADTS040.1050	1050	1050	65	50	400	
4015.ADTS040.1100	1100	1100	60	50	425	
4015.ADTS040.1150	1150	1150	55	50	450	
4015.ADTS040.1200	1200	1200	50	50	475	



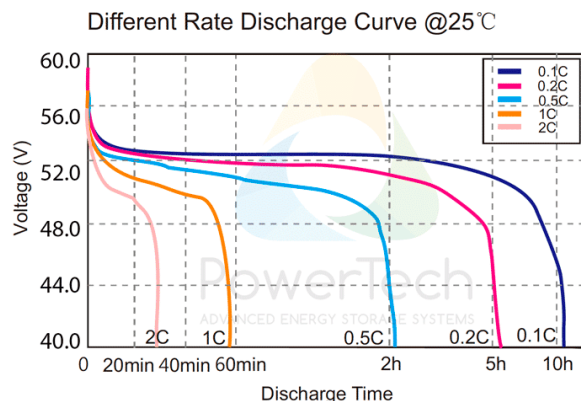
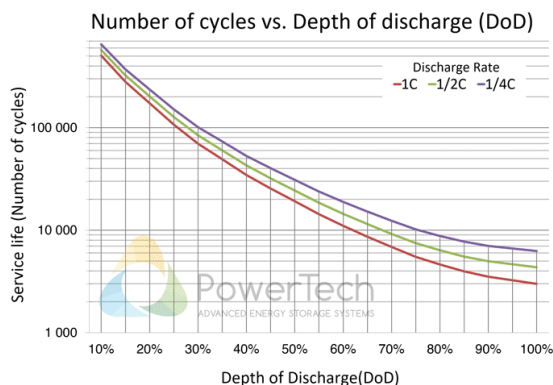
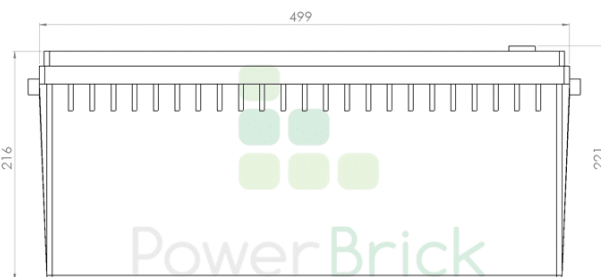
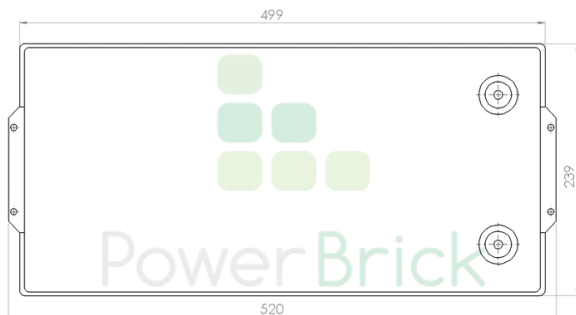
## ATTACHMENT A.7 – 48 V battery

### 48V battery pack - Lithium Iron-Phosphate (LiFePO<sub>4</sub>) - 105Ah

- **High Service Life : 3000 cycles** and more (see chart)
- **Deep discharge** allowed up to 100 %
- Ultra safe **Lithium Iron Phosphate** chemistry (no thermal run-away, no fire or explosion risks)
- **Embedded BMS** (Battery Management System) : **improve lifespan AND secure the battery**
- No **Lead**, no **rare earths**, no **acid**, no **degassing**
- Calendar life > **10 years**
- Excellent **temperature** robustness (-20 °C up to +60 °C)
- **Flexible** deployment : up to 16 packs in parallel and 4 in series
- **Constant power** during discharge (very low internal resistance)
- **Very low Peukert's losses** (energy efficiency of 98 %)
- **Very low self discharge** (<3 % per month)
- **No memory effect**
- About **50 % lighter** and **40% smaller** than equivalent Lead-AGM battery with same usable energy
- **Certification : CE, RoHS, UN 38.3**

### Technical Specifications

Electric	Nominal voltage	51.2 V
	Nominal capacity	105 Ah
	Stored energy	5.38 kWh
	Internal resistance	≤ 50 mΩ
	Cycles	>3000 cycles (see chart)
	Self discharge	< 3% per month
	Energy efficiency	98 %
Standard Charge	Charge voltage	57.6 V ± 0.8V
	Charge mode	CC/CV : Constant Current / Constant Voltage
	Continuous charge current / Maximum charge current	50 A / 100 A
	BMS charge cut-off voltage	59.2 V ± 0.4V
Standard Discharge	Continuous discharge current	120 A (6.14 kW)
	Maximum discharge current (< 30s)	200 A (10.24 kW)
	BMS discharge cut-off voltage	40V
Environment	Charge temperature range	0°C to +60°C
	Discharge temperature range	-20°C to +60°C
	Storage temperature	0°C to +50°C @60±25% relative humidity
	IP protection level	IP 66
Mechanical	Cell assembly	16S1P
	Casing material	ABS
	Dimensions	L : 500mm (520mm) x P : 239mm x H : 217 mm
	Weight	37.5 kg
	Terminal	M8





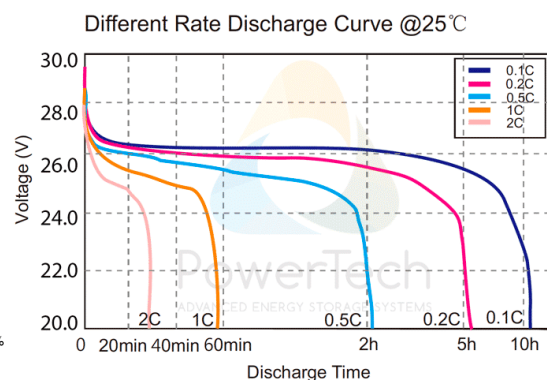
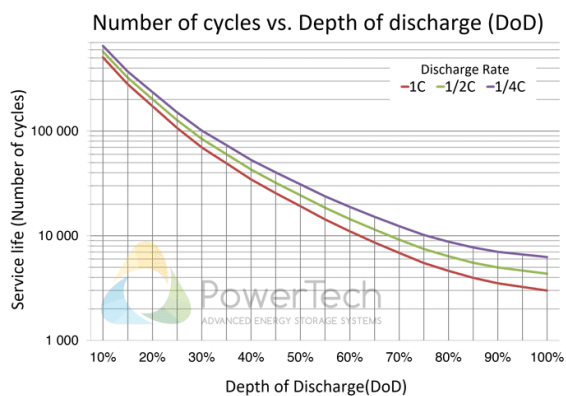
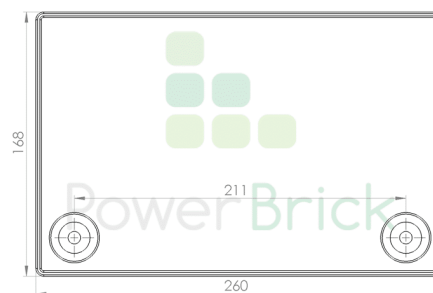
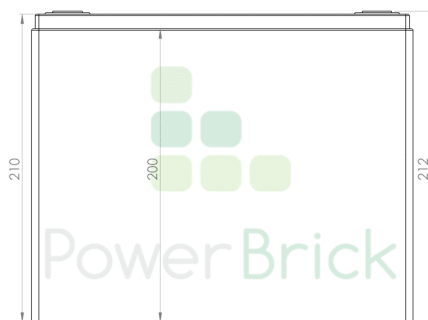
## ATTACHMENT A.8 – 24 V battery

### 24V battery pack - Lithium Iron-Phosphate (LiFePO<sub>4</sub>) - 50Ah

- **High Service Life : 3000 cycles** and more (see chart)
- **Deep discharge** allowed up to 100 %
- Ultra safe **Lithium Iron Phosphate** chemistry (no thermal run-away, no fire or explosion risks)
- **Embedded BMS** (Battery Management System) : **improve lifespan AND secure the battery**
- No **Lead**, no **rare earths**, no **acid**, no **degassing**
- Calendar life **> 10 years**
- Excellent **temperature** robustness (-20 °C up to +60 °C)
- **Flexible** deployment : up to 16 packs in parallel and 4 in series
- **Constant power** during discharge (very low internal resistance)
- **Very low Peukert's losses** (energy efficiency >98 %)
- **Very low self discharge** (<3 % per month)
- **No memory effect**
- About **50 % lighter** and **40% smaller** than equivalent Lead-AGM battery with same usable energy
- **Certification : CE, RoHS, UN 38.3, UL and CB**

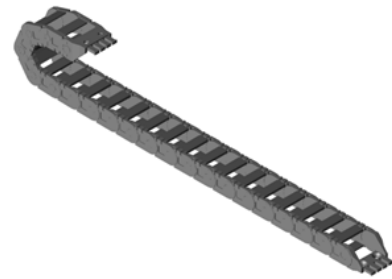
### Technical Specifications

Electric	Nominal voltage	25.6V
	Nominal capacity	50 Ah
	Stored energy	1280 Wh
	Internal resistance	≤ 50mΩ
	Cycles	>3000 cycles (see chart)
	Self discharge	< 3% per month
	Energy efficiency	> 98%
Standard Charge	Charge voltage	28.8V ± 0.4V
	Charge mode	CC/CV : Constant Current / Constant Voltage
	Continuous charge current / Maximum charge current	25 A / 50 A
Standard Discharge	BMS charge cut-off voltage	29.4V ± 0.2V
	Continuous discharge current	75 A (1.92 kW)
	Maximum discharge current (< 30s)	115 A (3.0 kW)
Environment	BMS discharge cut-off voltage	20 V
	Charge temperature range	0°C to +60°C
	Discharge temperature range	-20°C to +60°C
	Storage temperature	0°C to +50°C @60±25% relative humidity
Mecanical	IP protection level	IP 66
	Cell assembly	26650 - 8S16P
	Casing material	ABS
	Dimensions	L : 260mm x P : 168mm x H : 212 mm
	Weight	11.8 kg
	Terminal	M8

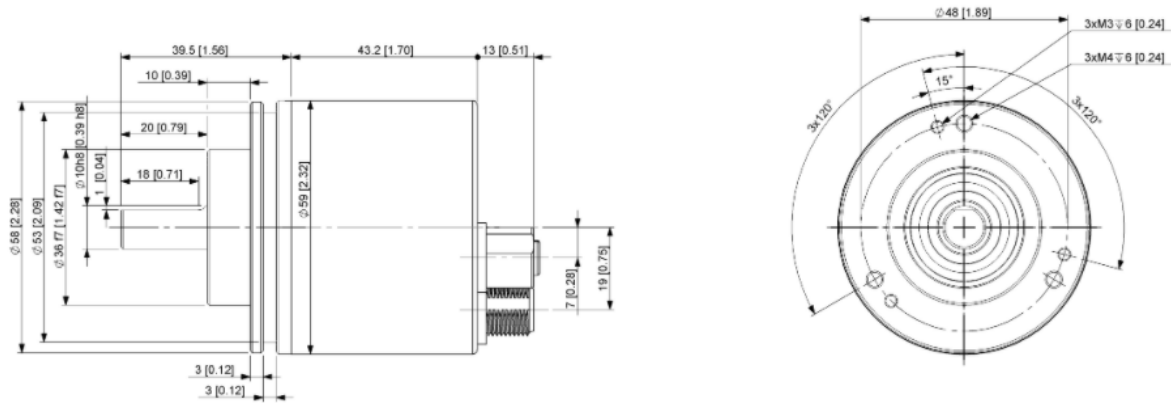


## ATTACHMENT A.9 – Cable carrier

▼ e-chain®	
Part No.	1400.038.035.0
Inner E-Chain width Bi (mm)	38
E-Chain outer width Ba (mm)	51.5
Bending radius R (mm)	35
<b>i</b> Application	unsupported ▼
Nominal clearance height H (mm)	98
Required clearance height HF (mm)	123
<b>i</b> Chain length	Calculation ▼
<b>i</b> Fixed end in the middle of travel distance	Yes ▼
Travel S [0 - 1000000]	950
<b>i</b> Position moving end [-475 - 475]	-475
Mounting bracket moving end	Polymer locking, one-piece ▼
Mounting bracket fixed end	Polymer locking, one-piece ▼
Possible installation conditions	A1 ▼
<hr/>	
e-chain®	1400.038.035.0
Mounting bracket set	14038.12PZ.A1
Order text	0.666m 1400.038.035.0 + 14038.12PZ.A1
▼ Display options/Calculated values	
Level of detail	Standard ▼
Indicated part	entire E-Chain® ▼
Calculated chain length [mm]	666.6
Number of links	20



# ATTACHMENT A.10 – Encoder



interface		Mechanical Data	
interface	PROFINET	Housing Material	Steel
profile	Profidrive profile 4.x, encoder profile 4.x	Housing Coating	Wet coating (RAL 9006 White Aluminium) + Cathodic corrosion protection (>720 h salt spray resistance)
diagnosis	Storage	Flange Type	Clamp, ø 58 mm (L)
Furnishing	Boot loader, round axis, flashing LEDs	Flange Material	Aluminum
Transfer rate	10/100 Mbit	Shaft Type	Solid, Single Flat, Length = 20 mm
Interface cycle time	≥ 1 ms	Shaft Diameter	ø 10 mm (0.39")
Programming functions	Resolution, time base and filter for speed preset, counting direction, IP address	Shaft Material	Stainless Steel V2A (1.4305, 303)
<b>Outputs</b>		Max. Shaft Load	Axial 40 N, Radial 110 N
Output driver	Ethernet	Minimum Mechanical Lifetime	430 (20 N / 40 N), 150 (40 N / 60 N), 100 (40 N / 80 N), 55 (40 N / 110 N)
<b>Electrical data</b>		Rotor Inertia	≤ 30 gcm <sup>2</sup> [≤ 0.17 oz-in <sup>2</sup> ]
Supply voltage	10-30 VDC	Friction Torque	≤ 5 Ncm @ 20 °C, (7.1 oz-in @ 68 °F)
Power consumption	≤ 230 mA @ 10 V DC, ≤ 100 mA @ 24 V DC	Max. Permissible Mechanical Speed	≤ 3000 1/min
Power consumption	≤ 2.5 W	Shock Resistance	≤ 100 g (half sine 6 ms, EN 60068-2-27)
Switch-on time	<1 s	Permanent Shock Resistance	≤ 10 g (half sine 16 ms, EN 60068-2-29)
Reverse polarity protection	Yes	Vibration Resistance	≤ 10 g (10 Hz – 1000 Hz, EN 60068-2-6)
Short circuit protection	Yes	Length	52.7 mm (2.07")
EMC: emitted interference	DIN EN 61000-6-4	Weight	435 g (0.96 lb)
EMC: interference immunity	DIN EN 61000-6-2		
MTTF	65 years @ 40 °C		

Sensor	
Technology	Magnetic
Resolution Singleturn	16 bit
Resolution Multiturn	14 bit
Multiturn Technology	Self powered magnetic pulse counter (no battery, no gear)
Accuracy (INL)	±0.0878° (≤ 12 bit)
Code	Binary

Environmental Specifications	
Protection Class (Shaft)	IP66/IP67
Protection Class (Housing)	IP66/IP67
Operating Temperature	-40 °C (-40 °F) - +70 °C (+158 °F)
Storage Temperature	-40 °C (-40 °F) - +85 °C (+185 °F)
Humidity	98% RH, no condensation

UCD-EIB1B-1216-L10S-PAM



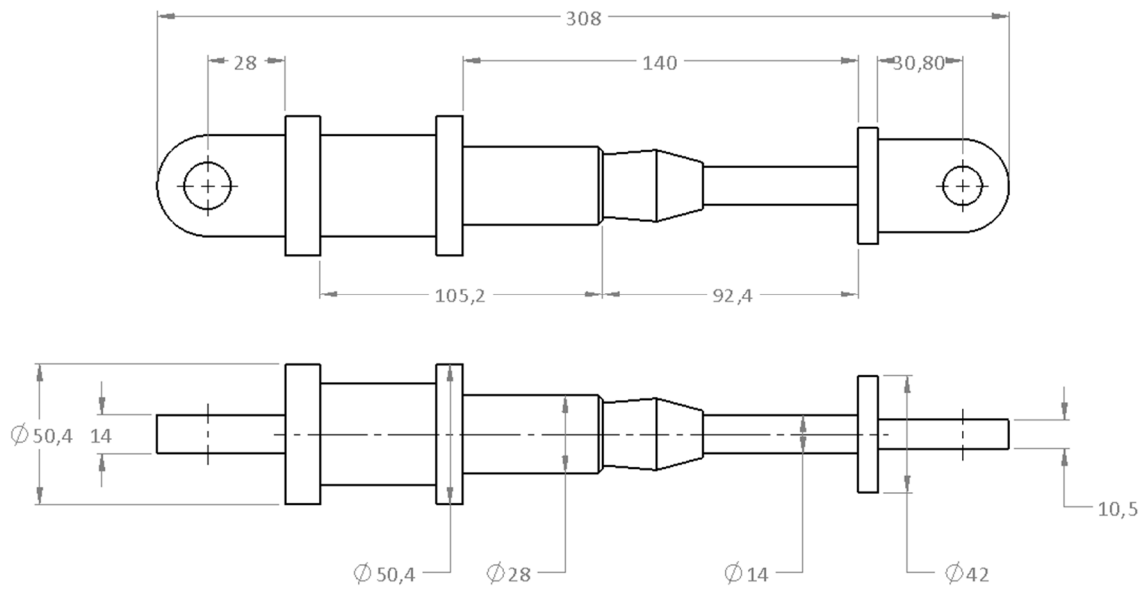
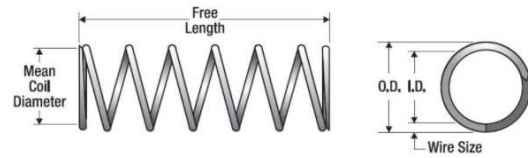
# ATTACHMENT A.11 – Damper

## 72923 - Compression Springs

### SPECIFICATIONS

English  Metric

Material	Music Wire - MW
Wire Dia (mm)	5.54
O. D. (mm)	42.85
I. D. (mm)	31.78
Free Length (mm)	139.7
Total Coils	13.30
Rate (N/mm)	15.937
Ends	Closed/Ground - CG
Suggested Max Load (N)	1,058.677
Suggested Max Deflection (mm)	66.04
Solid Length (mm)	73.4
Standard Finish	None - N



## ATTACHMENT A.12 – WHEEL

Industrial Wheel from pneumatic tyre block profile, precision ball bearing, Wheel-Ø 300mm,



### Product information

SKU	200506301
EAN	8718116116653

### Specifications

type	wheel
wheel centre	heavy pressed steel
tread	luchtband met blokprofiel
bearing type	precision ball bearing
Axle hole-Ø	20
Load capacity (static)	300
Hub length	75
Width of tread	100
Wheel-Ø	300

## ATTACHMENT B – Prices

### ATTACHMENT B.1 – Steering motor

Customizable



#### 100W 12V/24V 3000rpm BLDC Motor

★★★★★  
[Write a review](#)

**\$660.21**

Best 100W brushless DC motor kit for sales, 3 phase electric motor combines with bldc controller at affordable price, 3000rpm rated speed, working at 12V or 24V DC, 0.32Nm holding torque and peak torque up to 0.96Nm.

SKU: ATO-BLDC-100R3

Voltage (DC) *	24V ▼
With Brake *	Yes [+\$156.44] ▼
With Matched Controller *	No ▼
With Matched Gearbox *	Planetary Gearbox ▼
Planetary Gearbox *	Gear Ratio 80:1 [+\$325.19] ▼

### ATTACHMENT B.2 – Driving motor

Customizable



#### 1 kW 36V/48V 3000rpm Brushless DC Motor

★★★★★  
5 out of 5 based on [8 reviews](#) | [Write a review](#)

**\$856.53**

Good price 1 kW 36V/48V bldc motor and controller for sales, electric motor with 3000 rpm rated speed, 3.18 Nm holding torque, brushless design for long life, cost-effective replacement for brush dc motors. 3 phase brushless dc motor kit best for electric car.

SKU: ATO-BLDC-1000R3

Voltage (DC) *	48V ▼
With Brake *	Yes [+\$156.44] ▼
With Matched Controller *	No ▼
With Matched Gearbox *	Worm Gearbox ▼
Worm Gearbox *	Gear Ratio 7.5:1 [+\$284.24] ▼

## ATTACHMENT B.3 – ITEM products



**Motix NV**  
Nieuwlandlaan 111-89  
3200 Aarschot

**T** 016 140 710  
**E** item@motix.be  
**I** www.motix.be

<b>Offertenummer</b>	: 200026331	Betaalconditie	: Within 30 days Due net
Offertedatum	: 24-08-2020	Geldigheidsduur	: 30Dagen
Uw referentie	: Dimitri Hoogewijs	Leverwijze	: EXW
Totaal gewicht	: 24,97 kg	Levertijd	: 7Dagen

### Offerte

K.U. Leuven - Facturen bureau

Krakenstraat 3 Bus 5506  
3000 Leuven  
België

Pos	Itemnummer	Omschrijving	Aantal	Eenheids prijs	Bedrag
10	0.0.451.03	Profil 6 30x30, natur Lengte: 6000 mm	3 st	€ 86,94	€ 260,82
20	0.0.419.40	Nutenstein 6 St M6, verzinkt	100 st	€ 0,39	€ 38,85
30	0.0.672.86	Automatik-Verbindungssatz 6 30	16 st	€ 7,41	€ 118,61
40	0.0.419.67	Winkelsatz 6 30x30	16 st	€ 5,37	€ 85,85
50	0.0.391.34	Handgriff PA 80, schwarz	1 st	€ 2,61	€ 2,61
60	0.0.619.35	Verschlussystem 6, Zylinderschloss mit Rosette, linksschließend	1 st	€ 50,13	€ 50,13
70	TRANSPORT	Transportkost	1 st	€ 76,00	€ 76,00
<b>Totaal, Excl. BTW:</b>					<b>€ 632,87</b>

## ATTACHMENT B.4 – Slewing gear

### 01-0289-06 External Gear Slewing Ring Bearing Slewing Gear Slewing Ring

[Get Latest Price >](#)

[Leave a message.](#)

Purchase Qty. / Reference FOB Price	
1-19 Pieces	<b>US \$100</b>
20-199 Pieces	<b>US \$95</b>
200+ Pieces	<b>US \$90</b>

Port: Shanghai, China

Production Capacity: 600PCS Per Year

Payment Terms: L/C, T/T, Western Union, Paypal

Rolling Body: Roller Bearings

The Number of Rows: Single

Outer Dimension: 200-8000mm

Material: 50mn, 42CrMo

Spherical: Non-Aligning Bearings

Load Direction: Axial

## ATTACHMENT B.5 – Drawer slider

**SLIDING**  
SYSTEMS PROMOUNT

Providing quality Sliding Systems across:

[HOME](#) [SHOP](#) [FAQs](#) [ABOUT US](#)

[HOME](#) / [CART](#)

### Cart

ADTS-40 (50-110 kg/pr) Aluminium. Non Corrosive - **ARE SOLD AS SINGLE SLIDES (NOT A PAIR)**

PRODUCT	PRICE	QUANTITY	SUBTOTAL
ADTS-40 (50-110 kg/pr) Aluminium. Non Corrosive - ADTS-40 length 900mm. Extn 900mm. Load per pair 80kg	€135.61	<input type="text" value="2"/>	€271.22

PRODUCT	PRICE	QUANTITY	SUBTOTAL
ADTS-40 (50-110 kg/pr) Aluminium. Non Corrosive - ADTS-40 length 900mm. Extn 900mm. Load per pair 80kg	R\$767.62	<input type="text" value="2"/>	R\$1,535.24

Brazilian Real



## ATTACHMENT B.6 – 48 V Battery



### Lithium Ion battery 48V 105Ah – LiFePO4 – PowerBrick®

3 840.00 € – 4 416.00 €

LiFePO4 Battery pack 48V-105Ah  
with built-in BMS (Battery management System)

What difference between **STANDARD** and **PRO** ? CLEAR

Version :  ▼

PowerBrick+ 48V 105Ah – Professionnal – 2 years warranty

**3 840.00 €**

- 1 +

**ADD TO CART**

## ATTACHMENT B.7 – 24 V Battery



### Lithium Ion battery 24V 50Ah – LiFePO4 – PowerBrick®

★★★★★ (4 customer reviews)

1 008.00 € – 1 449.00 €

LiFePO4 Battery pack 24V-50Ah  
with built-in BMS (Battery management System)

What difference between **STANDARD** and **PRO** ?

Name	Discount
-15% on PRO versions	15 %

Version :  ▼ CLEAR

PowerBrick+ 24V 50Ah – Professionnal – 2 years warranty

~~1 260.00 €~~ **1 071.00 €**

## ATTACHMENT B.8 – Cable carrier

Energy chain systems and polymer plain bearings

Pos. 1



Energy chain 1400 series

Art.-No. : 1400.038.035.0

ready to ship within 24 - 48 hours

▶ Comments

Number

2

length (mm)

699

Price per piece

EUR 16.80

Total

EUR 33.60



## ATTACHMENT B.9 – Encoder

UCD-EIB1B-1213-L100-PAM



€ 419.00

Stock: 3 pieces

Delivery time if not in stock  
3-4 weeks.

Can only be ordered in  
NL BE

Code generator Profinet Multiturn Clamping flange,  
shaft 10mm, 4096 rev, 8192 steps / rev

Other versions

4096 rpm, 8192 steps / rev

Number

4

To order

Brand: Posital Fraba

Item No. : FUCD1213-006

Encoder with magnetic scanning

Favorites

## ATTACHMENT B.9 – COMPRESSION SPRING

72923 - Compression Springs

### SPECIFICATIONS

English Metric

Material	Music Wire - MW
Wire Dia (mm)	5.54
O. D. (mm)	42.85
I. D. (mm)	31.78
Free Length (mm)	139.7
Total Coils	13.30
Rate (N/mm)	15.937
Ends	Closed/Ground - CG
Suggested Max Load (N)	1,058.677
Suggested Max Deflection (mm)	66.04
Solid Length (mm)	73.4
Standard Finish	None - N

### CONFIGURE & BUY

Standard Finish

None - N

Please note: adding a finish (passivation ,zinc, etc...) will extend your lead time by 4 days and is subject to a lot charge as noted in the dropdown above (single lot charge applies to the entire quantity of this part ordered).

### VOLUME PRICING

QTY	1-9	10-24	25-49	50-99	100-249	250-499	500-999
UNIT PRICE	\$42.77	\$34.22	\$17.11	\$10.69	\$7.27	\$4.70	\$2.99

For quantities 1000 or greater, please contact us at [info@centuryspring.com](mailto:info@centuryspring.com) for quote.

QTY 8

Unit Price: \$42.77

Total Price: \$342.16

ADD TO CART

## ATTACHMENT B.10 – Wheel

**Van:** [Kit Cheung](#)

**Verzonden:** donderdag 30 juli 2020 9:29

**Aan:** [dimitrihoogewijs](#)

**Onderwerp:** RE: Price wheel 200506301

Good morning Dimitri,

Thank you for your request.]

The price for 4 wheels is as followed:

- 200506301 - €49 per wheel
- Transport - €40 from NL to UK

If you have any questions please contact us.


Have a nice day.

Met vriendelijke groet, Kind regards,

2.5.1 Kit Cheung  
Export sales and Transportation  
Konijnenburg B.V.



---

 +31 (0) 20 682 1051 | +31 (0) 20 584 9743

 [purchase@konijnenburg.nl](mailto:purchase@konijnenburg.nl)

 [www.wielen.nl](http://www.wielen.nl)

 Elektronstraat 19, 1014 AP, Amsterdam, The Netherlands

